Regulation of TrkB activity by PTPN11 is mediated through transmembrane protein Caveolin in the inner retina

Mojdeh Abbasi (MSc)

(44690665)

A thesis submitted for the partial fulfilment of the requirements for the degree of Master of Research in Neuroscience

Supervisor:

Professor Stuart Graham

Associate Supervisor:

Dr. Vivek Gupta

Adjunct Supervisor:

Dr. Seyyed Mojtaba Golzan

MACQUARIE University

Declaration of originality

I hereby declare that the work presented in this thesis has not been submitted for a higher degree to any other university or institution. To the best of my knowledge this submission contains no material previously published or written by another person, except where due reference is stated otherwise. Any contribution made to the research by others is explicitly acknowledged.

Mojdeh Abbasi
Student number: 44690665
Department of Clinical Medicine
Faculty of Medicine and Health Sciences
Macquarie University

Date of Submission
10/10/2016

Acknowledgements

Firstly, I would like to thank my principal supervisor, Professor Stuart Graham for his wisdom and guidance through this endeavour. It has been a privilege to be part of his team. I would like to thank my associate supervisor, Dr. Vivek Gupta. I could go to him with questions or whenever I came upon a difficult problem, for which he always offered sound advice and assistance.

I would like to acknowledge Dr. Mojtaba Golzan, my co-supervisor at the University of Technology Sydney for his assistance. I would also like to extend my thanks to the following members of the Graham group who made me feel welcome and who helped me learn the skills I needed; Roshana, Nitin and Dr. Anita Turner.

Finally, I would like to thank my loving husband and my family for all their support. Without them this would not have been possible.

Publications arising from this candidature

Conference presentations

Mojdeh Abbasi, Vivek Gupta, Nitin Chitranshi, Yogita Dheer, Anita Turner, Roshana Vanderwall, Stuart L. Graham. Cav-1 ablation protects against loss of inner retinal function caused by PTPN11 overexpression. Australian Neurosciences Society 36th Annual Scientific Meeting **2016**

Publications

Gupta V, Gupta VB, Chitranshi N, Gangoda S, Vander Wall R, **Abbasi M**, Golzan M, Dheer Y, Shah T, Avolio A, Chung R, Martins R, Graham S. One protein, multiple pathologies: multifaceted involvement of amyloid β in neurodegenerative disorders of the brain and retina. Cell Mol Life Sci. **2016** Jun 22.

Nitin Chitranshi, Yogita Dheer, Roshana Vander Wall, Veer Gupta, **Mojdeh Abbasi**, Stuart L. Graham, Vivek Gupta. Computational analysis unravels novel destructive single nucleotide polymorphisms in the non-synonymous region of human caveolin gene. Gene reports. **2016** Aug.

Abstract

Brain derived neurotrophic factor (BDNF) and its high affinity receptor tropomyosin-related kinase receptor B (TrkB) play a protective role in the survival of retinal ganglion cells (RGCs) in healthy and disease states. SH2 domain tyrosine phosphatase PTPN11 (Shp2) is a ubiquitously expressed tyrosine phosphatase that regulates TrkB receptor and its activation is mediated through its interactions with the adapter protein Caveolin (Cav-1). This study determines the involvement of Cav-1 in facilitating Shp2 mediated inner retinal effects by genetically upregulating Shp2 expression in Cav-1 knockout mice.

Shp2 was over-expressed in mice retina (n=38) through intravitreal injection of recombinant adeno-associated virus vector (AAV2). Wildtype and Cav-1 transgenic mice were used and for each animal one eye was transduced with PTPN11 transgene whereas GFP expression in the contralateral eye was used as control. Retinal functional changes were assessed by electroretinogram (ERG) and scotopic threshold response (STR) recordings. *In vivo* imaging using optical coherence tomography (OCT) and histological analysis were used to evaluate structural changes in the retinal laminar structure.

Shp2 upregulation resulted in significantly reduced STR amplitude in both WT and Cav-$1^{+/-}$ mice ($p<0.001$ and $p<0.01$ respectively). Cav-$1^{-/-}$ group on the other hand demonstrated only a slight loss of STR amplitudes upon Shp2 upregulation that was statistically insignificant. Cellular density in the ganglion cell layer (GCL) was also significantly reduced in WT and Het groups ($p<0.001$ and $p<0.01$ respectively). Shp2 upregulation did not result in a significant decrease in the GCL density in Cav-$1^{-/-}$ mice.

Together, these results suggest a novel role of Cav-1 in mediating Shp2 actions in retina particularly RGCs. Loss of Cav-1 exerts a protective effect particularly on the inner retinal function and structure. Future studies will help establish the pathophysiological cross talk between these two proteins.

Abbreviations

RGCs	Retinal ganglion cells
BDNF	Brain derived neurotrophic factor
Shp2	SH2 domain-containing tyrosine phosphatase-2
ERG	Electroretinogram
STR	Scotopic threshold response
SD-OCT	Spectral domain optical coherence tomography
GCL	Ganglion cell layer
CNS	Central nervous system
LGN	Lateral geniculate nucleus
RNFL	Retinal nerve fiber layer
IPL	Inner plexiform layer
OPL	Outer plexiform layer
IS/OS	Inner / outer segments
ONL	Outer nuclear layer
INL	Inner nuclear layer
AMD	Age related macular degeneration
POAG	Primary open-angle glaucoma
IOP	Intraocular pressure
NTG	Normal tension glaucoma
NTs	Neurotrophins
NGF	Nerve growth factor
TrkB	Tropomysin-related kinase receptor B
CREB	cAMP response element-binding protein
PTP	Protein tyrosine phosphatase
Cav	Caveolin
BRB	Blood–retinal barrier
MAPK	Mitogen activated protein kinase
Erk	Extracellular signal-regulated kinase

Table of Contents

Chapter 1
Introduction

The retina arises as an extension of the brain during development and is a part of the central nervous system (CNS). It comprises of several types of modified neuronal populations specialised to detect and response to various intensities of light stimuli and process the signals. These signals are then transmitted to higher processing centres in the brain by retinal ganglion cells and their axons. Retinal ganglion cells (RGCs) are particularly susceptible to progressive death in neurodegenerative eye disease such as glaucoma. Over the past decade there has been further understanding of the pathways underlying RGC survival and apoptotic processes in the retina. Further advances in understanding of the biochemical pathways determining RGC function and their survival in healthy and glaucoma conditions will help develop novel therapeutic approaches.

Accumulating evidence points to the pivotal role of brain derived neurotrophin factor/ tropomysin-related kinase receptor B (BDNF/TrkB) signalling pathway in preserving the RGCs. In this study, I have examined the previously poorly defined mode of TrkB regulation by Shp2 phosphatase and caveolin proteins. The study involves modulating these two proteins to evaluate their effects on TrkB activation and consequent retinal functional and structural indices.

1.1 Retina

1.1.1. Structure and cell biology

The retina is a multi-layered neural portion of the eye, formed as an outpouching extension of the diencephalon and is thereby considered as a part of central nervous system (London et al. 2012). Being a highly organized structure, the adult retina in mice and humans shares a laminar prototypic structure lining back of the eye.

Generally, the retina contains three distinct neural layers separated by two plexiform layers. Photoreceptor cells, the rods and cones, are located in outer nuclear layer (ONL) and are responsible for dim and bright light vision respectively (Harada et al. 2007). The great biological importance of these cells is to capture the photons and initiate a signalling cascade from which the light is converted to electrical signals (Pickard & Sollars 2012). Cones constitute approximately 2-5% of whole photoreceptor population and are closely packed in the centre of the retina, the fovea centralis, which is responsible for sharp and brilliant coloured vision (Rattner et al. 1999).

The inner nuclear layer (INL), the second inner layer in the retina, is occupied by bipolar (by far the most prolific), amacrine and horizontal cells which process and transmit the photoreceptors output. Recent evidences suggest that along with amacrine cells, bipolar cells have been extensively conserved in mammals (Jeon et al. 1998, Rattner et al. 1999). The innermost layer comprises of retinal ganglion cells, the axons of which converge at the optic disc where they extend to the lateral geniculate nucleus (LGN), the first major vision centre located in the dorsal part of the thalamus (Figure 1.1). There are at least 10 to 15 types of RGCs with distinct functional and structural features in mammalian retinas (Sand et al. 2012). The visual phototransduction pathway is initiated by photon capturing through rod and cone photoreceptors, converted to electrical signals and transmitted to bipolar and amacrine cells. The cascade of neuronal signals eventually reaches RGCs and is conveyed *via* RGC axons to the visual centres of the brain for higher order processing, enabling us to identify surrounding objects (Basavarajappa et al. 2011, Gupta et al. 2010, London et al. 2012).

A B

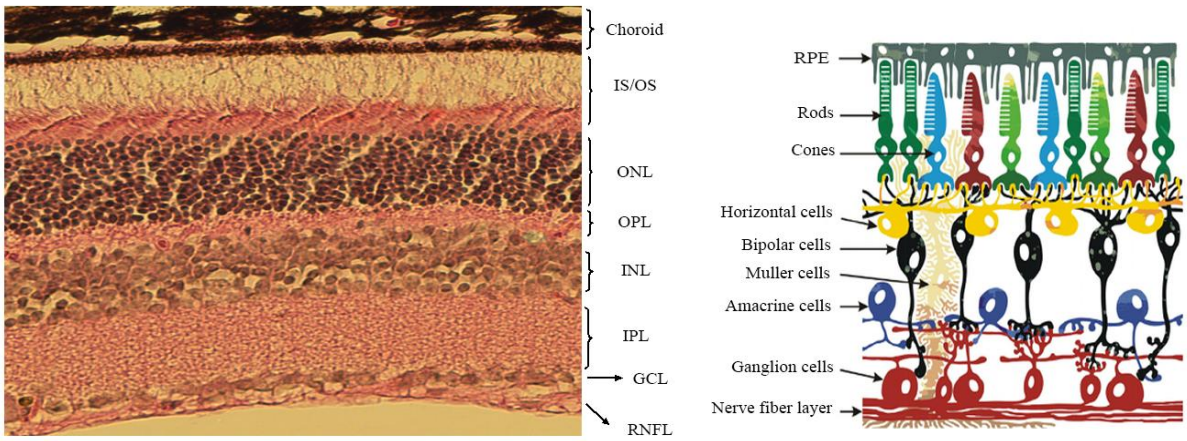

Figure 1.1: Histological (A) and corresponding schematic (B) (Slijkerman et al. 2015) representation of normal retinal structure. Cross-section of the retina indicating its laminated structure which involves RNFL, retinal nerve fiber layer; GCL, ganglion cell layer axons of which form the optic nerve; IPL, inner plexiform layer; INL, inner nuclear layer containing bipolar, horizontal and amacrine cells; OPL, outer plexiform layer; ONL, outer nuclear layer which contains the photoreceptor cells; IS/OS, inner and outer segments.

1.1.2. Retina displays similarities to the brain

There is much evidence to show that the retina displays characteristic properties of CNS neurons and shares several physiological, cellular and biochemical similarities with brain tissue. Several neurodegenerative conditions that impact the brain and impair neural function have distinct manifestations in the eye. Consequently, due to anatomical accessibility and the particular laminar organization, the eye can be considered as a convenient, non-invasive research system to study pathophysiological processes in the CNS (London et al. 2012). For instance, with the advancement of technology subtle changes in both human and animal retinas can be directly imaged and assessed *in vivo.* As such the retina is being increasingly used as a model to study not only local neurodegenerative disorders like glaucoma and age related macular degeneration (AMD) but also systemic brain disease such as Alzheimer's disease (AD), which together affect a significant proportion of the aging population (Gupta et al. 2016). As RGCs are particularly affected in glaucoma, I will be discussing this disorder in greater detail.

1.2 Glaucoma

Glaucoma is a common and multifactorial neurodegenerative retinal disorder characterised by optic neuropathy and retinal ganglion cell degeneration leading to irreversible vision defects and eventually blindness. Vision loss in glaucoma patients is primarily attributed to RGC death and associated axonal degeneration and as RGCs, being post-mitotic neurons have greatly limited regenerative capacity, strategies to protect these cells is of the utmost importance (Cheung et al. 2008, Weber & Harman 2005).

1.2.1 Clinical manifestations and prevalence

Based on iridocorneal angle changes, glaucoma can be clinically classified into two broad categories: angle-closure and primary open-angle glaucoma (POAG) with the latter being more prevalent in most populations (Lee & Higginbotham 2005). POAG is combined with slow progressive loss of visual sensitivity while the acute angle-closure is responsible for patients with serious vision loss and accounts for less than 10% of glaucoma cases with higher rates in Asian populations (Weinreb et al. 2014).

Common features of glaucoma include RGC degeneration, progressive thinning of the outer rim of optic nerve head and concurrent cupping of the optic nerve disc. The disease is often associated with increased intraocular pressure (IOP) and clinical management involves subsequent lowering of IOP which generally slows disease progression (Young H. Kwon, John H. Fingert 2009).

Only patients with acute glaucoma (usually angle closure glaucoma) have symptoms with sudden blurred vision, eye redness, pain, headache and nausea. The majority of glaucoma patients have a chronic form of glaucoma (POAG) where there is typically no warning sign and glaucoma progression can remain asymptomatic until the late stages, causing severe irreversible vision loss and tunnel vision. Hence it is also sometimes called the “silent thief of sight”. With deterioration in vision, the quality of life is reduced and associated morbidity includes; inability to perform daily activities such as driving, reading etc. leading to loss of individual independence (Lee & Higginbotham 2005, Weinreb et al. 2014).

Epidemiologic studies have shown glaucoma, the second leading cause of bilateral blindness, affects virtually more than 70 million people worldwide with approximately 2% of the population over the age of around 40. It is estimated that there will be around 80 million glaucoma patients by 2020 rendering more than 11.2 million people blind (Cheung et al. 2008, Quigley & Broman 2006, Weinreb et al. 2014).

1.2.2 Risk factors

Clinical evidence indicates that glaucoma is frequently associated with abnormally elevated IOP as the major risk factor; yet still not all patients have raised IOP. The normal IOP in human ranges from 10 to 21 mmHg, although 25% to 50 % of glaucoma patients have the IOP within the normal range (<21 mm Hg). These patients are referred to as normal tension glaucoma (NTG) (Lee & Higginbotham 2005, Quigley 1996, Weinreb et al. 2014).

Other strongly supported risk factors include advancing age, low diastolic perfusion pressure, myopia and relatively thin central cornea. Other systemic, risk factors such as diabetes mellitus, systemic hypertension and migraine are less consistent (Gupta et al. 2012b, Hewitt et al. 2006, Young H. Kwon, John H. Fingert 2009).

Apart from non-genetic components, the familial nature of POAG has also been well-established for decades (up to 5% with positive family history) suggesting that genetic defects similarly might associate with pathogenesis of glaucoma (Allingham et al. 2009). Genetic linkage studies have identified several genetic variations such as *MYOC*, *OPTN*, *WDR36* and *Cav1/Cav2* within different loci that might confer risk of glaucoma (Fan et al. 2006, Kumar et al. 2007, Rozsa et al. 2008, Wiggs et al. 2011). The *MYOC* gene encodes myocilin protein and intracellular accumulation of the mutant misfolded form fails to be adequately secreted from the cell and results in high IOP (Weinreb et al. 2014). Contrary to myocilin, *OPTN* is associated with an IOP-independent glaucoma phenotype and possibly increase the susceptibility of apoptosis in RGCs (Allingham et al. 2009). Genome-wide scans also resulted in discovery of *Cav1/Cav2* (caveolin-encoding genes) associations with POAG (Wiggs et al. 2011). *Cav1*, located on chromosome 7 in humans (7q31.1) and chromosome 6 in mice, comprise the main components of membrane lipid rafts caveolae, ubiquitously expressed in almost all mammalian cells including the retina and trabecular meshwork and plays pivotal role in signal transduction through interaction with various signalling proteins (Thorleifsson et al. 2010). Interestingly, these genes account for only about 10% of all glaucoma pathology (Weinreb et al. 2014). This indicates that a large number of relevant genetic polymorphisms linked with the disease pathology are yet to be identified. However, glaucoma is considered to be inherited as a complex trait in which interaction of both genes and environmental factors seem to influence the emergence (Allingham et al. 2009).

Glaucoma, particularly NTG, is also thought to have a strong vascular component, with reported changes in vascular regulation, retinal vascular pulsation, optic disc haemorrhages

and upregulation of hypoxia inducible factor in the retina (Golzan et al. 2014, Li et al. 2013, Sivak 2013) .

1.2.3 Clinical management

Currently, efficacious medical and surgical treatments are aimed exclusively at reducing IOP toward a target level at which the rate of glaucoma progression is decelerated sufficiently to avoid extra visual impairment. Clinical management commonly includes anti-glaucoma medications like prostaglandin analogues and if the disease progression continues, laser trabeculoplasty or incisional surgery is offered to achieve adequate intraocular pressure reduction to potentially slow down RGC and retinal nerve fiber layer (RFNL) loss (Rattner et al. 1999, Weinreb et al. 2014).

Unfortunately, despite effective IOP lowering, some patients still continue to progress and develop vision impairment and optic neuropathy. This paradigm indicates that an IOP-independent mechanisms may be involved in mediating the RGC degeneration in glaucoma disease (Gupta & Yücel 2007). Consequently, IOP is no longer regarded as the only target for glaucoma treatment and more effective strategies are required to protect RGCs.

In recent years, several new research strategies have been investigated in preclinical models to develop neuroprotective therapies for glaucoma to prevent, hinder or sometimes reverse RGCs death and prevent further optic nerve injury. If successful these may gradually find applications in the clinical management of the disease, along with current IOP lowering therapies (Cheung et al. 2008, Gupta & Yücel 2007).

For instance, in a pioneering study sphingosine-1-phosphate (S1P) analogue fingolimod (FTY720) is demonstrated to be functional as a neuroprotective agent to protect RGCs in experimental glaucoma (Gupta et al. 2012c, 2013a; You et al. 2014).

Nevertheless, currently no therapy is sufficiently developed for clinical applications to prevent glaucoma or completely halt its progression. The primary cause for this lack of treatment strategies is that we do not completely understand the molecular basis of the disease and how it affects the retinal structure and function (Lee & Higginbotham 2005, Zhou et al. 2005).

1.3 Mechanisms of cell injury in Glaucoma

Although RGC death and associated optic nerve dystrophy is major pathophysiological feature and leading cause of vision loss in glaucoma patients, the neurodegenerative

mechanism underlying glaucoma are poorly understood (Lebrun-Julien & Di Polo 2008). As mentioned previously, decreasing IOP helps but some patients continue to deteriorate despite responding well to IOP lowering medications (Leske et al. 2003). However, several signalling pathways involved in RGC loss have been identified over the last decades which may provide therapeutic targets for glaucoma that can effectively reach the clinic (Almasieh et al. 2012, Zhou et al. 2005). In this study, I have primarily focussed on exploiting the BDNF/TrkB signalling pathway and exploring the methods to analyse its effects on RGC survival.

1.3.1 Neurotrophic factors and their receptors

Neurotrophins (NTs) are a family of secreted proteins which are primarily expressed in neurons and regulate neural growth, survival and function by hindering the induction of cellular apoptotic pathways (Almasieh et al. 2012, Asai et al. 2007, Quigley 1999). The NT family consists of BDNF, nerve growth factor (NGF), neurotrophin-3 (NT-3) and neurotrophin-4/5 (NT-4/5). Amongst these, BDNF stands out in particular, as a powerful neurotrophin that plays a key role in maintaining the health of RGCs and protects them from apoptosis (Chen & Weber 2001, Cheng et al. 2002, Kido et al. 2000, Peinado-Ramon et al. 1996). Loss of neurotrophic support to the RGCs has widely been suggested to play a critical role in the apoptosis onset and resultant degeneration of RGCs. This may be due to disruption of axonal transport of the neurotrophins or sequestration of the secreted growth factors limiting their availability for the neurons. BDNF particularly has been shown to protect the optic nerve axonal loss in different models of optic nerve damage. The protective effects of BDNF were initially identified in 1986 by Johnson et al. when they rescued axotomized RGCs with BDNF treatment (Johnson et al. 1986, Lebrun-Julien & Di Polo 2008).

Neurotrophins activate two distinct classes of recetors: tropomysin-related kinases (Trk) receptor as well as p75 receptor ($p75^{NTR}$). Trk receptors generally mediate neural survival wheras $p75^{NTR}$ receptors are recruited in both survival and apoptotic events (Chao & Bothwell 2002).

BDNF is well expressed in superior collicolus, RGCs and inner nuclear cells and has been demonstrated to primarily exert its biological effects to the target cells through its high affinity receptor TrkB (Almasieh et al. 2012, Fu et al. 2009). TrkB is also well expressed in the developing as well as adults RGC dendrites and cell bodies (Pease et al. 2009). Trk receptors family hold various physiological roles in different tissues and have indispensable

role in signal transmission for neural development and survival. Other members of Trk receptors are TrkA and TrkC which mediate the trophic signal elicited by of NGF and NT-3 respectively (Gupta et al. 2013b).

1.3.2 BDNF/TrkB signalling

BDNF and its downstream signalling mediated through its high affinity receptor TrkB is critical in the development and preservation of vertebrate retina (Sánchez-Ramos et al. 2013). Consequent to BDNF binding, TrkB is activated by dimerization and autophosphorylation on its critical intracellular tyrosine residues (Bilderback et al. 1999). BDNF binding leads to activation of cellular survival signalling pathways such as mitogen activated protein kinase /extracellular signal-regulated kinase 1 and 2 (MAPK/Erk1/2) or phosphatidylinositol-3 kinase (PI3K/AKT) downstream signalling (Zhou et al. 2005). Both of these signalling networks promote cell growth, differentiation and survival by activating transcriptional factor cAMP response element-binding protein (CREB) which stimulates various pro-survival gene expression such as anti-apoptotic Bcl-2 protein. It was observed that inhibition of Erk1/2 upstream activator blocked the RGC survival whereas PI3K inhibition did not have discernible effect on neuroprotection and therefore the MAPK/Erk1/2 signalling pathway has been proposed to be the principal pathway in adult RGC survival in response to BDNF-TrkB stimulation (Cheng et al. 2002, Kaplan & Miller 2000, Walton & Dragunow 2000).

1.3.3 The SH2 domain-containing tyrosine phosphatase

Tyrosine kinase receptors like TrkB are susceptible to tandem phosphorylation and dephosphorylation and consequently need an appropriate regulatory control in order to efficiently perform their biological actions (Gupta et al. 2012b). In this regard, it has been recently reported that activation of Erk1/2 or PI3K pathways requires interaction of various proteins with TrkB (Almasieh et al. 2012, Walton & Dragunow 2000). One of the TrkB interactive proteins is SH2 domain-containing tyrosine phosphatase-2 (Shp2 also known as SH-PTP2, PTP1D, PTP2C) which is encoded by the *PTPN11* gene and has been identified as an essential intermediate in BDNF mediated MAPK pathway (Gupta et al. 2013b). Protein tyrosine phosphatase Shp2, is ubiquitously expressed in cytoplasm with a critical function in early development of vertebrate, cell proliferation, differentiation along with positive or negative regulatory role in Trk receptor signalling and neural fate in retina (Kontaridis et al. 2008, Neel et al. 2003). Shp2 consists of two Src homology-2 (SH2 and C-SH2) domains at

N-terminus, a single protein tyrosine phosphatase (PTP) region and a single phosphorylation site on C-terminal hydrophilic tail. SH2 motifs play a prominent role in response to hormones, growth factors or cytokines. However, PTP catalytic domain is located in close association with N-SH2, thereby inhibiting its phosphatase activity. Interaction between SH2 domain of the phosphatase and phosphotyrosine motifs of its binding partners can unlock the intrinsic catalytic activity of Shp2 (Dance et al. 2008).

Several studies in animal models demonstrated that Shp2 has a role in promoting growth factor-mediated Ras/MAPK pathway. The positive role of Shp2 is attributed to its scaffolding function to recruit mediators responsible for the negative regulation of MAPK activation such as SHPS-1 (Shp Substrate-1), Spry (Sprouty) or p120-RasGAP. For instance, loss of Shp2 resulted in retinal degeneration in Muller cells and its inhibition by glucocorticoids, repressed Erk signalling in neuronal cells (Cai et al. 2011, Dance et al. 2008, Kumamaru et al. 2011, Zhang et al. 2011).

However, there is also enough evidence to demonstrate the negative role of Shp2 in the same cascade (Gupta et al. 2012b, Peraldi et al. 1994, Reeves et al. 1995, Rusanescu et al. 2005). Shp2 participates in downstream signalling of TrkB receptor and negatively regulates TrkB by its phosphatase activity in RGCs (Gupta et al. 2012b, Rusanescu et al. 2005). Under normal *in vivo* physiological circumstances, TrkB and Shp2 have been shown to interact with each other however, these cellular interactions are suggested to increase further under various stress conditions promoting TrkB dephosphorylation.

Our group and others have identified that activation of Shp2 in RGCs is mediated through its interactions with the adapter protein caveolin (Cav). Shp2–caveolin interactions and consequent Shp2 activation is thus detrimental for TrkB receptor activity (Gupta et al. 2012b) (Figure 1.2).

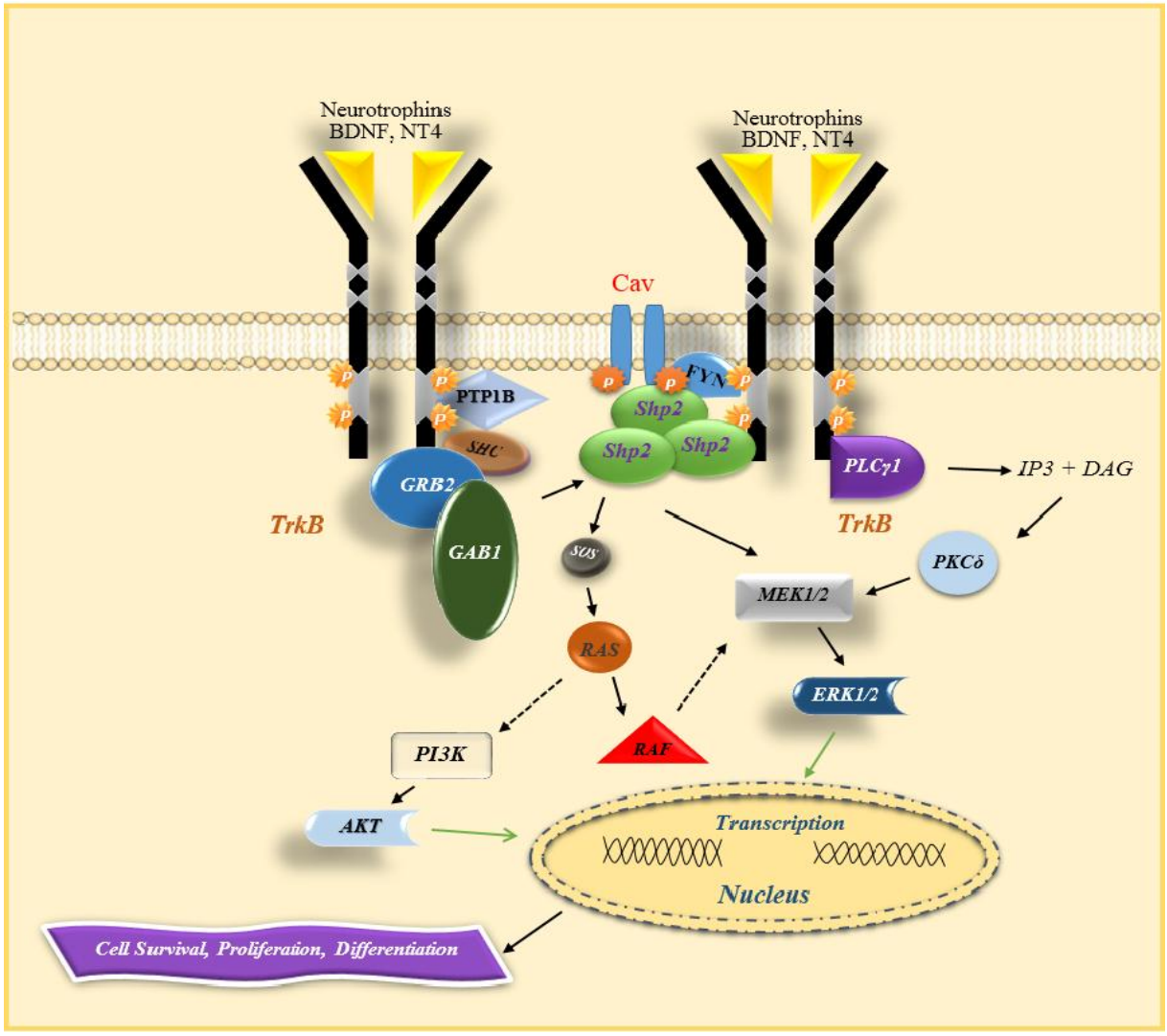

Figure 1.2: Schematic representation of major TrkB signalling-activated pathways. The interaction of Shp2 phosphatase with Cav-1 adaptor protein, TrkB receptor and various signalling molecules is depicted. Upon binding of neurotrophic factors to TrkB receptor, its activation occurs through dimerization and auto-phosphorylation of intracellular domain (Y515). TrkB activation leads to enhanced PI3K/Akt and MAPK/Erk1/2 signalling cascades in RGCs. Shp2-TrkB cross-talk *via* Cav-1 adaptor protein and its regulation on TrkB is shown. P, Phosphorylation; Cav, Caveolin; IP3, Inositol tri-phosphate; DAG, Diacylglycerol.

1.3.4 Strategies to regulate BDNF/TrkB signalling

Several theories that have been put forward to understand the mechanisms underlying RGC damage and neuronal apoptosis including excitotoxicity, oxidative stress, deprivation of neurotrophins (e.g. BDNF) and the related receptors and obstructed retrograde or anterograde transport of BDNF/TrkB proteins in RGCs' axons (Gupta et al. 2014, Martin et al. 2003, Wax & Tezel 2002). BDNF is considered as the most potent survival factor in the mammalian

visual system and the single intravitreal injection is demonstrated to rescue almost all RGCs for nearly one week (Mansour-Robaey et al. 1994). The role of BDNF was further investigated by repeated intraocular injection or by using osmotic mini-pumps, neither of which couldn't promote RGC protection for the longer term. Likewise, adenovirus mediated BDNF gene transfer to the superior colliculus or RGCs only addressed short-term outcomes only transiently delaying death of RGC which ultimately succumbed to the degenerative cascade. A possible explanation for the temporary neuroprotection effect is that RGCs become insensitive to the BDNF stimulating effect (Cheng et al. 2002, Lebrun-Julien & Di Polo 2008, Pernet & Di Polo 2006, Wax & Tezel 2002). Exogenous BDNF administration has also been associated with non-specific undesirable effects that limit the neuroprotective process. Moreover, the repeated BDNF injection has been stated to downregulate the expression of TrkB receptor (Frank et al. 1996, Klöcker et al. 2000, Zhou et al. 2005).

Additionally, optic nerve axotomy (experimental cutting or severing of the axons) and experimental glaucoma are both shown to induce a significant reduction in the expression of TrkB at both mRNA and protein levels in the RGC and thus limit the intrinsic capacity of these neurons to respond to exogenous neurotrophic factor stimulation (Fu et al. 2009). Accordingly experimental upregulation of TrkB and BDNF modulation resulted in increased RGC survival though the effects were transient (Cheng et al. 2002, Fu et al. 2009).

Several pharmacological compounds such as TrkB agonists and BDNF mimetic have also been investigated in modulation of TrkB signalling *in vivo*. For example our group has also evaluated the role of 7,8-Dihydroxyflavone (7,8 DHF) compound (a BDNF analog) that has been shown to prevent oxidative stress-mediated apoptosis in retinal neuronal precursor cell line by activating the TrkB downstream signalling (Gupta et al. 2013a).

1.3.5 Role of Caveolin in mediating Shp2-TrkB interactions

The evidence emerging from genome-wide association studies (GWAS) strongly links variations in the *Cav* gene locus as a risk factor in glaucoma pathogenesis (Wiggs et al. 2011). Cav is the prominent structural constituent of caveolae, with multiple isoforms including Cav-1, 2 and 3. Caveolae are special 50-100 nm ω-shaped invaginations of the plasma membrane functioning in vesicular trafficking events as well as providing a localized site for several signal transduction pathways. Cav-1 and Cav-2 are ubiquitously expressed in most human cells including endothelial cells, fibroblasts, majority of retinal layers such as outer plexiform layer (OPL) and photoreceptors, scleral spur cells as well as trabecular meshwork. However,

being mapped on chromosome 3, Cav-3 has distinct expression pattern which is mainly localised to muscle cell types (Kim et al. 2006, Razani & Lisanti 2001, Scherer et al. 1997).

Cav-1 is 21-24 kDa adapter protein that binds to a variety of proteins to modulate cellular signalling pathways (Jo et al. 2014). For instance, association between Cav-1 with G-proteins, Ras, protein kinase C, Src and tyrosine kinase receptor through protein-protein interactions has been revealed previously in several studies. Cav interactions with these proteins leads to alterations in signalling for example Cav negatively regulate p42/44 MAPK or inhibit protein kinase C isoforms (Berta et al. 2007, Bilderback et al. 1999, Lazo et al. 2002). Consistent with these functions, Cav-$1^{-/-}$ mice show hyperactivation of the p42/44 MAPK cascade in fibroblasts and cardiac tissue (Hnasko & Lisanti 2003). Cav-$1^{-/-}$ also exhibited an increase in Erk phosphorylation in hippocampus (Takayasu et al. 2010).

Additionally, under oxidative and hyperosmotic conditions, Cav-1 is shown to become hyperphosphorylated. Cav-1 hyperphosphorylation has been demonstrated in RGCs, astrocytes and fibroblasts while in cultured cell lines derived from trabecular meshwork of glaucoma patients, dexamethasone treatment decreased Cav phosphorylation, suggesting that Cav-1 phosphorylation in glaucoma is possibly restricted to RGCs (Bilderback et al. 1999, Rusanescu et al. 2005, Williams & Lisanti 2004).

Recent studies indicate that Shp2 phosphatase activity is enhanced through binding to Cav-1 adaptor protein resulting in negatively regulated TrkB/BDNF signalling. Cav-1 is likely to relieve Shp2 auto-inhibition by binding to Shp2 SH2 domain and release its latent phosphatase activity. This would result in prolonged dephosphorylation of TrkB leading to loss of axonal integrity and cellular survival through the BDNF mediated MAPK/Erk signalling cascade (Gupta et al. 2012b, Kim et al. 2006, Pawson et al. 2001). Shp2-Cav-1 interaction has been investigated in other studies as well. In astrocytes, complex formation between Shp2 and Cav-1 has been shown to hinder c-Src tyrosine kinase (CSK) function and positively regulate the Src signalling pathway in oxidative stressed condition suggesting different functions of Cav-1 in distinct cell types (Jo et al. 2014, Park et al. 2011). However, with a similar inhibitory effect, Cav-1 expression in PC12 cells was reported to interact with TrkA and decreased TrkA activation in these cells (Bilderback et al. 1999).

Other characteristics of transmembrane Cav-1 are retinal homeostasis as well as blood–retinal barrier (BRB) integrity. Caveolae numbers and Cav-1 expression significantly increased in retinal inflammatory disorders while Cav-1 ablation resulted in compromised BRB permeability. Additionally, expression of pro-inflammatory cytokines declined in Cav-1 deficiency elucidating its role in regulating inflammatory responses in the retina (Gu et al. 2014, Hauck et al. 2010, Klaassen et al. 2009, 2013).

1.4 Hypothesis and Aim

Studies from our group combined with a literature analysis indicate that enhanced Shp2 mediated dephosphorylation of TrkB receptors is dependent on Cav-1 adaptor protein. Consequently, I **hypothesise** that AAV mediated overexpression of Shp2 in the RGCs *in vivo* promotes dephosphorylation of TrkB receptor and impair endogenous BDNF signalling, reduce ganglion cell function and promotes inner retinal degeneration. I **hypothesise** that RGCs in Cav-$1^{-/-}$ mice will be protected against AAV mediated Shp2 over-expression compared to the wild type animals.

The main **aim** of this thesis is therefore to examine the effects of Shp2 overexpression on retinas of wild type (WT), heterozygous (Cav-$1^{+/-}$) and Cav-1 knockout (Cav-$1^{-/-}$) mice to evaluate and define the effects of Shp2-Cav-1 interactions *in vivo*.

Specific aims

- Determining the functional alterations in WT and Cav-1 deficient mice caused by Shp2 modulation. This will be achieved by *in vivo* measuring of the electroretinogram (ERG) and scotopic threshold response (STR).
- Determining the structural changes in WT and Cav-1 deficient mice caused by Shp2 modulation. This will be achieved by:
  1) Spectral domain optical coherence tomography (SD-OCT) for *in vivo* changes in retinal structure.
  2) Hematoxylin and Eosin (H and E) staining is applied for confirming *ex vivo* changes in retinal structure.

Chapter 2
Methods

2.1 Ethics

All the experimental procedures including animals in this study were performed in accordance with the Australian Code of Practice for the Care and Use of Animals for Scientific Purposes and the guidelines of the ARVO statement for the Use of Animals in Ophthalmic and Vision Research, and were approved by the Macquarie University Animal Ethics Committee (Ethics Approval No.: ARA 2014/058).

2.2 Methods

2.2.1 Animals

Experiments were conducted on Caveolin-1 knockout mice (on C57BL/6 background) bred and housed in Macquarie University central animal facility (CAF). Mice were genotyped at weaning using a fully automated genotyping system by Transnetyx (Cordova, TN). Mice genotypes were determined from ear cuttings using real time PCR with specific probes for neomycin and *Cav1* genes. Age-matched mice from different Cav-1 genotypes including Cav-1 null (KO), Cav-1 heterozygous (Het) and wildtype (WT) were used in this study. A total of 38 mice were used with n=12-14 in each experimental group. Animals were group housed in an air-conditioned room with constant temperature (21±2 °C) on a 12-h light /12-h dark cycle

(lights on at 6:00 AM). Mice were provided with *ad libitum* access of regular lab chow and water during the ensuing 24 hours and before the treatments.

2.2.2 Anaesthesia and Electrophysiology

Adult mice above 5 weeks of age were used in this study. Mice had varied range of body weight (approximately 10-27g) with the males being notably heavier than females.

Retinal function was measured using electroretinogram (ERG). The standard ERG response consists of an initial corneal negative deflection (a-wave) resulting from primary light response in photoreceptors and the large positive b-wave which reflects the activity of ON-bipolar and Muller cells (Rösch et al. 2014). Prior to the ERG recordings, all animals were dark adapted overnight for at least 12 hours and then anaesthesia was induced under dim red light *via* intraperitoneal injection (i.p.) of ketamine (50mg/ml, i.p., Ceva, Australia) and medetomidine (0.5 mg/ml, i.p., Pfizer, Australia) mixture (Li et al. 2013, You et al. 2012). All efforts were made to minimize the suffering and stress of animals caused by handling and restraining. After anaesthesia pupillary dilation was achieved by administration of 1.0% tropicamide followed by lubricant eye drops (Allergan, Inc) to maintain corneal moisturisation during the experiment. A thermostatically controlled heating pad was fixed to the ERG stage to maintain the animal's body temperature at 36-37°C during anaesthesia and recording sessions. The animal was placed on the heating pad so that the nose of the animal was extended almost 1cm beyond the exam table. A silver embedded thread recording electrode (3.0mm, Ocuscience) was positioned centrally across the corneal surface of each eye and a small contact lens was applied to maintain the connection between the cornea and the electrode to minimize the recording noise. Two stainless steel reference electrodes (Ocuscience) were placed subcutaneously in the forehead and an identical ground electrode was positioned subcutaneously near the base of the tail. A particular subtype of ERG recording termed the scotopic threshold response (STR) which reflects inner retinal function (Saszik et al. 2002) was recorded at full dark adaptation and performed at very dim light stimulation using flash intensities of -3.4 log cd·s/m^2 which were delivered 30 times at a stimulation rate of 0.5 Hz. A single bright flash electroretinogram (ERG) was then recorded according to the standardized protocol described by McCulloch et al (McCulloch et al. 2015) using a Ganzfeld ERG recording system (Ocuscience, Xenotec, Inc., MO, USA) with a flash intensity of 3 log cd·s/m^2 (Figure 2.1). After completion of the recording procedure atipamezole (5mg/ml, i.p., Zoetis, Australia) was administered to reverse the sedative effect of medetomidine and animals were allowed to recover from anaesthesia on a warming pad

which resulted in quick recovery after 2-3 minutes. Mice were returned to the CAF after they were able to walk normally in the cage and carefully monitored the next day. The ERG/STR recorded files were analysed using ERGVIEW (version 4.13). For all ERG recordings, the a-wave amplitude was measured from baseline (prior to the light stimulus) to the initial of the most negative voltage recorded and b-wave amplitude was measured from trough of the a-wave to the peak of positive b-wave. For STR analysis, the amplitudes of positive STR (pSTR) responses were obtained from flash intensities ranging from baseline to the peak of positive deflection which was observed at approximately 120 ms.

Electrophysiology recording was additionally acquired at the experimental end point. These experiments were performed over a time course of 2 months following all the treatments to evaluate the retinal function of retinal layers over time.

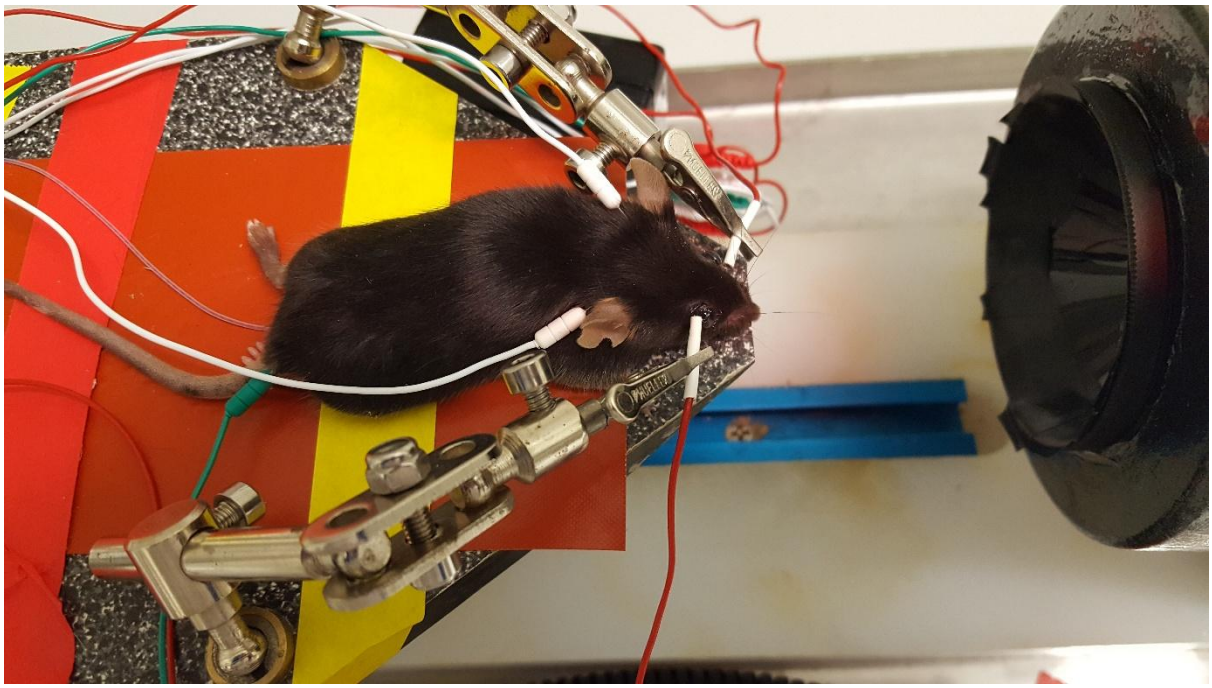

Figure 2.1: Full-field electroretinogram (ERG) and scotopic threshold response (STR) recording in mice. The mouse is positioned on heating pad and the reference (white) and ground (green) electrodes are subcutaneously connected to the forehead and tail respectively. The position of the mice was carefully adjusted ensuring a consistent position for the mouse eye to precisely align with the Ganzfeld bowl.

2.2.3 Spectral domain optical coherence tomography (SD-OCT)

Spectral domain optical coherence tomography (SD-OCT) is an advanced retinal imaging technique that provides cross-sectional images of the retina *in vivo*. SD-OCT imaging

technique provides non-invasive cross-sectional visualization of the eye and facilitate retinal thickness measurement which is valuable in evaluating retinal structure (Dysli et al. 2015, Kocaoglu et al. 2007, You et al. 2013). Mice were relocated from the central animal holding facility (CAHF) to the laboratory for the SD-OCT-assessment. Anaesthetic was administered intraperitoneally using the anaesthesia cocktail described previously. Pupils were sufficiently dilated by administration of 1% tropicamide (Mydriacyl, Alcon) eye drops. Two minutes after dilation, a corneal lubricant gel (3mg/g Gen Teal Hypromellose ophthalmic gel) was also applied on the surface of the cornea to maintain cornea moisture and clarity. To avoid further dehydration through the examination period the cornea was irrigated at frequent intervals with the same solution. The animal was then placed on the warming pad of the imaging platform. Spectral domain optical coherence tomography (SD-OCT) was accomplished in both eyes with the guidance of a bright-field live fundus image utilizing the image-guided SD-OCT system (Micron IV, Phoenix Research Laboratories) consistent with manufactures' instructions. The animal was properly positioned in front of the camera lens so that the eye was centered in the image frame (Figure 2.2). The lens was brought closer gently to come in contact with the cornea to reduce refractive power of corneal air interface and continued until the OCT image appeared. Illumination and focus was adjusted to optimize the details of the retinal features and images of the animals' optic nerve head and surroundings were obtained. Subsequently, the supplier's Insight software was employed to generate segmentation and measurement of different retinal layers including RGC + inner plexiform layer (GCL/IPL), INL as well as total retinal thickness. Retinal thickness was measured in 1025 positions of each layer by the software and averaged manually.

At the experimental end point SD-OCT measurements were performed to evaluate the retinal thickness variations over time.

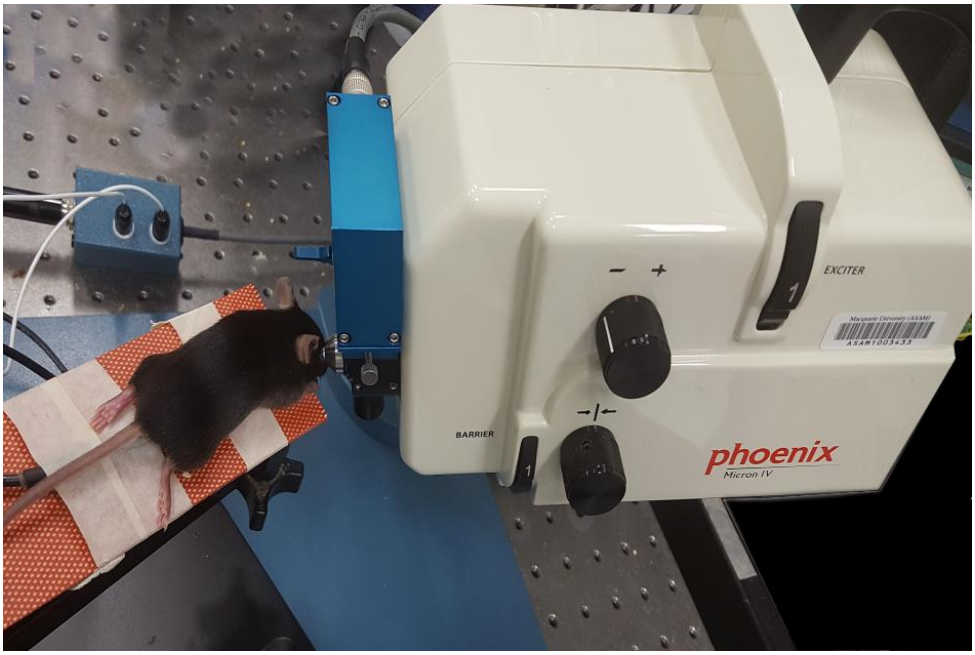

Figure 2.2: *In vivo* SD-OCT recording set up in mice. Mouse eye was prepared with tropicamide and corneal lubricant gel application and positioned on the heating pad attached to imaging platform. The mouse eye was directly in contact with the SD-OCT recording unit using specialized objective lens for mouse.

2.2.4 Shp2 overexpression

A. AAV Vectors-Design and packaging

The *in vivo* overexpression of Shp2 protein in the RGCs of all groups of mice was carried out using AAV virus gene therapy approach (Martin et al. 2002). Pre-validated AAV2 constructs carrying the *PTPN11* gene were obtained commercially (Vector Biolabs, PA, USA). The murine PTPN11 cDNA sequence was located under transcriptional control of the cytomegalovirus/chicken β-actin hybrid (CAG) promoter and inserted into commercially available AAV-Basic eGFP vector to produce ITR-AAV2-CAG2-EGFP-T2A-mSHP2-bGH-ITR poly(A)-ITR construct (briefly referred to AAV-PTPN11) (Figure 2.3). The co-packaging of GFP in the same cassette with PTPN11 was carried out to ensure the appropriate expression of Shp2 protein in retina. Enhanced green fluorescent protein (eGFP) control vector was also expressed under the control CAG promoter flanked by AAV terminal repeats (briefly referred to AAV-GFP). Both expression cassettes had the concentration of 1.8×10^{12} particles per millilitre and contained 7331 kb and 1.2 kb sequences respectively.

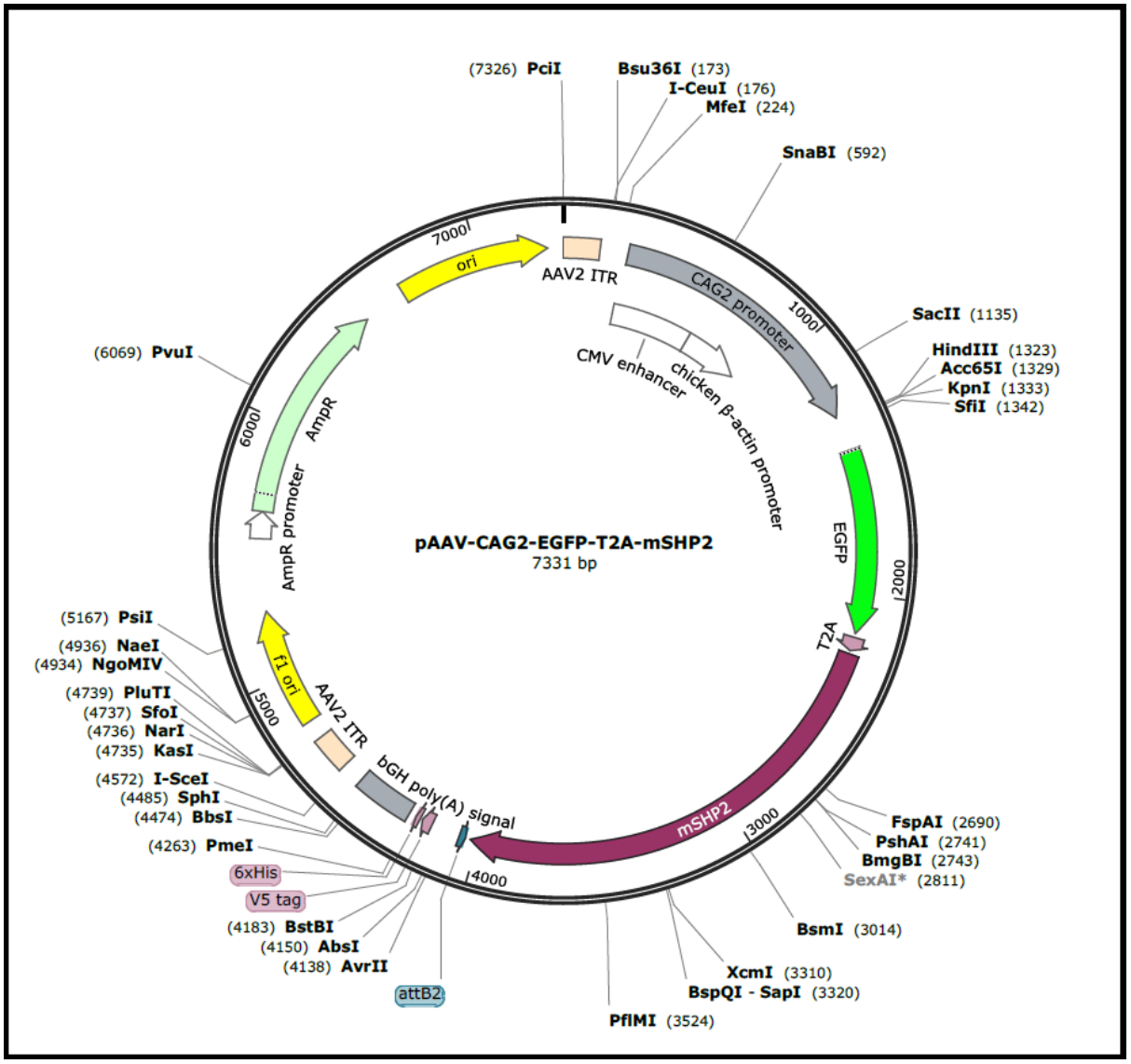

Figure 2.3: Map of the AAV-mShp2 (AAV-PTPN11) virus vector. Ori, origin of replication; CAG2 promoter, CMV i.e. enhancer, cytomegalovirus immediate early enhancer/chicken β-actin; EGFP, enhanced green fluorescent protein; mSHP2, mouse Shp2, bGH poly(A), bovine growth hormone polyA sequence; ITR, inverted terminal repeat.

B. AAV injections

Following retinal imaging, while the mice were still anaesthetized, the right eye was covered with one drop of Proxymetacaine hydrochloride 0.5% (Alcaine, Alcon) to relieve the injection pain. Using sterile procedures, a Hamilton syringe (Hamilton Co., Bonaduz, AG) with 33-gauge needle guided by a three-dimensional manipulator was used to deliver an intravitreal injection of either AAV-GFP or AAV-PTPN11 (1.8×10^{12} GC/ml) into the vitreous adjacent to the ora serrata but avoiding the lens (Figure 2.4). The procedure performed through a surgical microscope (Carl Zeiss Surgical GmbH, OPMI VARIO) to facilitate accurate focusing on

intravitreal injection. Non-injected eyes were also maintained as controls in addition to the GFP control-injected eyes. A period of 30 seconds was allowed before removing the needle to permit a suitable diffusion of the virus stock and prevent leakage from the injection track.

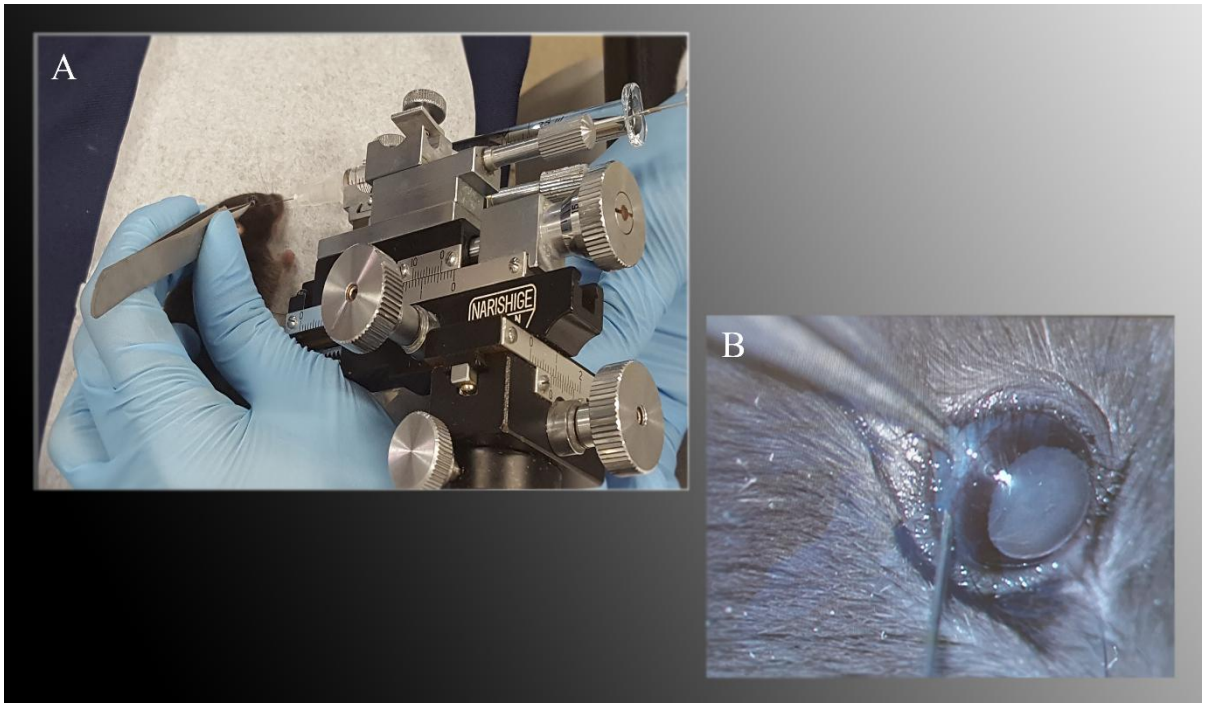

Figure 2.4: Intravitreal injection of AAV-PTPN11 and AAV-GFP into vitreous humour, the space between lens and the retina which is the efficient and safe gene delivery to the inner retina (the closest retinal layer to the lens). (A). Intravitreal injection using Hamilton syringe clamped to the syringe holder of a 3-axis manipulator with the mouse positioned on the heating pad. (B). the eye was carefully fixed in a place with the iris forceps and the needle inserted avoiding contact with lens. Injection was performed over a 30 second timeframe to prevent the leakage of the virus solution.

C. Animals' recovery and follow-up

Following the injection, 0.1% dexamethasone (Maxidex, Alcon) and 0.3% Tobramycin (3mg/ml, Tobrex, Alcon) eye drops along with 2% povidone-iodine were administered to prevent ocular inflammation and infection after the treatment. 5% carprofen was administered subcutaneously (50mg/ml Norbrook laboratories, Australia) as pain relief. The entire procedure of SD-OCT imaging procedure and virus injection took approximately 20 minutes and anaesthetic was reversed by atipamezole injection. Animals were allowed to recover in individual cages, returned to CAHF and carefully monitored for two consecutive days after the injection. The mice were tracked weekly thereafter over a 2-month period to allow for significant changes in gene expression.

2.2.5 Tissue preparation and histological retinal evaluations

A. Tissue fixation, embedding and sectioning:

At the completion of the experimental time points, animals were humanly euthanized under deep anaesthesia by an overdose of intraperitoneal injection of sodium pentobarbitone (100mg/kg Lethabarb, Virbac Pty, Australia). Eyes were harvested for morphometric and immunofluorescent studies and the marking dye (polysciences) was used to mark orientation of excised eyes. For morphometric analysis, the eyes were fixed for 2 hours with 4% paraformaldehyde (Sigma) and then immersed in 70% ethanol overnight at 4°C. Eyeballs were placed in embedding cassette and processed *via* automatic tissue processor (ASP200S, Leica). Eyes were subsequently embedded in molten paraffin wax. Using a rotator microtome (Microm, GmbH), 7 µm thick paraffin embedded sections involving the whole retina as well as the optic disc, were cut from the vertical meridian of each eye and mounted onto Superfrost Plus slides (Menzel-Glaser Lomb).

For immunofluorescent study (see below), eye globes were immersed in 4% paraformaldehyde fixative solution for 2 hours at room temperature, followed by 3 washings in PBS. Tissues were cryopreserved in 30% sucrose (in 1x PBS with 0.01% sodium azide) in 4°C until the tissue sank in the solution. Afterwards, the sample was embedded in OCT cryostat embedding medium (TissueTek) and the 10 µm thick cryosections were made using the cryostat (CM1950, Leica).

B. 2.2.5.2. Hematoxylin and eosin (H and E) staining

Paraffin-embedded retinal histological sections were used for H and E staining. Subsequent to the standard deparaffinization (histolene) and rehydration (a series of decreasing ethanol concentrations, 100%, 95%, 70%), retinal cross sections were stained with haematoxylin solution (Sigma) for 6 min, followed by 0.1% eosin (Sigma) solution for 15 seconds and finally mounted with ultramount (Fronine, Australia). Digitized images were obtained using a Zeiss axio Imager microscope (Zeiss) equipped with a Zeiss AxiocCam HRM digital camera system and analysed using ZEN imaging software. Retinal changes were evaluated in cross-

sections (superior and inferior to the optic nerve head) and data compiled in Excel spread sheets and transferred to the statistical program GrapPad Prism 6 for further analysis.
H and E images were also subjected to morphometric examination to measure the thicknesses of different retinal layers including GCL/IPL, INL as well as total retinal thickness superior and inferior of the ONH; 700µm from optic disc nerve head margin. The thicknesses values acquired from H and E staining were subsequently averaged for each retina and compared with the thickness averages obtained by SD-OCT assessments.

C. 2.2.5.3. Immunofluorescence assay

Immunofluorescence analyses were carried out on frozen retinal sections (Gupta et al. 2012a, Rajala et al. 2013). Briefly, retinal sections (10 µm thick) were made and blocked with 5% normal donkey serum in phosphate buffer saline (PBS, pH 8) supplemented with 0.3% Triton X-100 for 60 min. Next, samples were incubated with primary antibodies; Shp2 (1:100, Cell Signalling); GFP (1:100, Cell Signalling); TrkB (1:250, Abcam); pTrkB (1:250, phospho y515, Abcam); Cav-1 (1:100, Cell Signalling) at 4°C overnight, rinsed in PBS 3x 5 min followed by incubation with Alexa-Fluor 488 Donkey anti-rabbit IgG (1:250, Invitrogen,) and Alexa-Fluor 594 Donkey anti-goat IgG (1:250, Invitrogen,) (diluted in 1% Bovine Serum Albumin (BSA) PBS and 0.3 Triton X-100) for 1 hour. Thereafter, sections were washed in PBS 3x 5 min, mounted with Prolong Diamond Antifade Mountant DAPI (Life Technologies), cover-slipped and visualized by the Zeiss fluorescence microscope. Various photos were taken from randomly chosen fields of retinal sections which represented each protein expression (GFP, Shp2, TrkB and pTrkB) and mean fluorescent intensities were quantified by ImageJ software (version 1.50i) and compared with the controls.

2.2.6 Statistical analysis:

The ERG/STR responses, ganglion cell density in GCL, mean thickness of individual retinal layers in both histology and SD-OCT assessments were compared between the experimental and control groups. All data were analysed statistically and graphed using commercially available GraphPad Prism software (version 6.04) (GraphPad Software, CA). All values expressed as mean ± SD from given n sizes. Statistical analysis was performed by Student's t-test for unpaired data for comparisons between two variables. The level of statistical significance was set at $P<0.05$.

Chapter 3
Results

3.1 Cav-1 expression is uniformly distributed in the retina

Cav-1 expression in various retinal layers of WT, Cav-$1^{+/-}$ and Cav-$1^{-/-}$ mice was investigated using immunofluorescence staining followed by microscopic examination. As shown in figure 3.1 the Cav-1 was observed to evenly distribute within all layers of the retina in WT mice. These results corroborate previous reports of Cav-1 expression in neural and non-neural retinal parts including Muller glia, inner nuclear layer (INL), cytoplasm of cells in the ganglion cell layer (GCL), outer plexiform layer (OPL), along photoreceptor cells(Elliott et al. 2003, Li et al. 2012, Roesch et al. 2008). Cav-$1^{+/-}$ mice also demonstrated Cav-1 expression, however the immunoreactivity was absent in Cav-$1^{-/-}$ mice confirming the knockout status at the protein level. DAPI was used to identify various retinal regions (Figure 3.1).

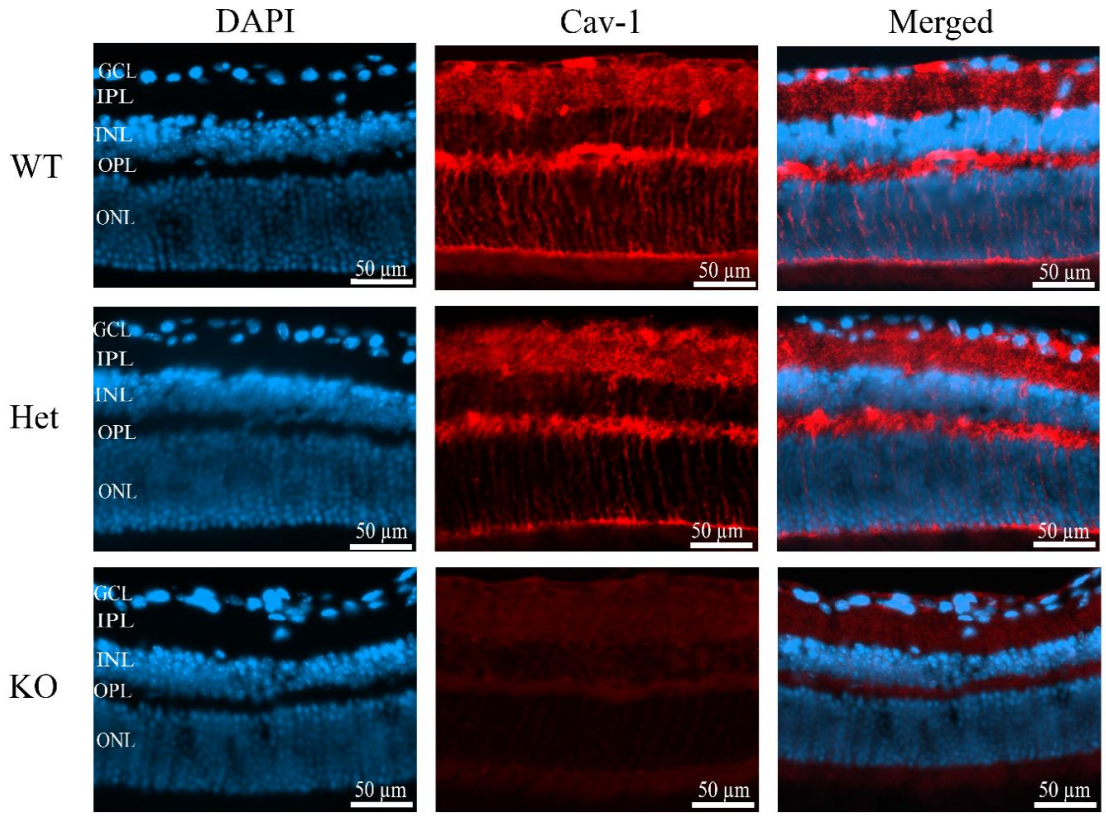

Figure 3.1: Immunofluorescence for Cav-1 and its localization in different retinal layers. Cav-1 was expressed throughout the whole retina in WT and Cav-$1^{+/-}$ mice (red, middle panels). However, the absence of Cav-1 immunoreactivity confirmed the knockout status at protein level. Cell nuclei are depicted with DAPI staining (left panel) to delineate the position of distinct retinal layers. GCL, ganglion cell layer; IPL, inner plexiform layer; INL, inner nuclear layer; OPL, outer plexiform layer; ONL, outer nuclear layer.

3.2 Retinal Ganglion cell targeting of AAV mediated PTPN11 upregulation

Mice were subjected to AAV-mediated PTPN11 and AAV-GFP overexpression at 5 weeks of age. All experimental groups were carefully monitored for 2 months and assessed for changes in Shp2 protein expression at the end point. For this purpose, following the euthanasia, mice eyes were enucleated and the cryosections prepared for immunofluorescence assay (IFA). Retinas were probed for changes in Shp2 expression in each of three genotypes viz. WT, Cav-$1^{+/-}$ and Cav-$1^{-/-}$ animal (Figure 3.2, 3.3 and 3.4 respectively). The relative *PTPN11* gene

expression was evaluated by densitometric measurements of the intensity of Shp2 immunostaining. Intensity was measured in AAV-PTPN11 injected eyes in each group and compared with AAV-GFP transduced control eyes and finally analyzed using ImageJ software (Figure 3.2). The results indicated that mice eyes injected with AAV-PTPN11 depicted a sustained high level of Shp2 expression (2.2-fold increase, mean: 60%), while the GFP transduced control eyes did not show enhanced immunostaining indicating that Shp2 protein expression was not affected. EGFP expression within Shp2 expression cassette was also used to trace the AAV delivery and Shp2 overexpression in the RGCs. Concomitantly staining with anti-GFP and anti-Shp2 antibodies showed the AAV expression and changes in protein expression was primarily localized to the GCL. The relative abundance of GFP-positive cells in retina was compared with the total number of DAPI stained cells in the GCL to approximate the percentage of cells targeted in the GCL. For this purpose, the DAPI-labeled cell in the GCL of each eye were checked for GFP immunoreactivity in 4 different areas of 350 µm dimension, counted and finally averaged in each separate group (Figure 3.2C, 3.3C and 3.4C). The results suggest that GFP expression in GFP controls and Shp2 overexpression groups reached 69% and 66% respectively which reflects a reasonably high efficiency of AAV2 mediated gene delivery to the GCL in mice retinas.

A

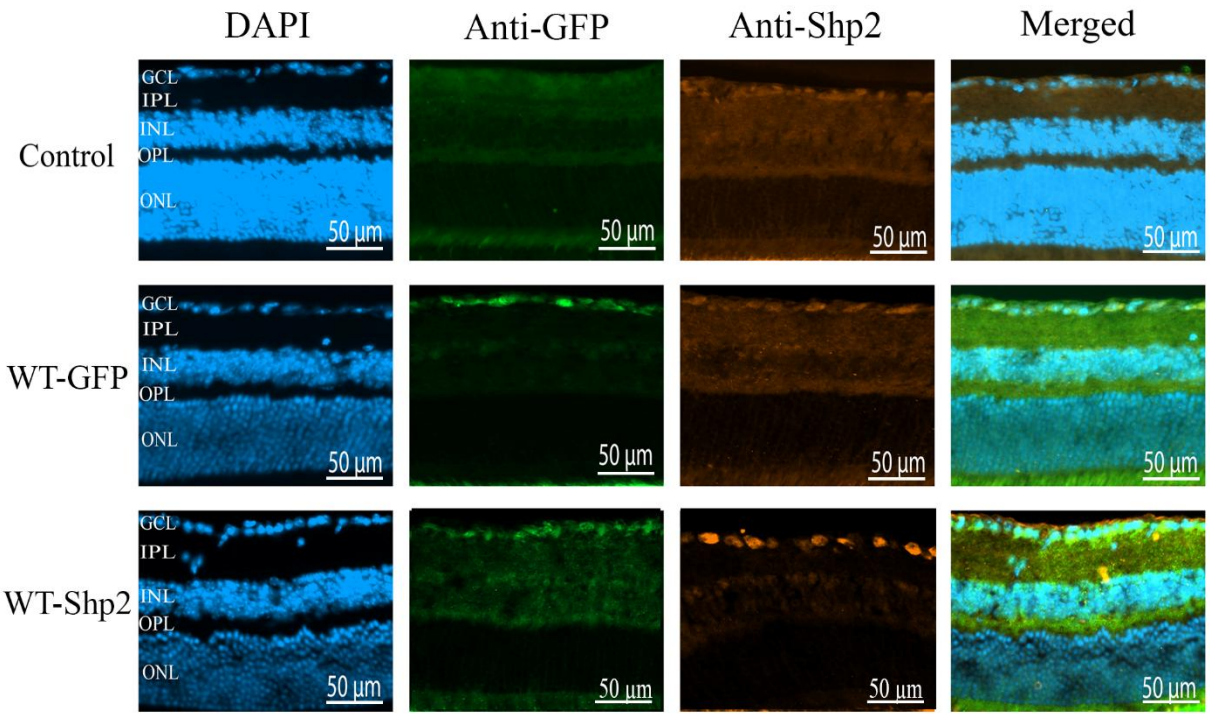

B

C

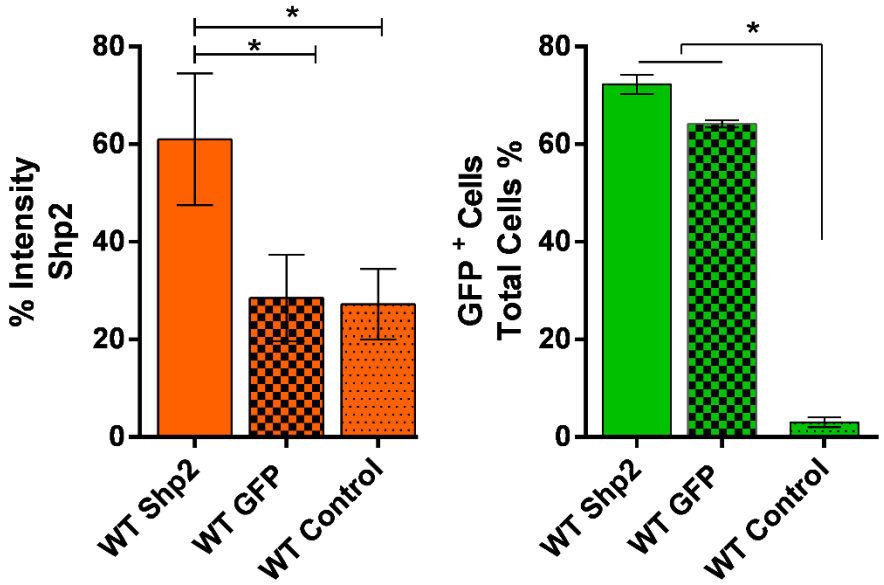

Figure 3.2: Immunostaining of the retinal sections in WT mice using anti-Shp2 and anti-GFP antibodies. (A) Overexpression of Shp2 protein (WT-Shp2) and GFP expression (WT-Shp2/WT-GFP) in GCL of WT mouse retina 2 months subsequent to intravitreal injection of AAV-PTPN11 and AAV-GFP vectors. Left panel shows DAPI staining to delineate different retinal layers. Second and third panels illustrate GFP expression and Shp2 expression respectively. (B) Comparison of the intensity of Shp2 expression. Two groups of control and WT-GFP showed normal expression of Shp2 (average of 25%) while WT-Shp2 group demonstrated statistically significant Shp2 upregulation of about 58%

compare to Shp2 normal expression (n=4 in each group, $p<0.05$). (C) GFP expression in WT-Shp2, WT-GFP and non-injected controls. Note that GFP gene was present in both AAV-GFP and AAV-PTPN11 vectors and GFP is well expressed in both experimental and GFP control groups while no GFP immunoreactivity is observed in non-injected controls. (n=4 in, average of expression was 63% and 73% in AAV-PTPN11 and AAV-GFP groups respectively).

A

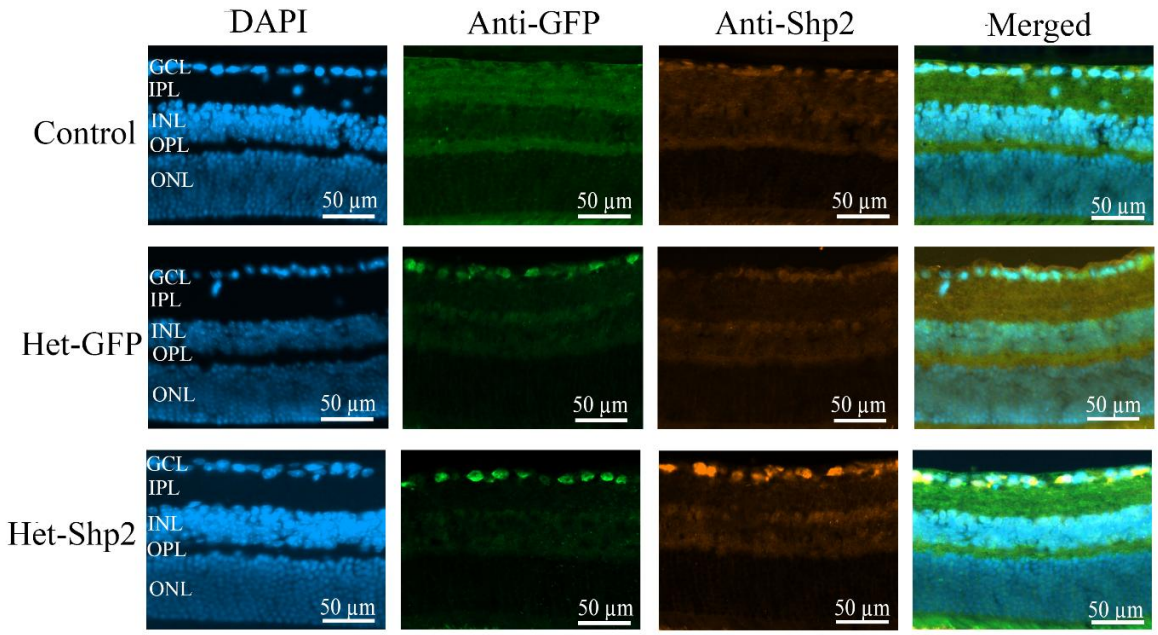

B

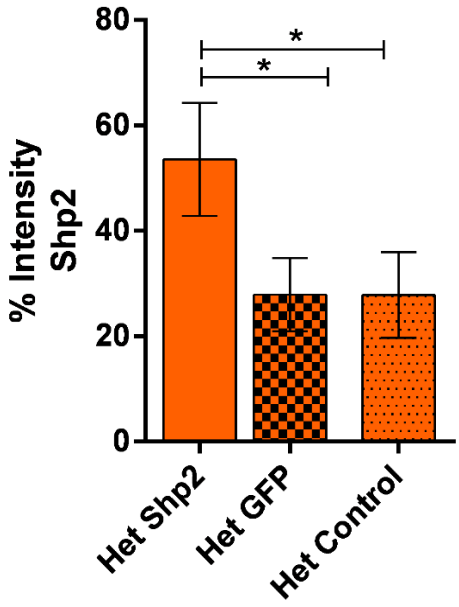

C

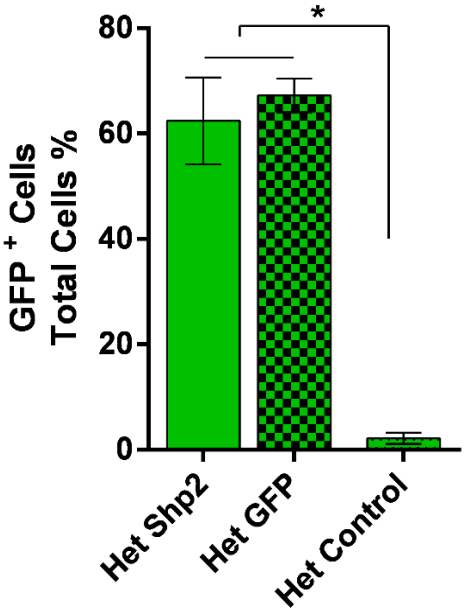

Figure 3.3: Immunostaining of the retinal sections in Het mice using anti-Shp2 and anti-GFP antibodies. (A, B and C) As noted in previous figure (3.2) Shp2 expression in AAV-PTPN11 injected group showed statistically significant expression in comparison to GFP and non-injected controls. ($n=4$, $p<0.05$) and GFP expression (Het-Shp2/Het-GFP) revealed an average 65% intensity in both groups.

A

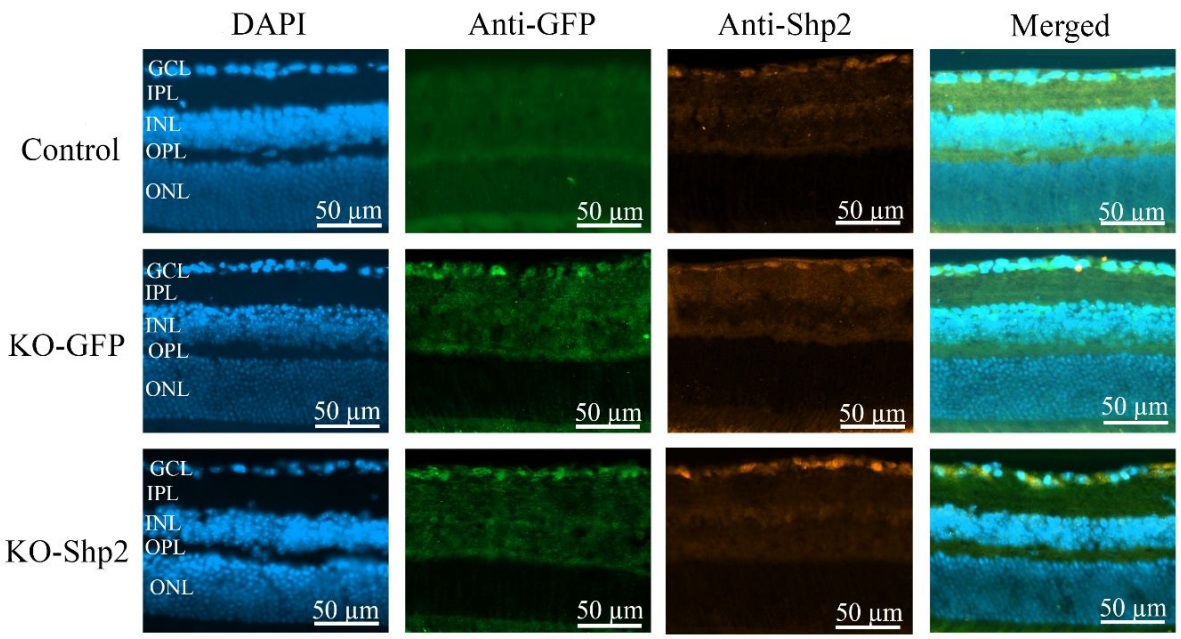

B

C

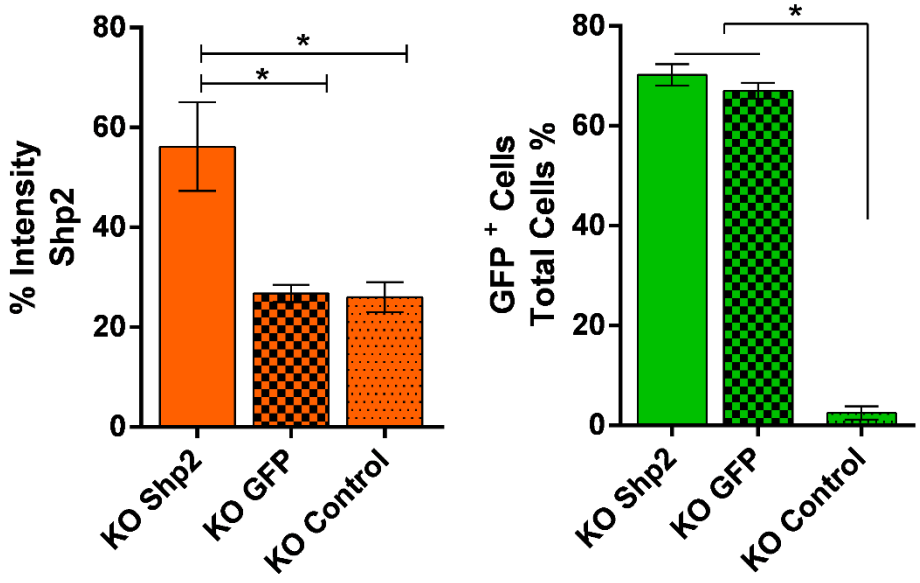

Figure 3.4: Similar to WT and Cav-$1^{+/-}$ mice, Immunostaining the retina in Cav-$1^{-/-}$ mice (A) confirmed the Shp2 overexpression (B) (n=4, $p<0.001$) and GFP expression (C) (average of 68.5%) in AAV-PTPN11 and AAV-GFP groups.

3.3 Inner retinal functional loss associated with Shp2 overexpression is mediated via Cav-1

Previous studies suggest that Shp2 interacts with Cav-1 which functions as an adapter protein. In order to understand the relevance of this interaction in the retina *in vivo*, Shp2 upregulated and control eyes in both WT and Cav-1 transgenic mice were assessed for potential electrophysiological changes. Electrophysiological responses were measured at the baseline and 2 months subsequent to Shp2 modulation. Figure 3.5 displays the average trace of pSTR recorded from the retina of Cav-1 mice 2 months following Shp2 upregulation. Analysis revealed that there was a notable decline in pSTR amplitude in AAV-PTPN11 injected WT animals compared to their AAV-GFP counterparts ($n=16$; $P<0.001$) (Figure 3.5A). Similarly, when compared with GFP-labelled animals, the Cav-$1^{+/-}$ group manifested statistically significant reduction in pSTR amplitude ($n=20$; $P<0.01$) (Figure 3.5B). The diminished STR is indicative of GCL functional loss that occurred in WT and Cav-$1^{+/-}$ mice under Shp2 upregulation conditions, which implies cellular effects of Shp2 are at least partially dependent on the Cav-1 protein in the retina.

The AAV-PTPN11 treated Cav-$1^{-/-}$ mice only demonstrated a slight decrease in pSTR amplitude compared to GFP-transduced controls that was statistically insignificant (Figure 3.5C). Collectively these results suggest that Cav-1 plays a critical role in the RGCs to mediate Shp2 actions and therefore pathological effects of Shp2 dysregulation could be partially prevented by Cav-1 ablation.

Non-injected eyes in all groups presented comparable RGC function with no significant differences to GFP-Injected eyes, indicating that GFP expression did not have any negative effects on ganglion cell function throughout the experimental period.

The pSTR amplitudes in AAV-Shp2 treated mice were also compared to their baseline responses recorded before any treatment was initiated. Results illustrated that with respect to their baseline, WT and Cav-$1^{+/-}$ mice experienced a respective 43% and 22% reduction in pSTR amplitude 2 months following Shp2 upregulation ($n=18$; $p<0.01$ and $n=20$; $p<0.05$ respectively) whereas the Cav-$1^{-/-}$ mice depicted about 11% decline in comparison with the baseline pSTR amplitude.

Quantitative evaluation of ERG revealed no statistically significant differences in the average of a-wave and b-wave 2 months after treatment, although all groups exhibited a slight decline in both waveforms in comparison with that observed in GFP-treated controls (Figure 3.6, 3.7 and 3.8). These results further suggest that Shp2 upregulation in the GCL preferentially affected inner retinal function.

A1

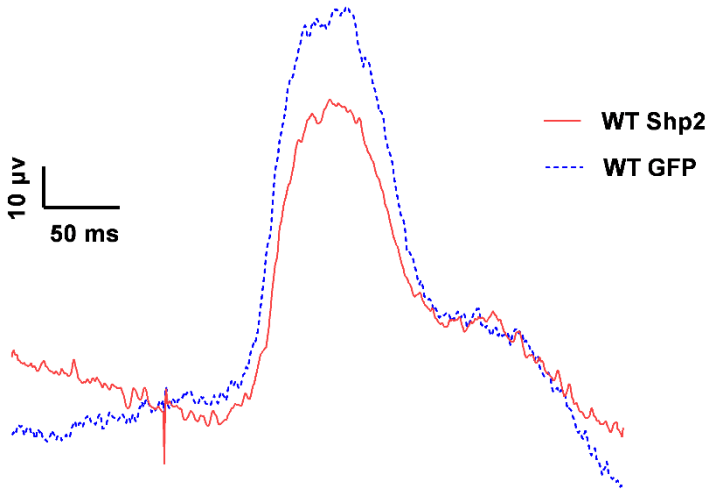
10 µv
50 ms
WT Shp2
WT GFP

A2

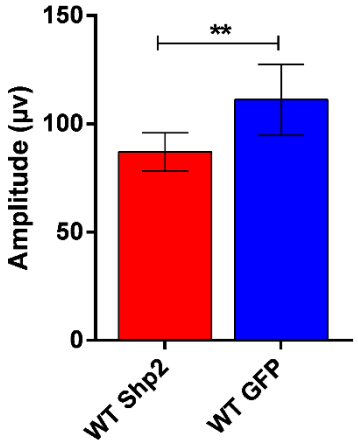
150
100
50
0
Amplitude (µv)
**
WT Shp2
WT GFP

B1

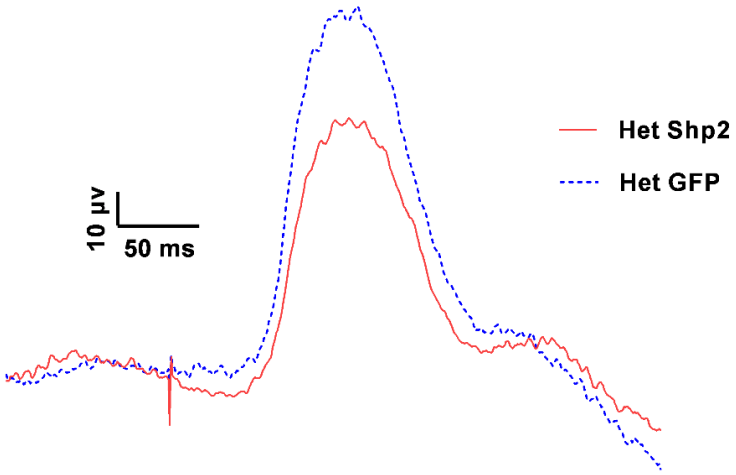
10 µv
50 ms
Het Shp2
Het GFP

B2

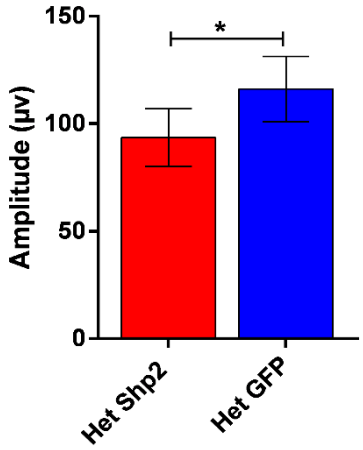
150
100
50
0
Amplitude (µv)
*
Het Shp2
Het GFP

C1 C2

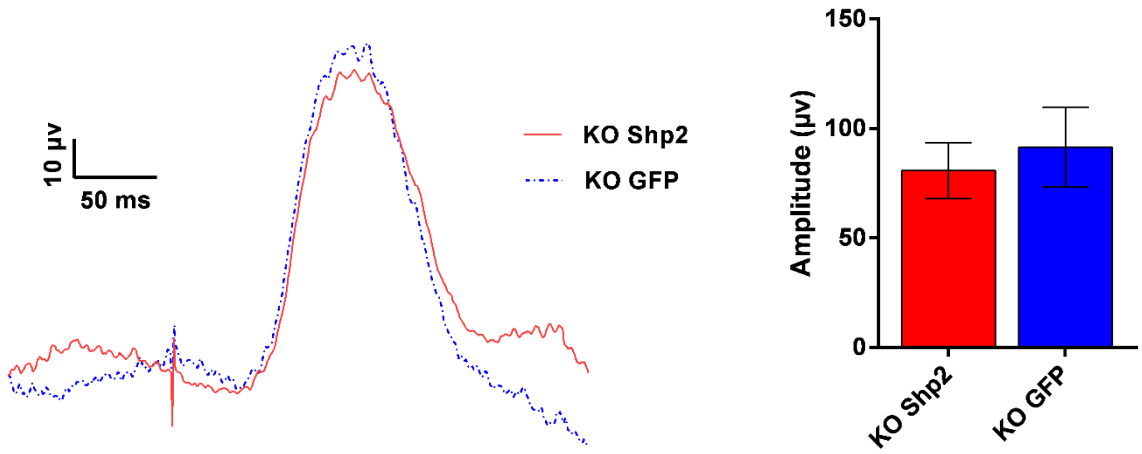

Figure 3.5: WT and Cav-$1^{+/-}$ are more susceptible to loss in pSTR amplitudes following Shp2 upregulation. (A1, B1) Average trace of pSTR signal from AAV-PTPN11 treated WT and Cav-$1^{+/-}$ mice (red) and their related AAV-GFP controls (dotted blue) 2 months following the treatment. (A2, B2) Quantification indicates that AAV-PTPN11 injected WT and Cav-$1^{+/-}$ mice have statistically significant lower pSTR amplitude in comparison with their relative AAV-GFP treated controls. (WT mice: n=16; P<0.001), (Cav-$1^{+/-}$ mice: n=20; P<0.01). (C1) Average pSTR responses of AAV-PTPN11 injected and AAV-GFP Cav-$1^{-/-}$ mice (red and blue respectively). (C2) quantification reveals a non-significant slight decline indicating that genetic ablation of Cav-1 partially protects the RGCs against loss of function caused by Shp2 upregulation. (n=16)

A

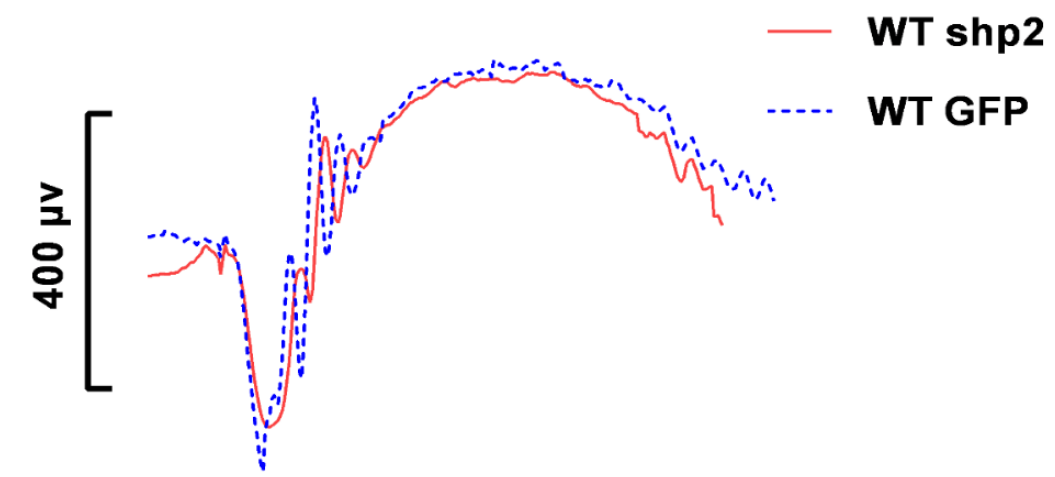

B

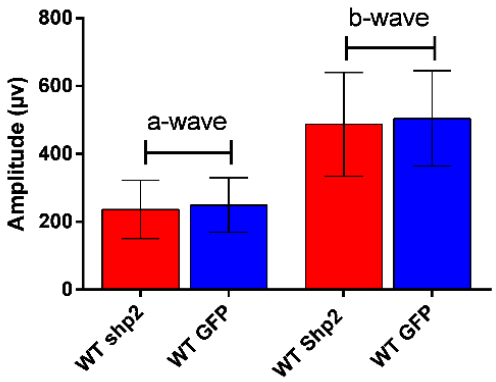

Figure 3.6: Changes in scotopic whole retinal ERG response in WT groups subsequent to AAV-PTPN11 treatment. (A) The average ERG traces in AAV-PTPN11 injected WT (red) and their AAV-GFP treated counterparts (dotted blue). (B) Graphical representation of a-wave and b-wave amplitudes which revealed no alteration to any significant extent (n=16).

A

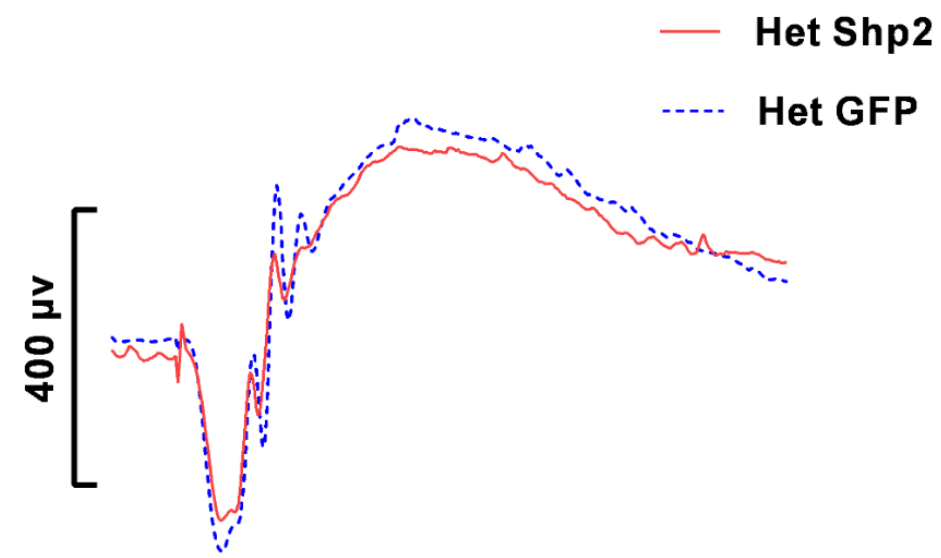

B

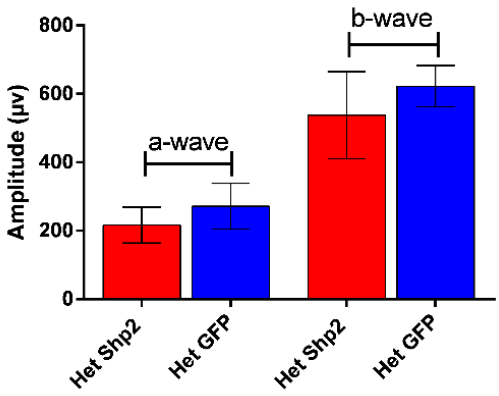

Figure 3.7: ERG response in AAV-PTPN11 injected Cav-$1^{+/-}$ group. (A) The average ERG components in experimental (red) and AAV-GFP control group (dotted blue). (B) Quantification of a-wave and b-wave showed no statistically significant in Cav-1 Het group compared to their related controls (n=20).

A

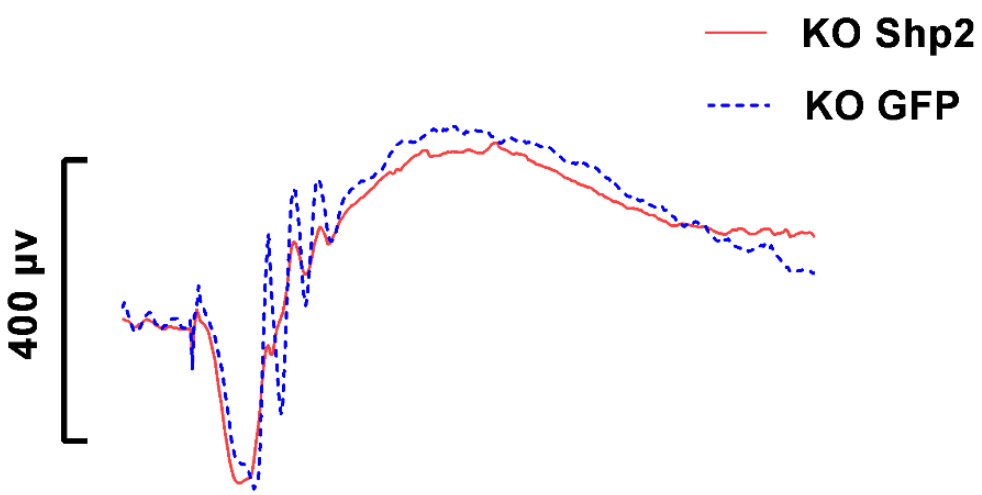

B

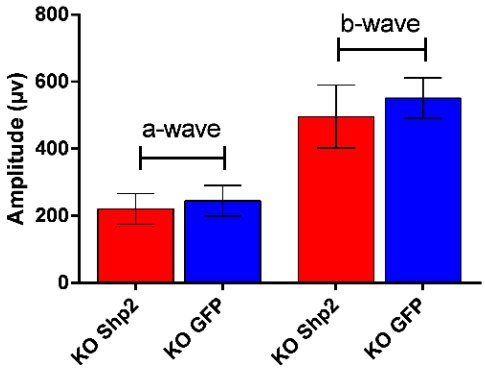

Figure 3.8: ERG responses in Cav-1 KO group. (A) Similar to WT and Het groups Cav-1 KO mice did not show any statistically significant alteration in a-wave and b-wave when compared to the GFP treated controls. (B) Graphical representation of a-wave and b-wave amplitudes (n=16).

3.4 Cav-1 is required for the inner retinal functional homeostasis

Previous studies have shown the important role played by Cav-1 in the retinal function, with Cav-1 mice demonstrating reduced whole retinal electrophysiological responses. In order to determine effects of loss of Cav-1 on the inner retinal function, the mice retinas were

specifically examined using pSTR recordings at the baseline and at the final time point. Electrophysiological analysis illustrated that Cav-$1^{-/-}$ mice had a statistically significant lower pSTR amplitudes when compared with the age-matched WT counterparts ($n=23$, $P<0.01$) (Figure 3.9). These findings suggest that Cav-1 although important for the whole retinal function, plays an even more important role in the inner retina. Evaluation of full-field ERG measurements also revealed that amplitudes of ERG components (a-wave and b-wave) in Cav-1 null mice were smaller than WT mice (Figure 3.10) and these results support the previous observations. These negative effects of Cav-1 loss were speculated to arise from ion transport in the retinal pigment epithelium (RPE) and Muller glial cells, resulting in photoreceptor dysfunction (Li et al. 2012). Cav-1 ablation may also affect the caveolae formation thereby disturbing the cellular micro-environment and increase the susceptibility of RGCs to negative effects of Shp2 upregulation.

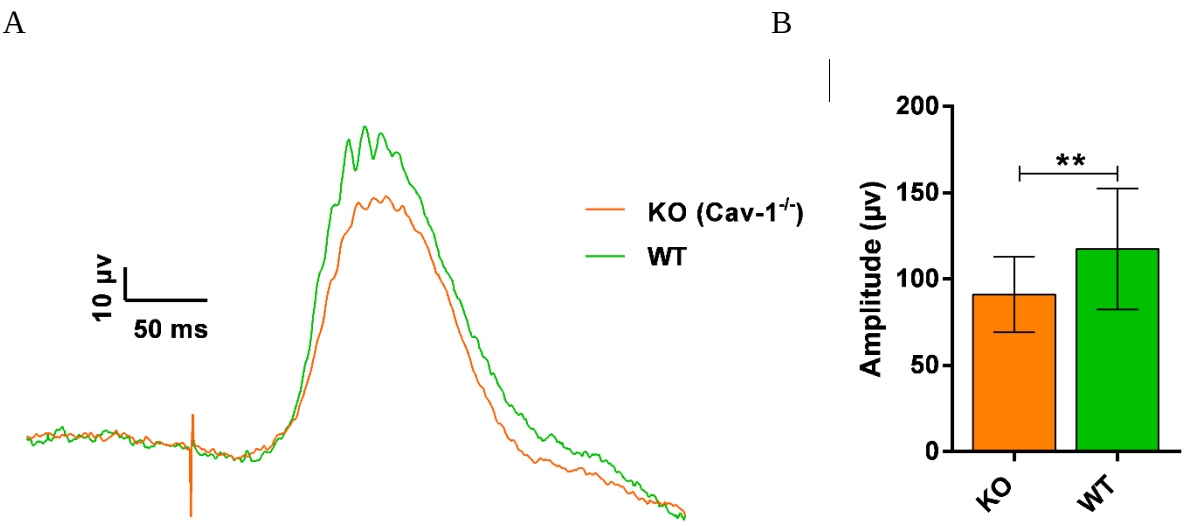

Figure 3.9: Reduced RGC function in Cav-$1^{-/-}$ mice. (A1) Traces of pSTR of KO (orange) and WT (green) mice measured before any treatment was initiated. KO mice shows a lower pSTR amplitudes when compared to the age-matched WT. (B) Quantification highlighting a statistically significant lower pSTR amplitudes in Cav-1 KO mice compared to their WT counterparts (n=23, P<0.01).

A

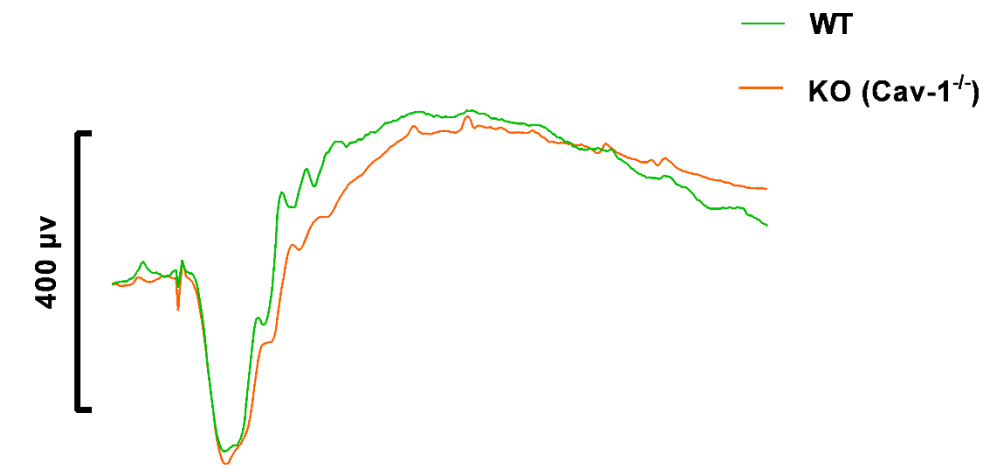

B

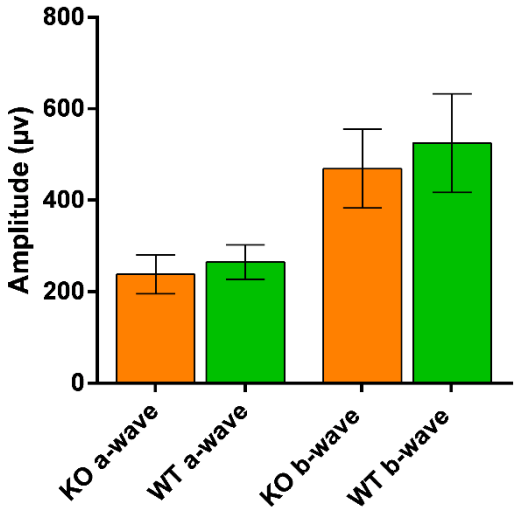

Figure 3.10: Whole retinal scotopic ERG recordings in Cav-1$^{-/-}$ mice and the WT mice (A) Average ERG traces of Cav-1 KO and their WT counterparts highlights albeit non-significant showed decreased a-wave and b-wave amplitude. (B) Quantification of a-wave and b-wave amplitudes (n=23).

3.5 Shp2 induced TrkB dephosphorylation is partially rescued in Cav-1 ablated retinas

In order to explore the role of Cav-1 in regulating Shp2-mediated TrkB dephosphorylation, we investigated the phosphorylation status of TrkB as depicted by anti-phospho-TrkB (pTrkB Y515) staining of retinal sections and the subsequent fluorescent imaging. Intensity-based

analysis revealed a sharp decline in pTrkB immunoreactivity in WT as well as Cav-$1^{+/-}$ animals 2 months post AAV-PTPN11 injection compared to GFP-injected control eyes which showed robust TrkB tyrosine phosphorylation (n=4 in each group, $p<0.05$) (Figure 3.11 and 3.12). Quantification showed that TrkB phosphorylation in these groups were approximately 65% of the original intensity in GFP-treated controls suggesting a Cav-1 dependent enhanced Shp2-TrkB cross-talk and resultant loss of TrkB phosphorylation. However, pTrkB immunoreactivity revealed no statistically significant changes in Cav-$1^{-/-}$ mice compare to GFP treated controls (Figure 3.13). AAV-GFP injected eyes and non-injected control eyes demonstrated no noticeable alterations in phosphorylated TrkB levels.

However, there was no obvious alteration in expression levels of total TrkB protein in response to Shp2 overexpression as TrkB intensity was consistent in almost all groups at the experimental end point. These data highlight that Shp-2 overexpression did not directly affect TrkB expression in either WT or Cav-1 transgenic mice suggesting *bonafide* changes in the TrkB activity caused by posttranslational modification (Figure 3.14).

A

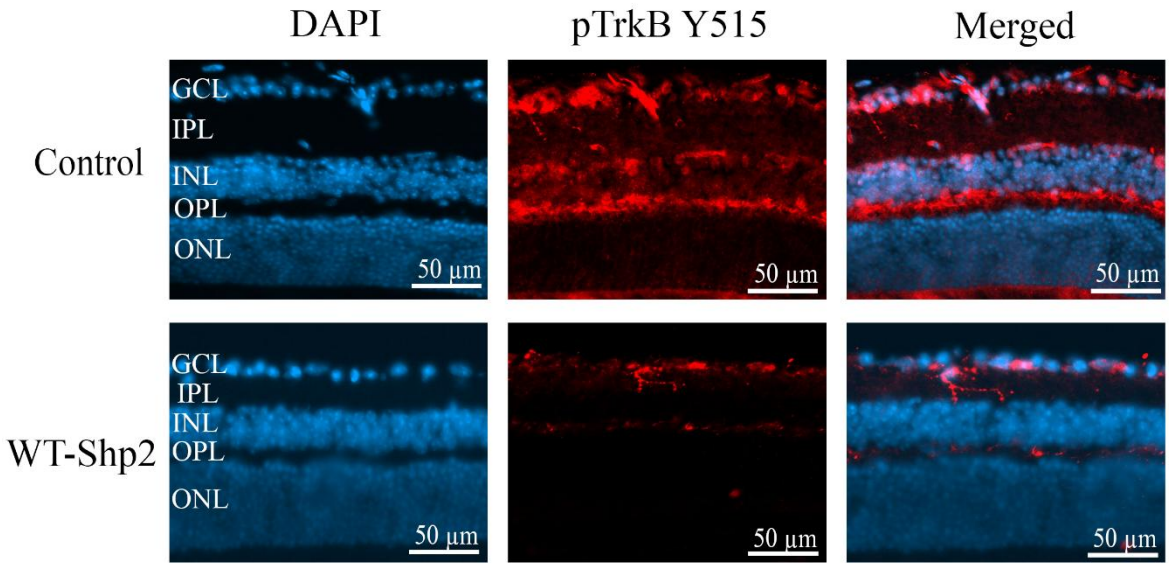

B

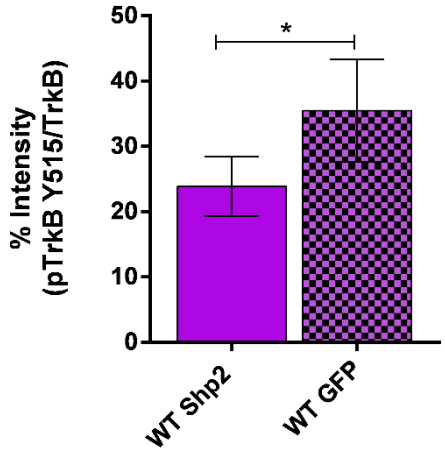

Figure 3.11: Immunofluorescent staining of WT mice retinal sections using anti-phospho-TrkB (pTrkB Y515) antibody. (A) Left panels shows the DAPI staining labelled retinal cells nuclei (blue) and the middle panel presents pTrkB immunostaining (red) in AAV-PTPN11 injected WT compared to their relative GFP injected controls. (B) Quantification of pTrkB intensity using imageJ software. The intensity of phosphorylated TrkB was significantly declined in AAV-PTPN11 treated WT mice when compared to their related AAV-GFP injected controls. Data are mean±SD. (n=4, $p<0.05$)

A

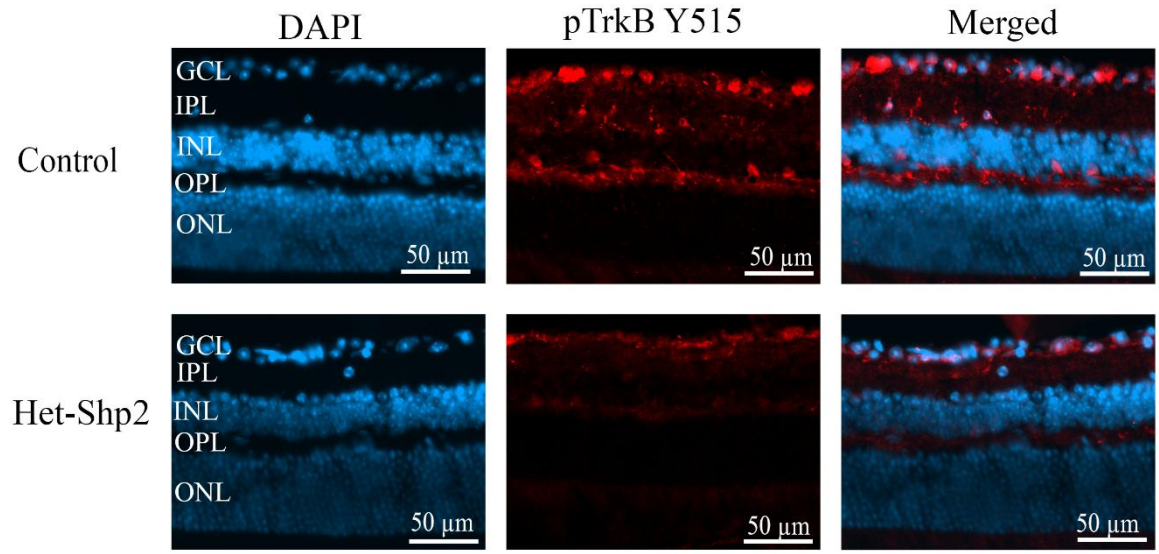

B

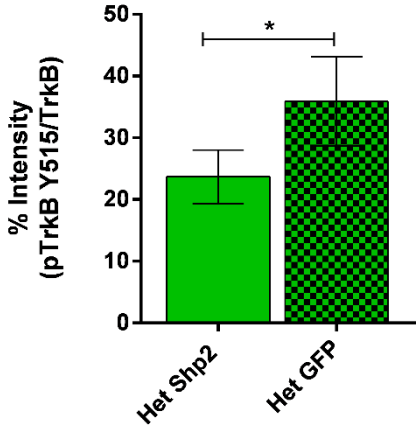

Figure 3.12: Phosphorylated TrkB immunoreactivity in Cav-1 Het mice 2 months following Shp2 upregulation. (A) Similar to WT mice Cav-$1^{+/-}$ mice revealed decreased pTrkB immunostaining (red) in Het-Shp2 groups compare to Het-GFP mice. (B) The intensity of phosphorylated TrkB was significantly declined in AAV-PTPN11 treated Cav-$1^{+/-}$ mice when compared to their related AAV-GFP injected controls. Data are mean±SD. (n=4, $p<0.05$)

A

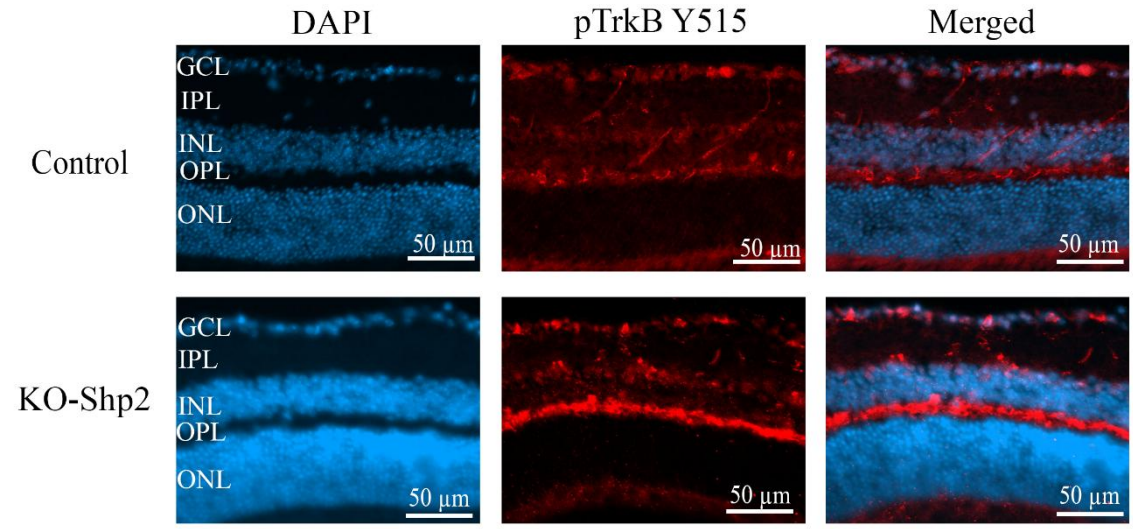

B

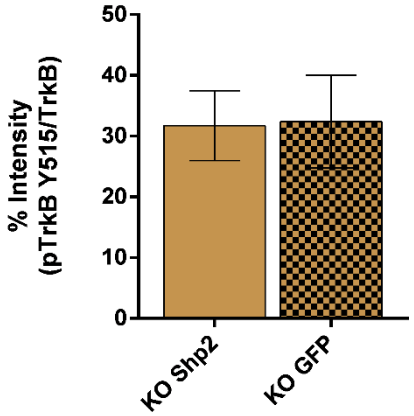

Figure 3.13: Immunofluorescent staining of mouse retinal sections using anti-phospho-TrkB (pTrkB Y515) antibody. Shp2-induced TrkB dephosphorylation was partially rescued in AAV-PTPN11 treated Cav-1 KO mice. (A) Comparison of phosphorylated TrkB immunoreactivity in AAV-PTPN11 injected Cav-1 KO mice and their relative GFP treated controls. (B) Quantification elucidated no significant differences in pTrkB intensity in abovementioned group. (n=4 in each group)

A

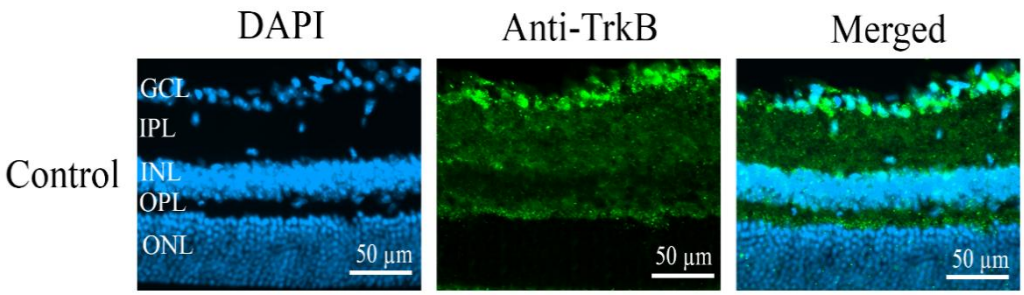

B

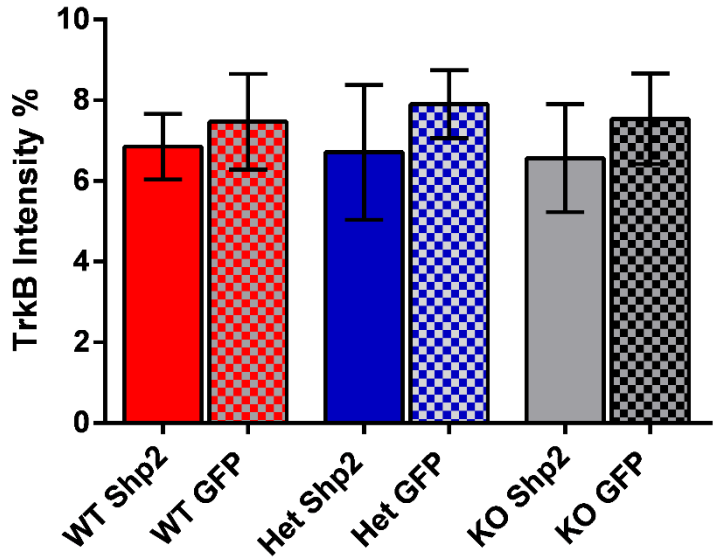

Figure 3.14: Immunostaining analysis of TrkB. (A) TrkB immunoreactivity in GCL was consistent in both AAV-PTPN11 and AAV-GFP treated groups. The image shown here presents TrkB expression in GCL of control groups which was comparable with TrkB expression in other experimental groups. (B) Quantification of TrkB expression using ImageJ software revealed no significant changes in intensity of TrkB expression among the experimental and control mice groups.

3.6 Retinal structural analysis

3.6.1 Interpretation of *in vivo* SD-OCT image data

The *in vivo* Spectral domain optical coherence tomography (SD-OCT) was carried out with the simultaneous capture of fundus photography and assessed at two different time points, prior to and after Shp2 overexpression. Optical parameters were adjusted to allow high resolution imaging of the optic nerve head (ONH) and distinct identification of various retinal layers. Figure 3.15 illustrates a typical SD-OCT imaging scan obtained from a representative healthy murine retina (control C57Bl/6) along with corresponding fundus photograph (Figure 3.15A). The circular OCT scan (Figure 3.15) was undertaken at defined distance of approximately 0.3mm from the edge of the optic disc as indicated.

The retinal thickness including GCL/IPL, INL and total retinal thickness (TRT) quantified by Insight software revealed no significant alterations in retinal thickness between AAV-PTPN11 injected mice and the related GFP-treated groups. All mice, displayed normal retinal structure and similar retinal thickness compared to their original measurement at 4 weeks of age. Briefly, by measuring segmentation results, the mean thickness of the GCL/IPL, INL and TRT measured 58.53 ± 3.7, 29.79±2.7 and 206.7 ± 12.9 respectively (Figure 3.16). No abnormalities were detected in the fundus indicating that retinal injections were not associated with retinal injury, vessel rupture or significant inflammation.

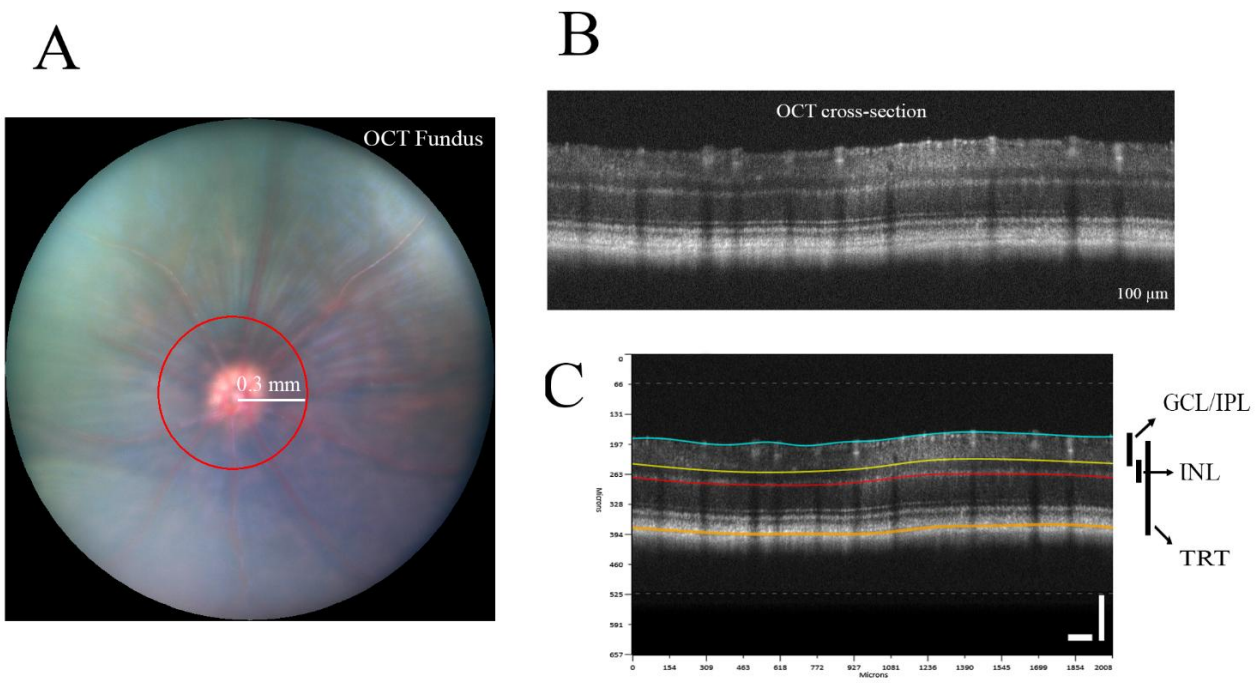

Figure 3.15: SD-OCT recording in mice. (A) Fundus image of a representative WT C57BL/6 mouse recorded concomitantly with the SD-OCT scan. (B) The SD-OCT was acquired on circular scan which was shown on fundus image with the distance of about 0.3 around the optic nerve head. (C) Manual retinal layer segmentation in SD-OCT of WT C57BL/6 mouse. Three distinct layers of GCL/IPL, INL and TRT were recognized, segmented and quantified using Insight software. The averaged thickness of each group were used for comparison between experimental and control groups. GCL, ganglion cell layer; IPL, inner plexiform layer; INL, inner nuclear layer; TRT, total retinal thickness

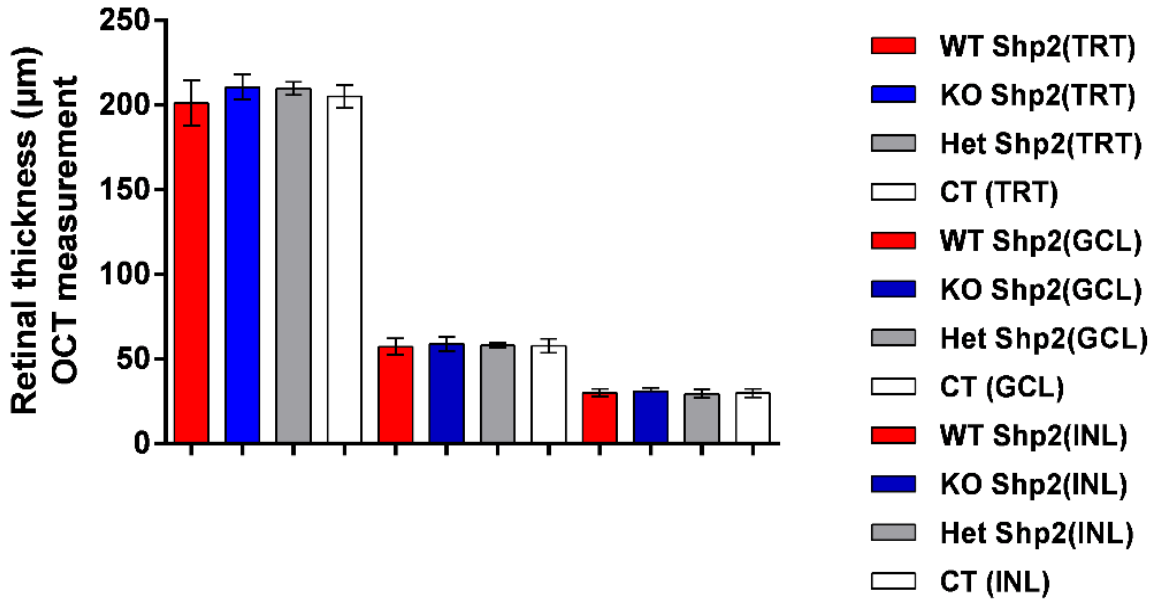

Figure 3.16: Quantification of retinal layer thickness using Insight software (Phoenix). No significant differences were shown in retinal thickness among AAV-PTPN11 injected experimental groups and AAV-GFP treated controls. (n=10 in WT and Cav-$1^{+/-}$ group and n=12 in Cav-$1^{-/-}$ mice). The control group (white) shows the average of all AAV-GFP groups since there was not any significant differences among the controls of each individual group.

3.6.2 Cav-1 partially protects the retina against Shp2 induced GCL loss

Mice eye sections embedded in paraffin were stained with haematoxylin and eosin (H and E) and thickness of various retinal layers analysed using light microscopy. Using ZEN software cells in the GCL were imaged and counted in six photographs superior and inferior to the optic nerve head, averaged and plotted in each group as depicted in figures 3.17-3.19. Quantification analysis revealed 24±1.9 mean numbers (± Standard error) of GCL cells in Shp2 transduced WT while the counts were 38±0.7 in GFP injected controls. This data demonstrated a significant decrease in ganglion cell density in Shp2 treated WT compared to GFP-treated counterparts (n=8; P<0.001) (Figure 3.17B). A). A similar reduction was observed for Cav-$1^{+/-}$ group which showed ~ 20% loss in RGC density with a mean of 28±1.6 compared to 35±1.1in control animals (n=8; p<0.01) (Figure 3.18B).

In contrast, in Cav-$1^{-/-}$ mice, although the mean number of GCL cells was less than that of GFP controls (31±2.4 versus 36±0.6), a statistically significant difference was not identified (n=8) (Figure 3.19B). Data analysis reveals that the percentage of ganglion cell loss 2 months subsequent to Shp2 overexpression was significantly higher in WT group compared to the

Cav-$1^{+/-}$ and Cav-$1^{-/-}$ groups under the equivalent treatment conditions, suggesting that Cav-1 deficit exerted a significant protective effect against retinal damage mediated by Shp2 upregulation.

To confirm the SD-OCT results, H and E stained sections were also assessed for thickness of various retinal layers. Similar to SD-OCT analysis histological analysis of retinal layers (GCL, INL or TRT) revealed no significant changes in the thickness of retinal layers to Shp2 overexpression in all 3 genotype groups when compared with GFP injected counterparts (Figure 3.17-3.19 C).

A

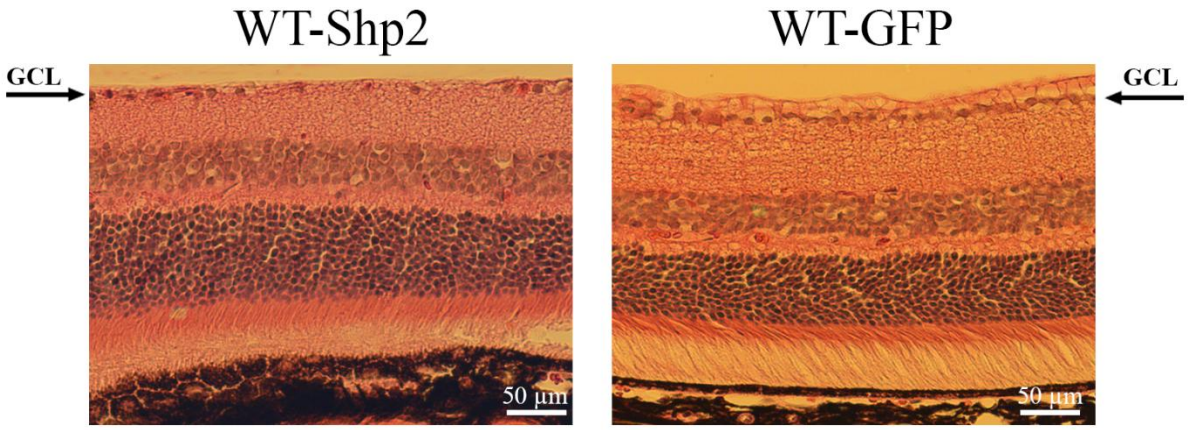

B

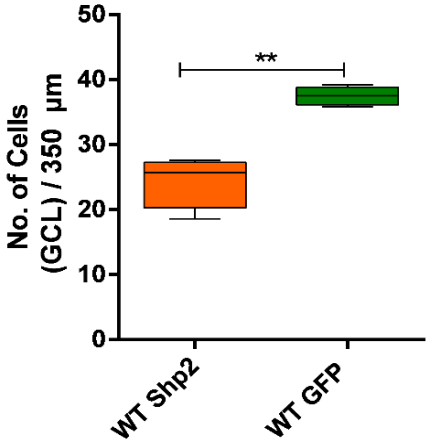

C

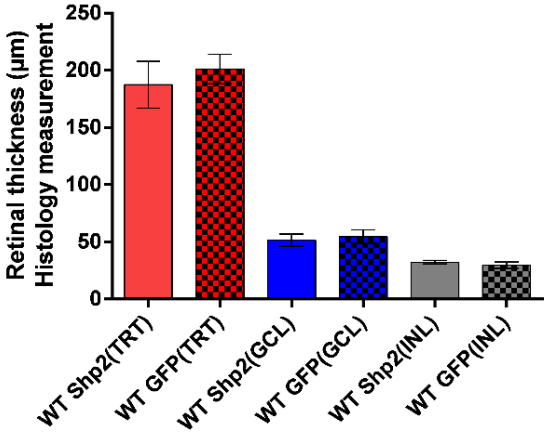

Figure 3.17: Histological analysis of WT mice 2 months subsequent to Shp2 upregulation. (A) H and E staining of the paraffin-embedded retinal histological sections. The GCL layer is indicated by arrows. (B) Quantification of GCL density revealed a significant decrease in AAV-PTPN11 treated WT when compared to their related GFP injected controls. (n=8, $P<0.001$) (C) Morphometric analysis of H and E staining indicated no significant differences in retinal thickness (GCL, INL or TRT) between experimental and the related GFP controls.

A

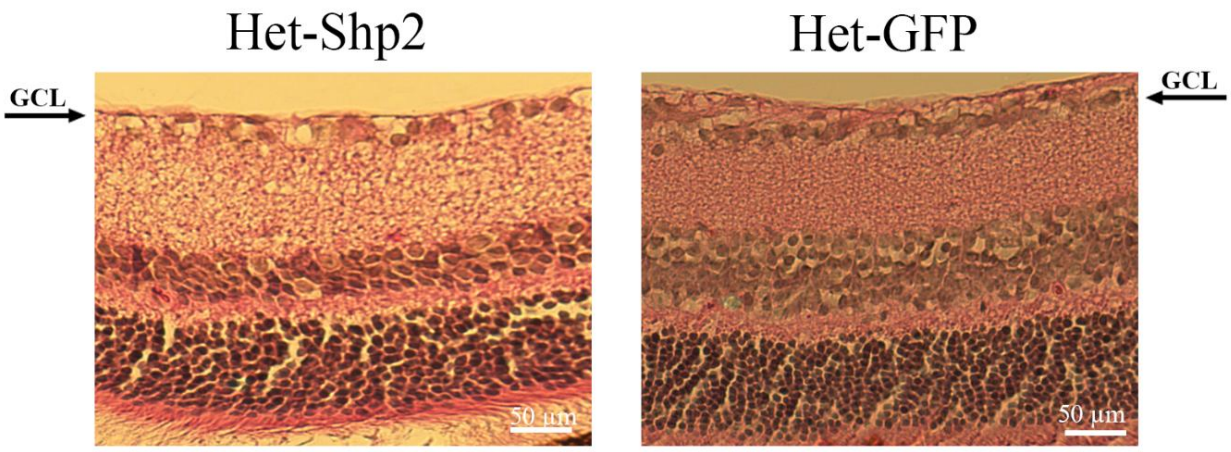

B

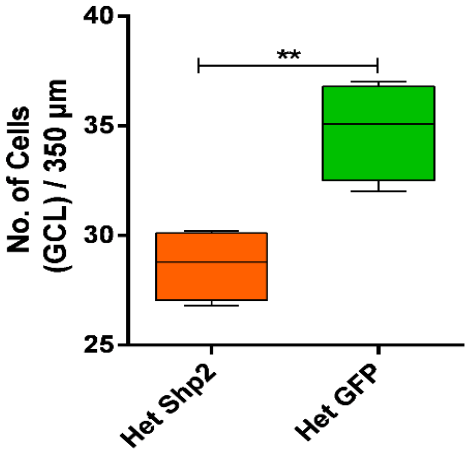

C

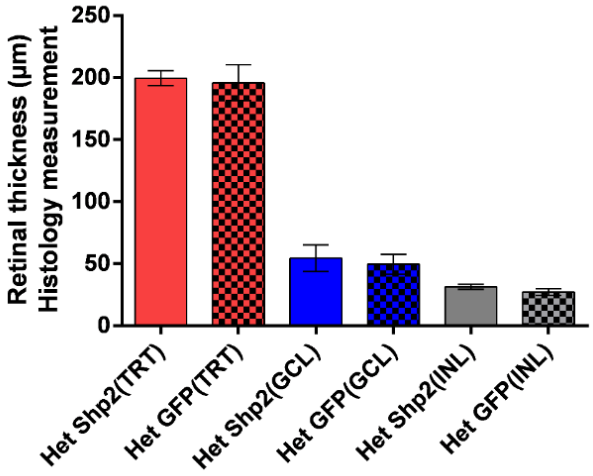

Figure 3.18: Histological analysis of Het mice 2 months following Shp2 upregulation (A) H and E staining of Cav-$1^{+/-}$ retinal histological sections. The GCL layer is indicated by arrows. (B) quantification of GCL density revealed a significant decrease in AAV-PTPN11 treated Cav-$1^{+/-}$ when compared with their related GFP injected controls. (n=8, $p<0.01$). (C) No statistically significant difference was seen in retinal thickness between experimental and the GFP controls.

A

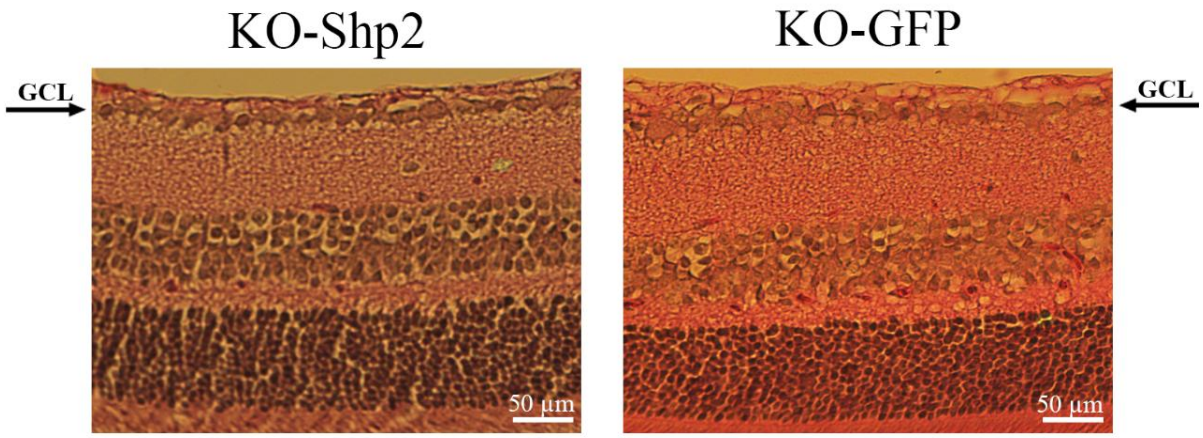

B

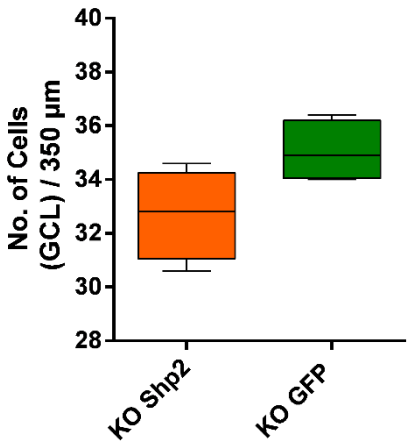

C

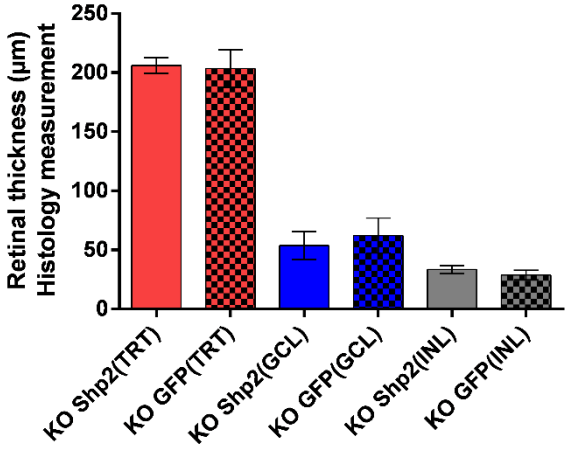

Figure 3.19: Histological evaluation of Cav-1$^{-/-}$ mice 2 months after Shp2 upregulation. (A) H and E staining demonstrates comparable GCL density in experimental and GFP control groups. (B) quantification indicate a slight non-significant decrease in GCL density of AAV-PTPN11 injected Cav-1 KO mice compare to their GFP treated counterparts. Scale 50 µm. (C) Similar to other groups, Morphometric analysis of H and E staining indicated no significant differences in retinal thickness between experimental and the related GFP controls.

3.6.3 Retinal *in vivo* imaging correlates with histological observations

The correlation of morphometric data with non-invasive SD-OCT scanning was examined in WT and Cav-1 transgenic mice. The dimensions of each distinct layer together with their respective standard deviations were calculated for both histological sections and SD-OCT imaging and averaged separately for comparison.

As displayed in figure 3.20, the retina consists of several cell types organized in separate layers imparting it a distinct laminar structure. The retinal structure including nerve fiber layer (NFL) on top, to retinal pigment epithelium (RPE) defined as choroid-sclera boundary, at the bottom were determined by the high-resolution SD-OCT setup (Figure 3.20A). For the appropriate measurement, the retinal regions were chosen around the optic nerve head which are analogous to cross-sectional images of SD-OCT system (as described in previous section). The thickness of each individual layer including GCL/IPL, INL and TRT were compared between two aforementioned methods within each distinct group (Figure 3.21A, B and C). Since no significant differences were observed in SD-OCT measurement among all groups prior and subsequent to AAV-PTPN11 treatment, each individual layer was also assessed among all animals to confirm the consistency of the values obtained by SD-OCT and histology measurement methods (Figure 3.21D). It is to be noted that tissue thickness in H and E may be different from the *in vivo* imaging as the tissues need to be processed for fixation, embedding and staining procedures.

We observed that the thickness of three individual layers by the two above mentioned methods revealed no significant differences among each individual genotype as well as all groups compared together (Student's t-test at a significance level of $p<0.05$). Table 3.1 demonstrates the mean of thickness for each individual layer measured by both methods of SD-OCT and histology.

The comparison between two methods revealed that SD-OCT *in vivo* imaging system enables high resolution images almost resembling histology images.

Table 3.1: The mean and standard deviation of different retinal layer thickness acquired by SD-OCT and histology techniques among all mice groups. The values are similar in each layer (n=24)

	His (INL)	OCT (INL)	His (GCL/IPL)	OCT (GCL/IPL)	His (TRT)	OCT (TRT)
Mean	31.4	29.79	53.78	58.53	199.6	206.7
Std. Deviation	3.028	2.704	9.5	3.7	14.29	12.98

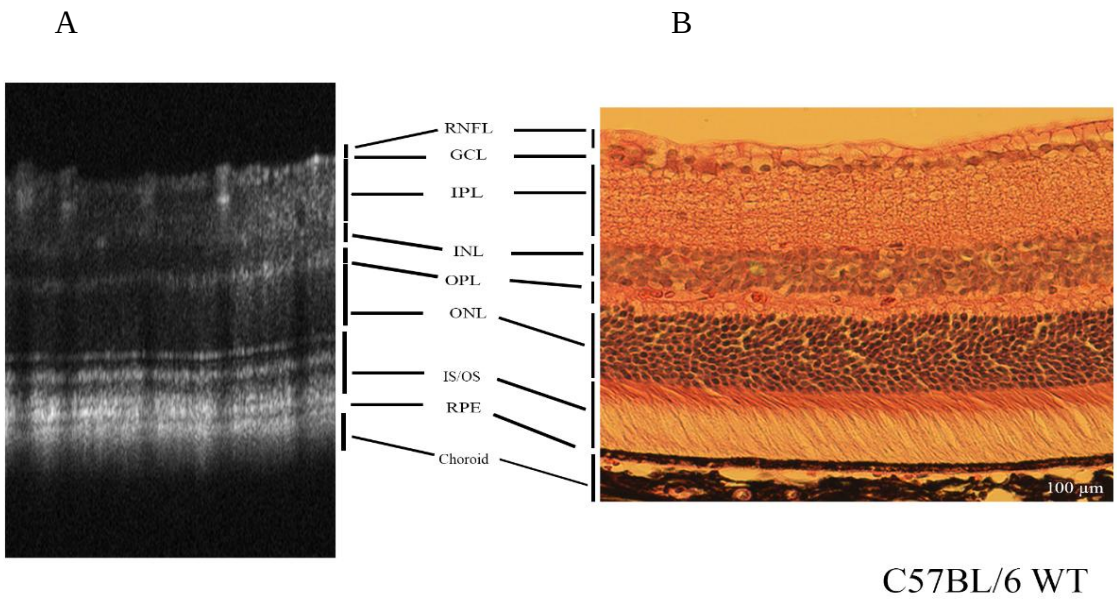

Figure 3.20: Comparison SD-OCT scan and histologic image of the C57BL/6 WT mouse for retinal layers. Distinct retinal layers are identifiable and labelled.

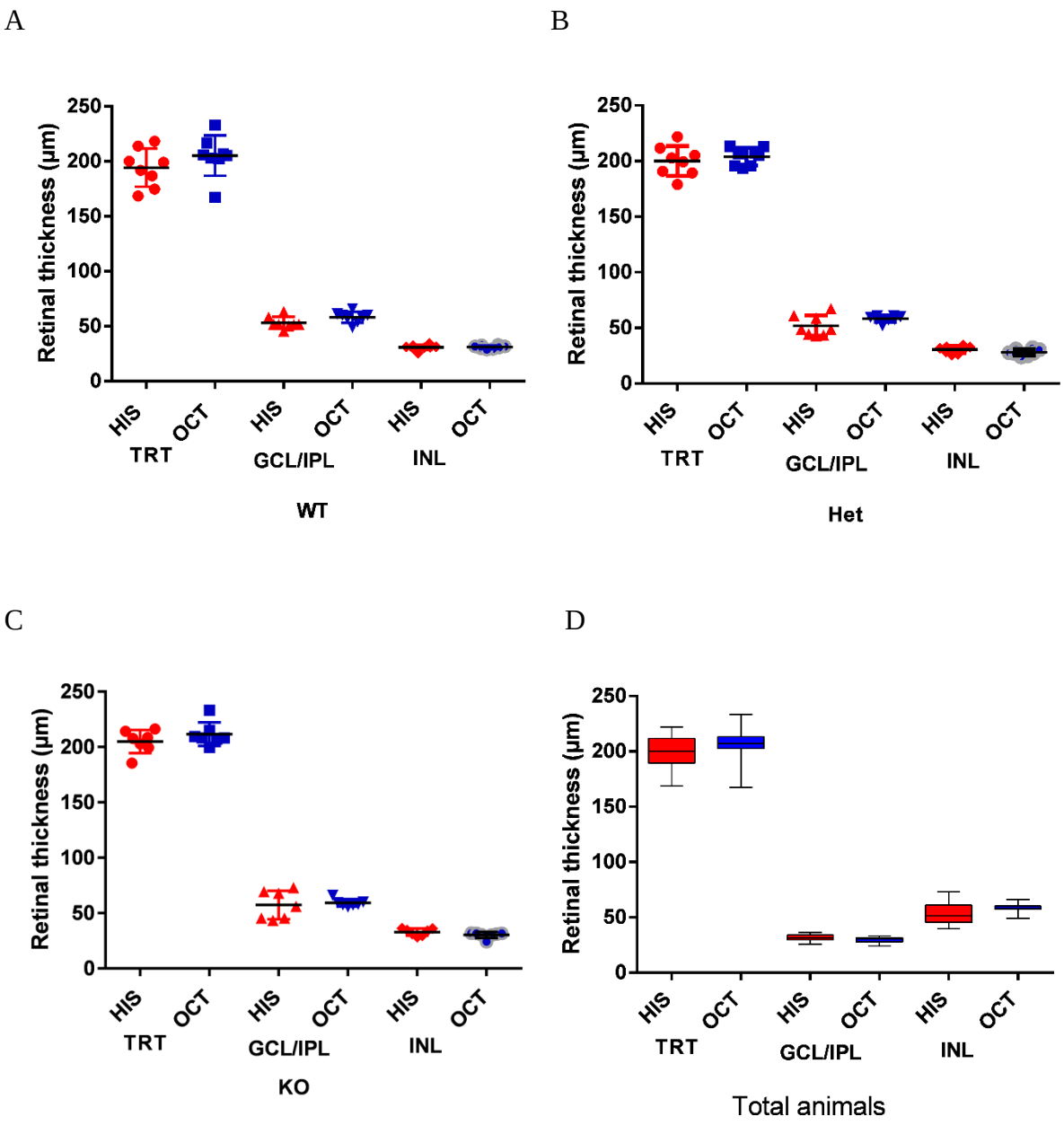

Figure 3.21: SD-OCT and histologic morphometric data obtained from H and E staining of sections in WT and Cav-1 transgenic mice and relationship between both methods plotted. (A, B, C) Comparison of retinal thickness (TRT, GCL/IPL and INL) between histology (blue) and SD-OCT (red) data. Using Student's t-test no statistically significant difference was illustrated between SD-OCT quantification and histological measurements in WT (A), Cav-$1^{+/-}$ (B) and Cav-$1^{-/-}$ (C) (n=8 in each group). (D) Since no significant differences were observed in SD-OCT measurement among all groups prior and subsequent to Shp2 upregulation, retinal thickness by both methods was also compared in all groups which revealed no significant difference. (n=24)

Chapter 4
Discussion

4.1 Major findings and implications

Several recent studies have highlighted the role of the Src homology domain containing protein tyrosine phosphatase Shp2 in neurotrophin signalling through its association with receptor tyrosine kinases (TrkA and TrkB) (Goldsmith & Koizumi 2002; Gupta et al. 2012b, 2013b; Marsh et al. 2003, Mattson 2000, Rusanescu et al. 2005). Neurotrophic factors, particularly BDNF and its high affinity receptor TrkB play critical roles in protecting the RGC survival during normal conditions and under various forms of stress (Chen & Weber 2001, Cheng et al. 2002). Shp2 has been implicated to regulate TrkB phosphorylation in BDNF-TrkB signalling pathway and inhibit BDNF-induced TrkB autophosphorylation in both cerebellar neurons in culture and retinal ganglion cells (Gupta et al. 2012b, Rusanescu et al. 2005). Our group has recently presented novel molecular evidence that the Shp2-TrkB interaction is mediated *via* the adaptor protein Cav-1 (Gupta et al. 2012b). *Cav* gene variations have been implicated in glaucoma (Thorleifsson et al. 2010).

However, little is known about the functional and biochemical impact of Shp2 and Cav-1 interaction on RGCs *in vivo* either under normal or stress conditions. To investigate this issue, this study considered the impact of Shp2 modulation on functional, biochemical and anatomical aspects of Shp2 modulation on the retina in particular the GCL of WT and Cav-1 mice. The major finding of this study was that the genetic ablation of Cav-1 can protect against the inner retinal functional deficits subsequent to AAV-mediated *PTPN11* gene overexpression. The functional findings correlated well with the biochemical and structural observations wherein TrkB activity was significantly reduced upon Shp2 upregulation and GCL density was significantly reduced in the WT mice but Cav-1 null mice depicted

protection against this reduction. To conclude, while Shp2 upregulation was demonstrated to be detrimental for the inner retinal microenvironment, Cav-1 ablation was observed to partially, protect against inner retinal deficits induced by the phosphatase upregulation.

4.2 Shp2-Cav-1 interaction affects functional integrity of the inner retina

The relative preservation of pSTR amplitudes in Cav-1 deficient mice (Figure 3.5C) implied that Cav-1 ablation was effective in preserving the inner retinal integrity following neurodegenerative effects induced by AAV-PTPN11 upregulation in the RGCs.

However, the significant decrease in pSTR amplitudes of WT mice (Figure 3.5A) under the same treatment, suggested that Cav-1 is involved in facilitating the neurodegenerative effects induced by Shp2 upregulation. Cav-$1^{+/-}$ mice similarly depicted results comparable to that of WT animals suggesting that Cav-1 heterozygosity was sufficient to mediate its effects on Shp2 actions (Figure 3.5B) although it was previously shown that ablation in one locus was sufficient enough to reduce the protein levels by virtually half (Park et al. 2003, Razani et al. 2001). These results clearly raised an interesting point that Cav-1 adaptor protein may modulate the function of Shp2 phosphatase in the ganglion cell layer which in turn negatively influences retinal function. The Shp2 active site, the PTP domain, is directly inactivated in the resting state by intramolecular association with N-SH2 domain and thus Shp2 is auto-inhibited unless it comes in contact with tyrosine-phosphorylated binding partners (Lu et al. 2001). Moreover, although Shp2 is a cytosolic phosphatase, it is found to be involved in dephosphorylation of many membrane proteins including TrkB receptor tyrosine kinase (RTK). Membrane binding has been suggested to be supported by the adapter functions of the integral membrane protein Cav-1. Cav-1 may recruit Shp2 to the raft microdomains as a signalling platform, translocating a pool of Shp2 protein into the vicinity of its crucial substrates, the RTKs (Kim et al. 2003, Park et al. 2015, Pawson et al. 2001). This binding could potentially relieve the allosteric constraints that sustained the Shp2 auto-inhibited condition and facilitate its activation. Intriguingly, recent published work from our group supports these findings by demonstrating that Cav-1 and Cav-3 proteins undergo hyperphosphorylation in RGCs in stress condition and depict several fold increased binding to Shp2 phosphatase (Gupta et al. 2012b). This may lead to concurrent Shp2 mediated TrkB interactions as observed in co-immunoprecipitations and this interaction was eliminated RGCs subjected to Cav-1 knockdown.

Cav-1 is a major isoform amongst the caveolin family, and is also well-known for its adapter functions in signal transduction cascades through providing a docking site to recruit diverse proteins (Park et al. 2002, 2015). Lipid raft-mediated regulation of Shp2 is reported to facilitate Shp2 interaction with tyrosyl phosphorylated growth hormone receptors (GHR) and negatively regulate the GH signalling pathway in mouse 3T3-F442A fibroblast cell line (Stofega et al. 2000). In microglia Shp2 was identified to directly associate with JAK leading to negative regulation of the JAK-STAT cascade in a raft-dependent manner while filipin, a lipid raft disrupter, could restore the pathway through blocking Shp2 phosphorylation (Hee et al. 2006, Pawson et al. 2001, Yu et al. 2000). JAK-STAT pathway is implicated in numerous cell functions including cell proliferation, differentiation, and survival (O'Shea et al. 2002). Importantly, Cav-1 overexpression has been reported to dramatically block the prolonged NGF-mediated TrkA autophosphorylation in neuron-like cell line, PC12, leading to its inhibitory effect on neurite outgrowth (Bilderback et al. 1999).

Cav-1 has also been shown to exhibit positive regulatory functions on cellular signalling cascades. In astrocytes, Cav-1 was shown to stimulate H_2O_2-dependent phosphorylation of Shp2 and activate the Erk cascade following the H_2O_2-induced oxidative stress (Park et al. 2011).

In the current study, Cav-1 demonstrated *in vivo* interactions with Shp2 that manifested in the form of reduced TrkB phosphorylation and was associated with inner retinal deficits. However, further investigation is required to precisely describe the dynamic of Cav-1 interaction with Shp2 and the ambiguous role of Cav-1 in downstream targets involved in TrkB signalling. A preferential inner retinal functional loss is not entirely unexpected given that fact that the phosphatase was specifically expressed in the RGCs under the CAG promoter. Nevertheless, these findings support the effects of the phosphatase dysregulation in the RGCs and may be relevant to several neurodegenerative conditions affecting the neuronal cells (Barford & Neel).

This study also established that Shp2 modulation in the RGCs specifically affects the functional and structural aspects of the inner retina. The loss of pSTR in PTPN11-treated WT/Cav-$1^{+/-}$ group is indicative of inner retinal compromise (Fortune et al. 2004) (Figure 3.5A, B). One plausible scenario regarding ganglion cell damage is the negative influence of Cav-1 mediated Shp2 actions on modulating BDNF/TrkB neurotrophin signalling. BDNF and its high affinity receptor TrkB play a critical role in neuronal survival, differentiation, neurite development and synaptic plasticity in the central nervous system *via* activation of several intracellular signalling pathways (Cowley et al. 1994, Meakin et al. 1999). The indispensable role of TrkB in physiological functions is evident from early fetal death of TrkB deficient

mice which presents several abnormalities in motor neurons, small dorsal root and trigeminal ganglion (Gupta et al. 2013b, Huang & Reichardt 2003) In the retina BDNF stimulation of TrkB results in activation of pro-survival signalling pathway that can provide neuroprotection to the retina in glaucoma and other optic nerve stress conditions. Its impairment is reported to contribute to progressive molecular degenerative changes in inner retina and preferential ganglion cell loss under normal and stressed physiological conditions (Gupta et al. 2014). Shp2 tyrosine phosphatase is shown to be highly expressed in GCL and INL layer. Several lines of evidence indicate the association of Shp2 with tyrosine kinase cascades through the binding of its SH2 domain to tyrosine phosphorylated proteins (Hadari et al. 1998, Marsh et al. 2003, Ong et al. 1997, Rusanescu et al. 2005). It is previously reported by our group and others that Shp2 mediates TrkB activity in RGCs and other neural cells (Cai et al. 2011, Gupta et al. 2012b, Rusanescu et al. 2005). Trk receptors contain an intracellular tyrosine kinase domain that can be a target for tyrosine phosphatase Shp2 and can ultimately prevent the downstream MAPK/Erk signalling cascade required for TrkB-mediated survival in RGCs(Cheng et al. 2002, Easton et al. 2006, Gupta et al. 2013b, Rusanescu et al. 2005). Here we propose that the capacity of neurons to respond to neurotrophic factors is influenced by prolonged TrkB dephosphorylation caused by enhanced association of the Shp2-TrkB complex through Cav-1 signalling platform which would ultimately lead to negative effects on TrkB activity and associated inner retinal deficits. An important role of BDNF-TrkB signalling in maintaining inner retinal function was ascertained from a previous study by our group investigating $BDNF^{+/-}$ animals which showed age-related decline of inner retinal integrity and low pSTR amplitude under normal and glaucomatous condition (Gupta et al. 2014). Our result is also in agreement with the previous observation in cerebellar neuronal cultures by Rusanescu et al. (2005) in which Shp2 hindered BDNF-induced TrkB autophosphorylation through its negative cross-talk with TrkB. This concept elucidates the negative regulatory effect of Shp2 on Ca^{2+}-induced excitotoxic neuronal damage, through suppressing BDNF and other downstream survival effectors whereas Shp2 deletion inversely desensitized neurons to excitotoxicity (Rusanescu et al. 2005). Accumulating evidence also supports a negative role of Shp-2 on PI3k signalling in response to epidermal growth factor (EGF) in fibroblast cell lines. Interestingly, Grb2-associated binder 1 (Gab1) mediated PI3K signalling improved in Shp2 mutant fibroblast whereas PI3K activation appeared to reduce in $Shp2^{-/-}$ conditions following other growth factor stimulation (PDGF and IGF-1). This indicates that Shp2 inhibitory effects can be significantly mediated in an RTK specific manner (Reeves et al. 1995, Zhang et al. 2002).

Conversely, a series of studies addressed the positive role of Shp2 in tyrosine kinase signalling pathways. Cai et el (2011), elucidated that Shp2 deletion negatively affects Ras-MAPK signalling pathway in prenatal development leading to retinal degeneration phenotype (Zhang et al. 2011). This aspect of retinal degenerative changes associated with Shp2 ablation may be based on different roles of Shp2 in pre-/postnatal development and promoter specific expression of Shp2 in different retinal cells. In this regard, Shp2 has also been suggested to be a prerequisite of MAPK stimulation in cortical neurons. The mechanisms underlying this effect were thought be acting through BDNF/TrkB signalling and exert their effects by directly regulating Ras or other related signalling components (Easton et al. 2006, Kumamaru et al. 2011).

Shp2 is specifically involved in patterning the retinal morphogenesis during early embryonic stage while during development it was not observed to further impact retinal differentiation. This phosphatase has been emphasized to be indispensable for several RTK such as FGFR to activate the Ras-MAPK pathway in initial retinal morphogenesis during optic vesicle formation (Cai et al. 2010, Zhang et al. 2011). Likewise, in brain, Shp2 signalling was found to play a key role in neural cell-fate decisions to ensure that cortical precursor cells generate the neuronal cells rather than glia cell type during brain development (Gauthier et al. 2007, Lethality et al. 2007). In the embryonic nervous system of chick and mice, Shp2 was stated to be localized in retinal neurons taking part in Sema4D repulsive signalling to provide the axonal guidance (Fuchikawa et al. 2009).

In addition to the negative effects of Shp2 upregulation on the inner retinal function and protection conferred by the absence of Cav-1 against Shp2 effects, we identified that Cav-1 null mice exhibited a decline in pSTR amplitudes (Figure 3.9). The pSTR reduction corroborated with reduced amplitudes of whole retinal scotopic ERGs (Figure 3.10). Our findings substantiate previous observations that Cav-1 null mice exhibit loss of ERGs amplitudes (Li et al. 2012). Cav-1 participates in variety of cell function such as lipid trafficking, endocytosis, mechanotransduction and regulation of various signalling cascades (Berta et al. 2007, Gu et al. 2014, Song et al. 1996). Cav-1 also exhibits largely an even distribution in various retinal layers including ganglion layer cells. Cav-1 may directly affect the inner retinal function by affecting the integrity of ganglion cells in the inner retina or its loss may indirectly effect supporting cells such as Muller glia. Muller glial cells play fundamental roles in neuroprotection, neural regeneration and biochemical scaffolding of the retina and their dysfunction may compromise the survival of various retinal cells including RGCs. Besides, Cav-1 is reported to play a critical role in the preservation of retinal micro-environment by contributing to the maintenance of blood retinal barrier (BRB) integrity.

Furthermore, Cav-1 loss is associated with alterations in retinal ion homeostasis and blunted pro-inflammatory cytokine responses (Gu et al. 2014; Li et al. 2012, 2014; Reagan et al. 2016). This is in addition to the fact that Cav-$1^{-/-}$ loss may be associated with pre or postnatal developmental changes that may affect the retinal function with age (Head et al. 2010). Li et. al. (2012) also showed that Cav-1 ablation led to reduced retinal neural function and contributed to impaired subretinal homeostasis rather than a direct photoreceptor dysfunction (Li et al. 2012). Cav-$1^{-/-}$ mice also exhibit increased endothelial nitric oxide synthase (eNOS) activity (Kuehn et al. 2005, Razani et al. 2001). Nitric oxide (NO) performs important physiological functions in normal vascular responses, synaptic plasticity and neurotransmitter release and has recently been suggested to be involved in human glaucoma pathogenesis. Interestingly, Cav-1 absence leads to excessive eNOS activity resulting in loss of vascular tone, glial-cell mediated apoptosis and RGC death while blocking NO production has been directly correlated with a decrease RGC damage in rat glaucoma model (Kuehn et al. 2005, Razani et al. 2001). Cav-1 is also introduced as a tumor suppressor candidate negatively regulating Ras-p42/44 MAP and PI3K/AKT kinase pathway (Lin et al. 2010) and Cav-$1^{-/-}$ mice have demonstrated an enhanced Erk phosphorylation in the hippocampus (Takayasu et al. 2010). Recent genome wide studies have identified the association of *Cav1* gene locus genetic variants with primary open angle glaucoma and these observations lend further credence to our functional findings (Thorleifsson et al. 2010). In addition to the retina effects, it is also possible that Cav-1 alterations may affect other ocular structures such as trabecular meshwork and extracellular matrix ultrastructure thereby indirectly affecting to the retinal pathology (Surgucheva & Surguchov 2011, Vranka et al. 2015). Our findings further demonstrate that these animals showed greater reduction in the inner retinal function compared to the whole retinal electrophysiological response implicating a significant role that this transmembrane protein plays in the inner retinal function. Together, all these factors may contribute to the phenotypic effect that we observed in our experiments in Cav-1 mice. The confounding effects were minimised by maintaining corresponding Cav-1 knockout, Heterozygous and WT controls for all the experimental paradigms.

4.3 Regulatory effect of Shp2-Caveolin interactions on the TrkB tyrosine phosphorylation

In order to determine the involvement of Cav-1 in Shp2 induced TrkB regulation, we examined changes in TrkB phosphorylation in the retinas of Cav-1 deficient mice. RGCs in WT and Cav-$1^{+/-}$ mice which were subjected to Shp2 upregulation, showed 33% reduction in pTrkB Y515 immunoreactivity while compared to Cav-$1^{-/-}$ mice retinas of only 3% (Figure

3.11 and 3.12). This experiment demonstrated enhanced Shp2 induced TrkB negative modulation that was dependent to the Cav-1 adaptor protein. TrkB receptors, similarly to other tyrosine receptor kinases, are subject to tandem phosphorylation and dephosphorylation to be appropriately balanced for efficient performance of their biological functions. The PTPase Shp2 is one the TrkB interactive proteins which binds to TrkB and regulates its activity under stress condition (Gupta et al. 2012b, Rusanescu et al. 2005) Although neurotrophins play an important role in RGC survival after injury, long term studies revealed that positive effects of exogenous BDNF on RGCs in glaucoma patients or optic nerve injuries have not been long-lasting and that multiple or higher doses delay but do not prevent the onset of RGCs loss and ultimately RGCs surrender to the degenerative cascade (Cheng et al. 2002, Clarke et al. 1998, Di Polo et al. 1998, Mansour-Robaey et al. 1994). The plausible explanation for the transient effects of BDNF may be the prolonged dephosphorylation of its related receptor TrkB. Sustained dephosphorylation of TrkB receptor has also been reported to hinder the axonal regeneration and neuroprotective effects of neurotrophin 4 (NT-4) (Gupta et al. 2012b, Hollis et al. 2009).

TrkB phosphorylation is a perquisite for connecting to Shc adaptor protein and the subsequent downstream Ras-MAPK, PI3K/Akt and PLCγ1 signalling procedures (Minichiello et al. 1998).

These findings are congruent with the previous observations that illustrated Shp2 co-immunoprecipitation with TrkB in RGCs under either optic nerve axotomy or enhanced intraocular pressure stress conditions, while pharmacological inhibition of Shp2 resulted in maintenance of sustained TrkB phosphorylation (Gupta et al. 2012b). This negative regulatory effect of Shp2 on TrkB activity partially elucidates why the BDNF/TrkB targeting has yielded only transitory influences and has largely been ineffective in preventing the RGC damage (Cheng et al. 2002, Clarke et al. 1998, Mansour-Robaey et al. 1994). Cav-$1^{+/-}$ mice also demonstrated a loss of TrkB phosphorylation that was comparable to that observed in the WT mice suggesting that a subset of the total Cav-1 cellular fraction is sufficient to mediate Shp2 effects on TrkB activity (Figure 3.12).

Shp2 upregulation in Cav-$1^{-/-}$ mice however, did not significantly reduce TrkB activity (Figure 3.13). It is likely that in the absence of Cav-1, Shp2 could not be recruited into Cav-1 docking site to facilitate its enhanced association with TrkB. Kumamaru et al. (2011) have shown that glucocorticoids impeded the BDNF-induced MAPK/ErK signalling through the suppression of Shp2-TrkB coupling in cultured cortical neurons (Kumamaru et al. 2011). This variation may reflect that Shp2 actions are cell and tissue specific and also show that alterations in protein-protein interaction may be differentially affected in health and disease

conditions. No statistically significant alteration was observed in TrkB receptor expression under Shp2 upregulation conditions or in either of the WT, Cav-$1^{+/-}$ or Cav-$1^{-/-}$ mice genotypes (Figure 3.14) strongly implicating that Shp2 interaction manifested itself in the form of reduced tyrosine phsopshorylation on TrkB receptor.

4.4 Shp2 upregulation-associated structural deficits are ameliorated with Cav-1 loss

Analysis of the morphological differences in retinal sections revealed that genetic ablation of Cav-1 not only significantly protected RGCs against loss of function but also moderately preserved RGC density subsequent to AAV mediated Shp2 upregulation (Figure 3.19). This suggests that loss of Cav-1 abrogated the *in vivo* interactions of Shp2 with TrkB. The molecular degenerative changes upon Shp2 upregulation resulted in morphological alterations in WT and Cav-$1^{+/-}$ mice as depicted by a great loss in their GCL cell density (Figure 3.17 and 3.18), compared to the Cav-$1^{-/-}$ mice retinas. This suggests that Cav-1 expression exacerbated Shp2 induced inner retinal structural deficits. These findings corroborate previous observations that have demonstrated a significant decrease in GCL density of $BDNF^{+/-}$ mice under various stress conditions. Taken together these results support the hypothesis that Shp2 plays a regulatory effect on TrkB signalling partially in Cav-1 dependent manner and that this axis is essential to preserve inner retinal structural integrity. As BDNF is known to promote RGC survival through its high affinity receptor TrkB it is likely that in the Cav-$1^{-/-}$ mice Shp2 is not appropriately recruited or localised within the cells to mediate TrkB dephosphorylation (Gupta et al. 2014, Kido et al. 2000, Ren et al. 2012). In contrast to GCL density, evaluation of retinal thickness through either SD-OCT or histological measurement revealed no discernible effect on retinal laminar structure in either of the experimental groups. These results may be attributed to the fact that RGCs comprise a small population of total retinal neurons and GCL comprises a small percentage of total retinal thickness. Therefore, the corresponding changes in the GCL are not easily discernible using these measurement tools. High resolution ultrastructural analysis will further project insights into the anatomical changes induced by Cav-1 loss or the effects of Shp2 modulation. Relative preservation of thickness of various retinal layers also support our argument that AAV engaged its target cells in the GCL and had only minimal off target effects.

4.5 SD-OCT *in vivo* imaging directly correlates with retinal histological morphometric analysis

We were interested to determine whether OCT *in vivo* imaging reflects the true measure of retinal changes in our mice models and can be confidently compared to the data obtained from histological analysis. *In vivo* techniques such as electrophysiology (ERG and STR) can provide us with dynamic functional changes of the retina in animal models but quantification of retinal layers has relied on histological evaluation and remains the gold standard. The traditional histology technique has known shortcomings involving tissue distortion, visible artefacts and laborious technical procedure. High resolution SD-OCT has enabled non-invasive *in vivo* structural imaging in human and rodent retinas and is now being used for longitudinal studies. We quantified different retinal layers through SD-OCT and histological analysis and our results show that SD-OCT quantification comparable with the histological indices in Cav-1 null mice and in the AAV gene modulation paradigms (Figure 3.21A, B, C). By comparing the results of histology and SD-OCT measurement we confirmed the capability of SD-OCT for non-invasively monitoring the retinal layers and investigating possible damages in retinal layers (Yang et al. 2012). The histological preparation procedure may account for thickness differences of less than 10% in individual layers. Our results are in agreement with previous studies which found SD-OCT correlates well with histological measurement in various forms of retinal degeneration (Huber et al. 2009, Kim et al. 2008, Pang et al. 2011).

4.6 Methodological Considerations and limitations

4.6.1 Gene Knockout studies

Inactivating the gene for a specific protein and production of KO animals though technically difficult has emerged as a most promising way to elucidate the biological role of target proteins and determine their interactions with other molecules *in vivo*. Hence we utilized this technique in double transgenic mice (Cav-1 genetically modified mice) in order to explore the precise role of Cav-1 in interaction with Shp2 protein upregulation caused by AAV2 vector constructs. This technique facilitates the advances in genomic research by comparing the knockout organism to wild type controls (Galli-Taliadoros et al. 1995, Guan et al. 2010, Picciotto & Wickman 1998). However, a limitations of our study model was that global *Cav1* gene ablation (Cav-$1^{-/-}$) in addition to retinal neural effects may also affect vasculature or induce blood retinal barrier compromise, that in turn may facilitate subtle inflammatory changes and add additional confounding factors (Trushina et al. 2006). To compensate for this issue we applied the age-matched and litter matched Cav-$1^{-/-}$ mice for the AAV-GFP control in addition to the WT counterparts. However, two potential alternatives would be knockdown (KD) studies and use of conditional or inducible KO mice. Conditional knockout technique to study tissue specific effects by using "Cre-LoxP mediated recombination" may be another strategy to circumvent these limitations. This strategy enables manipulation of the gene of interest only in desired tissues and minimises phenotypic susceptibility to developmental changes or contribution of systemic alterations to tissue specific effects (Picciotto & Wickman 1998). It is commonly utilized in conditions where KO mutations would be lethal, since this is a complicated and time-consuming procedure and not every distinct gene can be trapped conditionally (Zhang et al. 2012).

4.6.2 AAV induced overexpression

The hypothesis of this study was to assess the effect of overexpression of Shp2 phosphatase in RGCs of Cav-1 transgenic mice. To address this speculation, we used recombinant AAV2 vector system to deliver *PTPN11* gene in to adult RGCs *via* intravitreal injection. The lynchpin of this experiment was the application of a highly efficient vector system for transduction of RGCs *in vivo* (Watanabe et al. 2013) which produced a sustained overexpression of Shp2 enabling us to evaluate the alterations of retinal function. AAV

vectors evoke minimal immune reactions and provide long-standing expression persisting for at least one year in the host. The optimal performance of transfection greatly depends on careful selection of AAV capsid serotype, designing the plasmid and the route of transmission. Serotype 2 (AAV2) was introduced as the potential vector to efficiently transduce RGCs after intravitreal injection in mouse eyes (Petrs-Silva et al. 2009, Reich et al. 2003, Yokoi et al. 2007). We also designed the Shp2 sequence to be placed under transcriptional control of cytomegalovirus/chicken β actin hybrid (CAG) hybrid promoters in AAV particles, known to work well in RGCs (Cunningham et al. 2008, Martin et al. 2003) Previous studies showed that intravitreal recombinant AAV expression vector successfully transferred to GCL and the beneficial effects of BDNF and TrkB on RGC survival was markedly detected following the IOP elevation (Klöcker et al. 2000, Martin et al. 2003, Qu 2002, Ren et al. 2012). In agreement with these reports, our data also revealed that GCL was the main target for AAV recombinant vector transduction leading to an average of 68% and 60% of GCL cell population to be efficiently transduced by GFP and Shp2 respectively. No deleterious effect was observed following the injection of control eyes with the AAV-GFP construct alone. Two main phenotypic findings of our study are that RGC function in WT and Cav-$1^{+/-}$ groups dramatically declined compared to Cav-$1^{-/-}$ mice and that the GCL cell counts significantly decreased in Shp2 upregulated WT and Cav-$1^{+/-}$ animals, which verified that AAV-PTPN11 worked accurately in mediating Shp2 overexpression. However, a few potential shortcomings might be imposed by this method such as Shp2 overexpression being not at physiological levels might introduce pathological artefacts. However, moderate fold change of only 2.2 suggests that expression changes were not disproportionately high. Such a limitation can be circumvented by utilizing an inducible promoter such as doxycycline to modulate transcription of the target gene in a tissue/time dependent manner (Hoppe et al. 2014).

4.6.3 Electrophysiological assessment

The full-field ERG commonly assess the dark-adapted retinal response to visual stimuli with its components a-wave and b-wave mainly associated with photoreceptors and bipolar cells respectively (Saszik et al. 2002). STR, is a modified recording technique in response to very dim light, close to the psychophysical scotopic threshold which has negative and positive components (nSTR and pSTR). Similar to other species, pSTR in mouse retina is assumed to be the most sensitive parameter of the ERG, 3-4 times more sensitive than b-wave (in C57/BL6 mice) and predominantly arises from the inner retina (Toda et al.). Since pSTR

response originates from proximal retinal neurons rather than distally positioned neurons, it is extremely sensitive to background light compare to the b-wave in ERG, which is in turn more sensitive than the a-wave (Frishman & Steinberg 1989, Naarendorp et al. 2001). Therefore, in our experiment, to remove any non-specific results, STR was carried out under low dim red light. Saszik et al. (2002) established the presence and nature of mouse STR for the first time, and showed that each STR component does not necessarily arise from a single class of neuron (Saszik et al. 2002). Several studies declare that pSTR in rodents is preferentially affecte in glaucoma and disappearance of STRs has been reported in experimental ganglion cell degeneration (You et al. 2013), suggesting that pSTR is valuable in evaluating ganglion cell activity. There is also enough evidence that STR is a combination response of RGCs and amacrine cells from the GCL and IPL and it may not be arising solely from RGCs (Frishman & Steinberg 1989, Hopkins 1999, Saszik et al. 2002). The origination of nSTR is also reported to be dominated in a species dependent manner. nSTR in humans for instance is considered to be more amacrine cell based and not a pure response of ganglion cells (You et al. 2013). The nSTR, in mouse however is most probably due to background noise such as respiratory movements which is not applied since it is small, albeit several strategies have evolved to recover it (Saszik et al. 2002).

4.7 Future directions

Possible future directions include:

1. RGCs damage occurs in several retinal disorders but in particular in glaucoma (Fu et al. 2009, Gupta et al. 2012b, Lee & Higginbotham 2005, Nickells 1999). Therefore, future studies will determine the consequence of Cav-1-Shp2 interaction under glaucomatous or other stress conditions in an animal model of glaucoma and in human post-mortem tissues.

2. To expand biochemical investigations to determine effects of Shp2 on the TrkB downstream signalling. This can be performed by pharmacologically blocking critical converging steps in neurotrophin pathways including Ras, Raf, MEK1/2, ERK, PI3K and Akt signalling molecules

3. Since Cav-1 is well known for providing a docking site to modulate several signal transductions, the effects of its association with Shp2 can also be explored on other neurotrophins (NGF, NT-3 and NT-4) and their related Trk receptors (TrkA and TrkC).

4. Another novel approach is to further identify the range of molecules particularly the signalling proteins which bind to caveolins. This can be carried out using interactome analysis using Cav-1 pull downs followed by mass spectrometry and by molecular modelling and *in silico* docking analysis (Gupta & Gowda 2008). Changes in this protein-protein interaction pattern caused by Shp2 modulation can then be compared with this data.

5. The physiological relevance can be tested by pharmacologically or genetically modulating various downstream effectors of TrkB that may impart functional or structural protective effects to animal models of RGC degeneration.

6. Shp1, another member of SH2-containing phosphatase, shares structural features with Shp2 and is known to be expressed in mouse and human retina. Due to negative regulation activity of Shp1 on signalling pathways such as RTK (TrkA)(Lu et al. 2001, Marsh et al. 2003) and its role in retinal photoreceptors (Geraldes et al. 2009, Lyons et al. 2006) further investigations can help to improve our understanding of its role on TrkB retinal preservation activity.

7. The retina is an integral part of CNS and the similarities of RGCs to CNS neurons along with easy accessibility make it an appropriate research model to study CNS neurons. Findings from this research could be adapted to other animal models of neurodegenerative diseases.

Conclusion

The present study provides evidence underlying the key role of Cav-1 adaptor protein in mediating an interactive association between Shp2 phosphatase and TrkB receptor *in vivo*. RGCs are affected in glaucoma but current therapeutic strategies are limited to lowering IOP to protect the retinal damage. There is an urgent need to understand the molecular mechanisms underlying the RGC damage that may in turn lead to better targeting for improved clinical management. Our results for the first time demonstrate that Shp2 phosphatase negatively regulates the BDNF/TrkB pathway in a Cav-1 dependent manner. We provide molecular, functional and structural evidence that Shp2 upregulation is detrimental to the RGC integrity and that these effects are partially dependent on Cav-1. Therefore, targeting Cav-1 or Shp2 proteins either pharmacologically or through AAV mediated approaches may enable us to modulate the pro-survival BDNF/TrkB pathway. This strategy may find applications in the retinal diseases such as in glaucoma and additionally may help advance the field in other neurodegenerative conditions.

References

Allingham RR, Liu Y, Rhee DJ. 2009. The genetics of primary open-angle glaucoma: A review. *Exp. Eye Res.* 88(4):837–44

Almasieh M, Wilson AM, Morquette B, Cueva Vargas JL, Di Polo A. 2012. The molecular basis of retinal ganglion cell death in glaucoma. *Prog. Retin. Eye Res.* 31(2):152–81

Asai N, Abe T, Saito T, Sato H, Ishiguro S ichi, Nishida K. 2007. Temporal and spatial differences in expression of TrkB isoforms in rat retina during constant light exposure. *Exp. Eye Res.* 85(3):346–55

Barford D, Neel BG. Revealing mechanisms for SH2 domain mediated regulation of the protein tyrosine phosphatase SHP-2. . 249–54

Basavarajappa DK, Gupta VK, Dighe R, Rajala A, Rajala RVS. 2011. Phosphorylated Grb14 is an endogenous inhibitor of retinal protein tyrosine phosphatase 1B, and light-dependent activation of Src phosphorylates Grb14. *Mol. Cell. Biol.* 31(19):3975–87

Berta AI, Kiss AL, Kemeny-Beke A, Lukats A, Szabó A, Szél A. 2007. Different caveolin isoforms in the retina of melanoma malignum affected human eye. *Mol. Vis.* 13(May 2006):881–86

Bilderback TR, Gazula V, Lisanti MP, Dobrowsky RT. 1999. CELL BIOLOGY AND METABOLISM : Caveolin Interacts with Trk A and p75 NTR and Regulates Neurotrophin Signaling Pathways Caveolin Interacts with Trk A and p75 NTR and Regulates Neurotrophin Signaling Pathways *. . 274(1):257–63

Cai Z, Feng G-S, Zhang X. 2010. Temporal Requirement of the Protein TyrosinePhosphatase Shp2 in Establishing the Neuronal Fatein Early Retinal Development. *J. Neurosci.* 30(11):4110–19

Cai Z, Simons DL, Fu X-Y, Feng G-S, Wu SM, Zhang X. 2011. Loss of Shp2-mediated mitogen-activated protein kinase signaling in muller glial cells results in retinal degeneration. *Mol. Cell. Biol.* 31(14):2973–83

Chao M V., Bothwell M. 2002. Neurotrophins: To Cleave or Not to Cleave. *Neuron*. 33(1):9–12

Chen H, Weber AJ. 2001. BDNF enhances retinal ganglion cell survival in cats with optic nerve damage. *Invest. Ophthalmol. Vis. Sci.* 42(5):966–74

Cheng L, Sapieha P, Kittlerova P, Hauswirth WW, Di Polo A. 2002. TrkB gene transfer protects retinal ganglion cells from axotomy-induced death in vivo. *J. Neurosci.* 22(10):3977–86

Cheung W, Guo L, Cordeiro MF. 2008. Neuroprotection in glaucoma: drug-based approaches. *Optom. Vis. Sci.* 85(6):406–16

Clarke DB, Bray GM, Aguayo AJ. 1998. Prolonged administration of NT-4/5 fails to rescue most axotomized retinal ganglion cells in adult rats. *Vision Res.* 38(10):1517–24

Cowley S, Paterson H, Kemp P, Marshall CJ. 1994. Activation of MAP kinase kinase is necessary and sufficient for PC12 differentiation and for transformation of NIH 3T3 cells. *Cell*. 77(6):841–52

Cunningham SC, Dane AP, Spinoulas A, Logan GJ, Alexander IE. 2008. Gene delivery to the juvenile mouse liver using AAV2/8 vectors. *Mol. Ther.* 16(6):1081–88

Dance M, Montagner A, Salles JP, Yart A, Raynal P. 2008. The molecular functions of Shp2 in the Ras/Mitogen-activated protein kinase (ERK1/2) pathway. *Cell. Signal.* 20(3):453–59

Di Polo A, Aigner LJ, Dunn RJ, Bray GM, Aguayo AJ. 1998. Prolonged delivery of brain-derived neurotrophic factor by adenovirus- infected Muller cells temporarily rescues injured retinal ganglion cells. *Pnas*. 95(7):3978–83

Dysli C, Enzmann V, Sznitman R, Zinkernagel MS. 2015. Quantitative Analysis of Mouse Retinal Layers Using Automated Segmentation of Spectral Domain Optical Coherence Tomography Images. *Transl. Vis. Sci. Technol.* 4(4):9

Easton JB, Royer AR, Middlemas DS. 2006. The protein tyrosine phosphatase, Shp2, is required for the complete activation of the RAS/MAPK pathway by brain-derived neurotrophic factor. *J. Neurochem.* 97(3):834–45

Elliott MH, Fliesler SJ, Ghalayini AJ. 2003. Cholesterol-dependent association of caveolin-1 with the transducin alpha subunit in bovine photoreceptor rod outer segments: disruption by cyclodextrin and guanosine 5'-O-(3-thiotriphosphate). *Biochemistry*. 42(26):7892–7903

Fan BJ, Wang DY, Lam DSC, Pang CP. 2006. Gene mapping for primary open angle glaucoma. *Clin. Biochem.* 39(3):249–58

Fortune B, Bui B V, Morrison JC, Johnson EC, Dong J, et al. 2004. Selective ganglion cell functional loss in rats with experimental glaucoma. *Invest. Ophthalmol. Vis. Sci.* 45(6):1854–62

Frank L, Ventimiglia R, Anderson K, Lindsay RM, Rudge JS. 1996. BDN F Down-regulates Neu rotrophin Responsiveness, TrkB Protein and TrkB mRNA Levels in Cultured Rat Hippocampal Neurons. *Eur. Neurosci. Assoc. Eur. J. Neurosci.* 8:1220–30

Frishman LJ, Steinberg RH. 1989. Light-evoked increases in [K+]o in proximal portion of the dark-adapted cat retina. *J. Neurophysiol.* 61(6):

Fu QL, Li X, Yip HK, Shao Z, Wu W, et al. 2009. Combined effect of brain-derived neurotrophic factor and LINGO-1 fusion protein on long-term survival of retinal ganglion cells in chronic glaucoma. *Neuroscience.* 162(2):375–82

Fuchikawa T, Nakamura F, Fukuda N, Takei K, Goshima Y. 2009. Biochemical and Biophysical Research Communications Protein tyrosine phosphatase SHP2 is involved in Semaphorin 4D-induced axon repulsion. *Biochem. Biophys. Res. Commun.* 385(1):6–10

Galli-Taliadoros LA a, Sedgwick JDD, Wood SA a, Körner H. 1995. Gene knock-out technology: a methodological overview for the interested novice. *J. Immunol. Methods*. 181(1):1–15

Gauthier S, Furstoss O, Araki T, Chan R, Neel BG, et al. 2007. Article Control of CNS Cell-

Fate Decisions by SHP-2 and Its Dysregulation in Noonan Syndrome. . 245–62

Geraldes P, Hiraoka-Yamamoto J, Matsumoto M, Clermont A, Leitges M, et al. 2009. Activation of PKC-δ and SHP-1 by hyperglycemia causes vascular cell apoptosis and diabetic retinopathy. *Nat. Med.* 15(11):1298–1306

Goldsmith BA, Koizumi S. 2002. Transient Association of the Phosphotyrosine Phosphatase SHP-2 with TrkA Is Induced by Nerve Growth Factor. *J. Neurochem.* 69(3):1014–19

Golzan SM, Butlin M, Kouchaki Z, Gupta V, Avolio A, Graham SL. 2014. Characterizing dynamic properties of retinal vessels in the rat eye using high speed imaging. *Microvasc. Res.* 92:56–61

Gu X, Fliesler SJ, Zhao Y-YY, Stallcup WB, Cohen AW, Elliott MH. 2014. Loss of caveolin-1 causes blood-retinal barrier breakdown, venous enlargement, and mural cell alteration. *Am. J. Pathol.* 184(2):541–55

Guan C, Ye C, Yang X, Gao J. 2010. A review of current large-scale mouse knockout efforts. *Genesis*. 48(2):73–85

Gupta N, Yücel YH. 2007. Glaucoma as a neurodegenerative disease. *Curr. Opin. Ophthalmol.* 18(2):110–14

Gupta VK, Chitranshi N, Gupta VB, Golzan M, Dheer Y, et al. 2016. Amyloid β accumulation and inner retinal degenerative changes in Alzheimer's disease transgenic mouse. *Neurosci. Lett.* 623:52–56

Gupta VK, Gowda LR. 2008. Alpha-1-proteinase inhibitor is a heparin binding serpin:

Molecular interactions with the Lys rich cluster of helix-F domain. *Biochimie*. 90(5):749–61

Gupta VK, Rajala A, Daly RJ, Rajala RVS. 2010. Growth factor receptor-bound protein 14: a new modulator of photoreceptor-specific cyclic-nucleotide-gated channel. *EMBO Rep.* 11(11):861–67

Gupta VK, Rajala A, Rajala RVS. 2012a. Insulin receptor regulates photoreceptor CNG channel activity. *Am. J. Physiol. - Endocrinol. Metab.* 303(11):

Gupta VK, You Y, Klistorner A, Graham SL. 2012b. Shp-2 regulates the TrkB receptor activity in the retinal ganglion cells under glaucomatous stress. *Biochim. Biophys. Acta - Mol. Basis Dis.* 1822(11):1643–49

Gupta VK, You Y, Klistorner A, Graham SL. 2012c. Focus on molecules: Sphingosine 1 phosphate (S1P). *Exp. Eye Res.* 103:119–20

Gupta VK, You Y, Li JC, Klistorner A, Graham SL. 2013a. Protective effects of 7,8-dihydroxyflavone on retinal ganglion and RGC-5 cells against excitotoxic and oxidative stress. *J. Mol. Neurosci.* 49(1):96–104

Gupta VKVB, You Y, Gupta VKVB, Klistorner A, Graham SL. 2013b. TrkB receptor signalling: Implications in neurodegenerative, psychiatric and proliferative disorders. *Int. J. Mol. Sci.* 14(5):10122–42

Gupta VV, You Y, Li J, Gupta VV, Golzan M, et al. 2014. BDNF impairment is associated with age-related changes in the inner retina and exacerbates experimental glaucoma. *Biochim. Biophys. Acta*. 1842(9):1567–78

Hadari YR, Kouhara H, Lax I, Schlessinger J. 1998. Binding of Shp2 tyrosine phosphatase to FRS2 is essential for fibroblast growth factor-induced PC12 cell differentiation. *Mol. Cell. Biol.* 18(7):3966–73

Harada T, Harada C, Parada LF. 2007. Molecular regulation of visual system development : more than meets the eye. . 367–78

Hauck SM, Dietter J, Kramer RL, Hofmaier F, Zipplies JK, et al. 2010. Deciphering membrane-associated molecular processes in target tissue of autoimmune uveitis by label-free quantitative mass spectrometry. *Mol. Cell. Proteomics*. 9(10):2292–2305

Head BP, Peart JN, Panneerselvam M, Yokoyama T, Pearn ML, et al. 2010. Loss of caveolin-1 accelerates neurodegeneration and aging. *PLoS One*. 5(12):e15697

Hee YK, Soo JP, Joe EH, Jou I. 2006. Raft-mediated Src homology 2 domain-containing protein-tyrosine phosphatase 2 (SHP-2) regulation in microglia. *J. Biol. Chem.* 281(17):11872–78

Hewitt AW, Dimasi DP, Mackey DA, Craig JE. 2006. A Glaucoma Case-control Study of the WDR36 Gene D658G sequence variant. *Am. J. Ophthalmol.* 142(2):324–25

Hnasko R, Lisanti MP. 2003. The biology of caveolae: lessons from caveolin knockout mice and implications for human disease. *Mol. Interv.* 3(8):445–64

Hollis ER, Jamshidi P, Löw K, Blesch A, Tuszynski MH. 2009. Induction of corticospinal regeneration by lentiviral trkB-induced Erk activation. *Proc. Natl. Acad. Sci. U. S. A.* 106(17):7215–20

Hopkins J. 1999. M g h r d. . 89–131

Hoppe PS, Coutu DL, Schroeder T. 2014. Single-cell technologies sharpen up mammalian stem cell research. *Nat. Cell Biol.* 16(10):919–27

Huang EJ, Reichardt LF. 2003. Trk receptors: roles in neuronal signal transduction. *Annu. Rev. Biochem.* 72:609–42

Huber G, Beck SC, Grimm C, Sahaboglu-Tekgoz A, Paquet-Durand F, et al. 2009. Spectral domain optical coherence tomography in mouse models of retinal degeneration. *Invest. Ophthalmol. Vis. Sci.* 50(12):5888–95

Jeon CJ, Strettoi E, Masland RH. 1998. The major cell populations of the mouse retina. *J Neurosci*. 18(21):8936–46

Jo A, Park H, Lee SH, Ahn SH, Kim HJ, et al. 2014. SHP-2 binds to caveolin-1 and regulates Src activity via competitive inhibition of CSK in response to H2O2 in astrocytes. *PLoS One*. 9(3):

Johnson JE, Barde YA, Schwab M, Thoenen H. 1986. Brain-derived neurotrophic factor supports the survival of cultured rat retinal ganglion cells. *J. Neurosci.* 6(10):3031–38

Kaplan DR, Miller FD. 2000. Neurotrophin signal transduction in the nervous system. *Curr. Opin. Neurobiol.* 10(3):381–91

Kido N, Tanihara H, Honjo M, Inatani M, Tatsuno T, et al. 2000. Neuroprotective effects of brain-derived neurotrophic factor in eyes with NMDA-induced neuronal death. *Brain Res.* 884(1–2):59–67

Kim H, Lee T, Lee J, Ahn M, Moon C, et al. 2006. Immunohistochemical study of caveolin-1 and -2 in the rat retina. *J. Vet. Sci.* 7(2):101–4

Kim HY, Park EJ, Joe E -h., Jou I. 2003. Curcumin Suppresses Janus Kinase-STAT Inflammatory Signaling through Activation of Src Homology 2 Domain-Containing Tyrosine Phosphatase 2 in Brain Microglia. *J. Immunol.* 171(11):6072–79

Kim KH, Puoris'haag M, Maguluri GN, Umino Y, Cusato K, et al. 2008. Monitoring mouse retinal degeneration with high-resolution spectral-domain optical coherence tomography. *J. Vis.* 8(1):17

Klaassen I, Hughes JM, Vogels IMC, Schalkwijk CG, Van Noorden CJF, Schlingemann RO. 2009. Altered expression of genes related to blood–retina barrier disruption in streptozotocin-induced diabetes. *Exp. Eye Res.* 89(1):4–15

Klaassen I, Van Noorden CJFF, Schlingemann RO. 2013. Molecular basis of the inner blood-retinal barrier and its breakdown in diabetic macular edema and other pathological conditions. *Prog. Retin. Eye Res.* 34(February):19–48

Klöcker N, Kermer P, Weishaupt JH, Labes M, Ankerhold R, Bähr M. 2000. Brain-derived neurotrophic factor-mediated neuroprotection of adult rat retinal ganglion cells in vivo does not exclusively depend on phosphatidyl-inositol-3'-kinase/protein kinase B signaling. *J. Neurosci.* 20(18):6962–67

Kocaoglu OP, Uhlhorn SR, Hernandez E, Juarez R a, Will R, et al. 2007. Simultaneous fundus imaging and optical coherence tomography of the mouse retina. *Invest. Ophthalmol. Vis. Sci.* 48(3):1283–89

Kontaridis MI, Yang W, Bence KK, Cullen D, Wang B, et al. 2008. Deletion of Ptpn11 (Shp2) in cardiomyocytes causes dilated cardiomyopathy via effects on the extracellular signal-regulated kinase/mitogen-activated protein kinase and RhoA signaling pathways. *Circulation*. 117(11):1423–35

Kuehn MH, Fingert JH, Kwon YH. 2005. Retinal ganglion cell death in glaucoma: Mechanisms and neuroprotective strategies. *Ophthalmol. Clin. North Am.* 18(3):383–95

Kumamaru E, Numakawa T, Adachi N, Kunugi H. 2011. Glucocorticoid suppresses BDNF-stimulated MAPK/ERK pathway via inhibiting interaction of Shp2 with TrkB. *FEBS Lett.* 585(20):3224–28

Kumar A, Basavaraj MG, Gupta SK, Qamar I, Ali AM, et al. 2007. Role of CYP1B1, MYOC, OPTN, and OPTC genes in adult-onset primary open-angle glaucoma: predominance of CYP1B1 mutations in Indian patients. *Mol. Vis.* 13:667–76

Lazo JS, Nemoto K, Pestell KE, Cooley K, Southwick EC, et al. 2002. Identification of a potent and selective pharmacophore for Cdc25 dual specificity phosphatase inhibitors. *Mol. Pharmacol.* 61(4):720–28

Lebrun-Julien F, Di Polo A. 2008. Molecular and cell-based approaches for neuroprotection in glaucoma. *Optom. Vis. Sci.* 85(6):417–24

Lee DA, Higginbotham EJ. 2005. Glaucoma and its treatment: A review. *Am. J. Heal. Pharm.* 62(7):691–99

Leske MC, Heijl A, Hussein M, Bengtsson B, Hyman L, et al. 2003. Factors for glaucoma progression and the effect of treatment: the early manifest glaucoma trial. *Arch.*

Ophthalmol. (Chicago, Ill. 1960). 121(1):48–56

Lethality P, Ke Y, Zhang EE, Hagihara K, Wu D, et al. 2007. Deletion of Shp2 in the Brain Leads to Defective Proliferation and Differentiation in Neural Stem Cells and Early. . 27(19):6706–17

Li JC, Gupta VK, You Y, Ng KW, Graham SL. 2013. The dynamic response of intraocular pressure and ocular pulse amplitude to acute hemodynamic changes in normal and glaucomatous eyes. *Invest. Ophthalmol. Vis. Sci.* 54(10):6960–67

Li X, Gu X, Boyce TM, Zheng M, Reagan AM, et al. 2014. Caveolin-1 increases proinflammatory chemoattractants and blood???retinal barrier breakdown but decreases leukocyte recruitment in inflammation. *Investig. Ophthalmol. Vis. Sci.* 55(10):6224–34

Li X, McClellan ME, Tanito M, Garteiser P, Towner R, et al. 2012. Loss of caveolin-1 impairs retinal function due to disturbance of subretinal microenvironment. *J. Biol. Chem.* 287(20):16424–34

Lin S, Wang XM, Nadeau PE, Mergia A. 2010. HIV infection upregulates caveolin 1 expression to restrict virus production. *J. Virol.* 84(18):9487–96

London A, Benhar I, Schwartz M. 2012. The retina as a window to the brain—from eye research to CNS disorders. *Nat. Rev. Neurol.* 9(1):44–53

Lu W, Gong D, Bar-Sagi D, Cole PA. 2001. Site-specific incorporation of a phosphotyrosine mimetic reveals a role for tyrosine phosphorylation of SHP-2 in cell signaling. *Mol. Cell*. 8(4):759–69

Lyons BL, Smith RS, Hurd RE, Hawes NL, Burzenski LM, et al. 2006. Deficiency of SHP-1 Protein-Tyrosine Phosphatase in “Viable Motheaten” Mice Results in Retinal Degeneration. *Investig. Opthalmology Vis. Sci.* 47(3):1201

Mansour-Robaey S, Clarke DB, Wang YC, Bray GM, Aguayo AJ. 1994. Effects of ocular injury and administration of brain-derived neurotrophic factor on survival and regrowth of axotomized retinal ganglion cells. *Proc. Natl. Acad. Sci. U. S. A.* 91(5):1632–36

Marsh HN, Dubreuil CI, Quevedo C, Lee A, Majdan M, et al. 2003. SHP-1 negatively regulates neuronal survival by functioning as a TrkA phosphatase. *J. Cell Biol.* 163(5):999–1010

Martin KRG, Klein RL, Quigley HA. 2002. Gene delivery to the eye using adeno-associated viral vectors. *Methods*. 28(2):267–75

Martin KRG, Quigley HA, Zack DJ, Levkovitch-Verbin H, Kielczewski J, et al. 2003. Gene therapy with brain-derived neurotrophic factor as a protection: retinal ganglion cells in a rat glaucoma model. *Invest Ophthalmol Vis Sci*. 44(10):4357–65

Mattson MP. 2000. Apoptosis in neurodegenerative disorders. *Nat. Rev. Mol. Cell Biol.* 1(2):120–30

McCulloch DL, Marmor MF, Brigell MG, Hamilton R, Holder GE, et al. 2015. ISCEV Standard for full-field clinical electroretinography (2015 update). *Doc. Ophthalmol.* 130(1):1–12

Meakin SO, MacDonald JI, Gryz EA, Kubu CJ, Verdi JM. 1999. The signaling adapter FRS-2 competes with Shc for binding to the nerve growth factor receptor TrkA. A model for

discriminating proliferation and differentiation. *J. Biol. Chem.* 274(14):9861–70

Minichiello L, Casagranda F, Tatche RS, Stucky CL, Postigo A, et al. 1998. Point mutation in trkB causes loss of NT4-dependent neurons without major effects on diverse BDNF responses. *Neuron*. 21(2):335–45

NAARENDORP F, SATO Y, CAJDRIC A, HUBBARD NP. 2001. Absolute and relative sensitivity of the scotopic system of rat: Electroretinography and behavior. *Vis. Neurosci.* 18(4):641–56

Neel BG, Gu H, Pao L. 2003. The "Shp"ing news: SH2 domain-containing tyrosine phosphatases in cell signaling. *Trends Biochem. Sci.* 28(6):284–93

Nickells RW. 1999. Apoptosis of Retinal Ganglion Cells in Glaucoma. *Surv. Ophthalmol.* 43(June):S151–61

O'Shea JJ, Gadina M, Schreiber RD. 2002. Cytokine signaling in 2002: new surprises in the Jak/Stat pathway. *Cell*. 109 Suppl:S121-31

Ong SH, Lim YP, Low BC, Guy GR. 1997. SHP2 Associates Directly with Tyrosine Phosphorylated p90 (SNT) Protein in FGF-Stimulated Cells. *Biochem. Biophys. Res. Commun.* 238(1):261–66

Pang J, Dai X, Boye SLSE, Barone I, Boye SLSE, et al. 2011. Long-term retinal function and structure rescue using capsid mutant AAV8 vector in the rd10 mouse, a model of recessive retinitis pigmentosa. *Mol. Ther.* 19(2):234–42

Park DS, Cohen AW, Frank PG, Razani B, Lee H, et al. 2003. Caveolin-1 null (-/-) mice show

dramatic reductions in life span. *Biochemistry*. 42(51):15124–31

Park DS, Woodman SE, Schubert W, Cohen AW, Frank PG, et al. 2002. Caveolin-1/3 double-knockout mice are viable, but lack both muscle and non-muscle caveolae, and develop a severe cardiomyopathic phenotype. *Am. J. Pathol.* 160(6):2207–17

Park H, Ahn KJ, Kang JL, Choi YH. 2015. Protein-protein interaction between caveolin-1 and SHP-2 is dependent on the N-SH2 domain of SHP-2. *BMB Rep.* 48(3):184–89

Park JS, Park SJ, Choi Y-H, Jo A, Kang JL, et al. 2011. Caveolin-1 is involved in reactive oxygen species-induced SHP-2 activation in astrocytes. *Exp. Mol. Med.* 43(12):660

Pawson T, Gish GD, Nash P. 2001. SH2 domains, interaction modules and cellular wiring. *Trends Cell Biol.* 11(12):504–11

Pease ME, Zack DJ, Berlinicke C, Bloom K, Cone F, et al. 2009. Effect of CNTF on Retinal Ganglion Cell Survival in Experimental Glaucoma. *Investig. Opthalmology Vis. Sci.* 50(5):2194

Peinado-Ramon P, Salvador M, Villegas-Perez MP, Vidal-Sanz M. 1996. Effects of axotomy and intraocular administration of NT-4, NT-3, and brain-derived neurotrophic factor on the survival of adult rat retinal ganglion cells. A quantitative in vivo study. *Invest Ophthalmol Vis Sci*. 37(4):489–500

Peraldi P, Zhao Z, Filloux C, Fischer EH, Van Obberghen E. 1994. Protein-tyrosine-phosphatase 2C is phosphorylated and inhibited by 44-kDa mitogen-activated protein kinase. *Proc. Natl. Acad. Sci. U. S. A.* 91(11):5002–6

Pernet V, Di Polo A. 2006. Synergistic action of brain-derived neurotrophic factor and lens injury promotes retinal ganglion cell survival, but leads to optic nerve dystrophy in vivo. *Brain*. 129(Pt 4):1014–26

Petrs-Silva H, Dinculescu A, Li Q, Min S-H, Chiodo V, et al. 2009. High-efficiency transduction of the mouse retina by tyrosine-mutant AAV serotype vectors. *Mol. Ther.* 17(3):463–71

Picciotto MR, Wickman K. 1998. Using knockout and transgenic mice to study neurophysiology and behavior. *Physiol. Rev.* 78(4):1131–63

Pickard GE, Sollars PJ. 2012. Intrinsically photosensitive retinal ganglion cells. *Rev. Physiol. Biochem. Pharmacol.* 162:59–90

Qu C-K. 2002. Role of the SHP-2 tyrosine phosphatase in cytokine-induced signaling and cellular response. *Biochim. Biophys. Acta*. 1592(3):297–301

Quigley HA. 1996. Number of people with glaucoma worldwide. *Br. J. Ophthalmol.* 80(5):389–93

Quigley HA. 1999. Neuronal death in glaucoma. *Prog. Retin. Eye Res.* 18(1):39–57

Quigley HA, Broman AT. 2006. The number of people with glaucoma worldwide in 2010 and 2020. *Br. J. Ophthalmol.* 90(3):262–67

Rajala A, Gupta VK, Anderson RE, Rajala RVS. 2013. Light activation of the insulin receptor regulates mitochondrial hexokinase. A possible mechanism of retinal neuroprotection. *Mitochondrion*. 13(6):566–76

Rattner A, Sun H, Nathans J. 1999. Molecular genetics of human retinal disease. *Annu. Rev. Genet.* 33:89–131

Razani B, Engelman JA, Wang XB, Schubert W, Zhang XL, et al. 2001. Caveolin-1 null mice are viable but show evidence of hyperproliferative and vascular abnormalities. *J. Biol. Chem.* 276(41):38121–38

Razani B, Lisanti MP. 2001. Caveolin-deficient mice:insights into caveolar function and human disease. *J.clin.invest*. 108(11):1553–61

Reagan A, Gu X, Hauck SM, Ash JD, Cao G, et al. 2016. Retinal Caveolin-1 Modulates Neuroprotective Signaling. *Adv. Exp. Med. Biol.* 854:411–18

Reeves SA, Sinha B, Baur I, Reinhold D, Harsh G. 1995. An alternative role for the src-homology-domain-containing phosphotyrosine phosphatase (SH-PTP2) in regulating epidermal-growth-factor-dependent cell growth. *Eur. J. Biochem.* 233(1):55–61

Reich SJ, Auricchio A, Hildinger M, Glover E, Maguire AM, et al. 2003. Efficient Trans-Splicing in the Retina Expands the Utility of Adeno-Associated Virus as a Vector for Gene Therapy. *Hum. Gene Ther.* 14(1):37–44

Ren R, Li Y, Liu Z, Liu K, He S. 2012. Long-term rescue of rat retinal ganglion cells and visual function by AAV-mediated BDNF expression after acute elevation of intraocular pressure. *Investig. Ophthalmol. Vis. Sci.* 53(2):1003–11

Roesch K, Jadhav AP, Trimarchi JM, Stadler MB, Roska B, et al. 2008. The transcriptome of retinal Müller glial cells. *J. Comp. Neurol.* 509(2):225–38

Rösch S, Johnen S, Müller F, Pfarrer C, Walter P, et al. 2014. Correlations between ERG, OCT, and Anatomical Findings in the *rd10* Mouse. *J. Ophthalmol.* 2014:1–10

Rozsa FW, Scott K, Pawar H, Moroi S, Richards JE. 2008. Effects of timolol on MYOC, OPTN, and WDR36 RNA levels. *Arch. Ophthalmol. (Chicago, Ill. 1960)*. 126(1):86–93

Rusanescu G, Yang W, Bai A, Neel BG, Feig L a. 2005. Tyrosine phosphatase SHP-2 is a mediator of activity-dependent neuronal excitotoxicity. *EMBO J.* 24(2):305–14

Sánchez-Ramos C, Bonnin-Arias C, Guerrera MC, Calavia MG, Chamorro E, et al. 2013. Light regulates the expression of the BDNF/TrkB system in the adult zebrafish retina. *Microsc. Res. Tech.* 76(1):42–49

Sand A, Schmidt TM, Kofuji P. 2012. Diverse types of ganglion cell photoreceptors in the mammalian retina. *Prog. Retin. Eye Res.* 31(4):287–302

Saszik SM, Robson JG, Frishman LJ. 2002. The scotopic threshold response of the dark-adapted electroretinogram of the mouse. *J. Physiol.* 543(Pt 3):899–916

Scherer PE, Lewis RY, Volonte D, Engelman JA, Galbiati F, et al. 1997. Cell-type and tissue-specific expression of caveolin-2. Caveolins 1 and 2 co-localize and form a stable hetero-oligomeric complex in vivo. *J. Biol. Chem.* 272(46):29337–46

Sivak JM. 2013. The aging eye: common degenerative mechanisms between the Alzheimer's brain and retinal disease. *Invest. Ophthalmol. Vis. Sci.* 54(1):871–80

Slijkerman RWN, Song F, Astuti GDN, Huynen MA, van Wijk E, et al. 2015. The pros and cons of vertebrate animal models for functional and therapeutic research on inherited

retinal dystrophies. *Prog. Retin. Eye Res.* 48:137–59

Song KS, Li Shengwen, Okamoto T, Quilliam LA, Sargiacomo M, Lisanti MP. 1996. Co-purification and direct interaction of Ras with caveolin, an integral membrane protein of caveolae microdomains. Detergent-free purification of caveolae microdomains. *J. Biol. Chem.* 271(16):9690–97

Stofega MR, Herrington J, Billestrup N, Carter-Su C. 2000. Mutation of the SHP-2 binding site in growth hormone (GH) receptor prolongs GH-promoted tyrosyl phosphorylation of GH receptor, JAK2, and STAT5B. *Mol. Endocrinol.* 14(September):1338–50

Surgucheva I, Surguchov A. 2011. Expression of caveolin in trabecular meshwork cells and its possible implication in pathogenesis of primary open angle glaucoma. *Mol. Vis.* 17:2878–88

Takayasu Y, Takeuchi K, Kumari R, Bennett MVL, Zukin RS, Francesconi A. 2010. Caveolin-1 knockout mice exhibit impaired induction of mGluR-dependent long-term depression at CA3-CA1 synapses. *Proc. Natl. Acad. Sci. U. S. A.* 107(50):21778–83

Thorleifsson G, Walters GB, Hewitt AW, Masson G, Helgason A, et al. 2010. Common variants near CAV1 and CAV2 are associated with primary open-angle glaucoma. *Nat. Genet.* 42(10):906–9

Toda K, Bush RA, Humphries P, Sieving PA. The electroretinogram of the rhodopsin knockout mouse. *Vis. Neurosci.* 16(2):391–98

Trushina E, Du Charme J, Parisi J, McMurray CT. 2006. Neurological abnormalities in caveolin-1 knock out mice. *Behav. Brain Res.* 172(1):24–32

Vranka JA, Kelley MJ, Acott TS, Keller KE. 2015. Extracellular matrix in the trabecular meshwork: intraocular pressure regulation and dysregulation in glaucoma. *Exp. Eye Res.* 133:112–25

Walton MR, Dragunow I. 2000. Is CREB a key to neuronal survival? *Trends Neurosci.* 23(2):48–53

Watanabe S, Sanuki R, Ueno S, Koyasu T, Hasegawa T, Furukawa T. 2013. Tropisms of AAV for Subretinal Delivery to the Neonatal Mouse Retina and Its Application for In Vivo Rescue of Developmental Photoreceptor Disorders. *PLoS One*. 8(1):

Wax MB, Tezel G. 2002. Neurobiology of glaucomatous optic neuropathy: diverse cellular events in neurodegeneration and neuroprotection. *Mol. Neurobiol.* 26(1):45–55

Weber AJ, Harman CD. 2005. Structure-function relations of parasol cells in the normal and glaucomatous primate retina. *Invest. Ophthalmol. Vis. Sci.* 46(9):3197–3207

Weinreb RN, Aung T, Medeiros FA. 2014. The pathophysiology and treatment of glaucoma: a review. *Jama*. 311(18):1901–11

Wiggs JL, Kang JH, Yaspan BL, Mirel DB, Laurie C, et al. 2011. Common variants near CAV1 and CAV2 are associated with primary open-angle glaucoma in Caucasians from the USA. *Hum. Mol. Genet.* 20(23):4707–13

Williams TM, Lisanti MP. 2004. The caveolin proteins. *Genome Biol.* 5(3):214

Yang Q, Cho KS, Chen H, Yu D, Wang WH, et al. 2012. Microbead-induced ocular hypertensive mouse model for screening and testing of aqueous production suppressants

for Glaucoma. *Investig. Ophthalmol. Vis. Sci.* 53(7):3733–41

Yokoi K, Kachi S, Zhang HS, Gregory PD, Spratt SK, et al. 2007. Ocular Gene Transfer with Self-Complementary AAV Vectors. *Investig. Opthalmology Vis. Sci.* 48(7):3324

You Y, Gupta VK, Li JC, Al-Adawy N, Klistorner A, Graham SL. 2014. FTY720 protects retinal ganglion cells in experimental glaucoma. *Invest. Ophthalmol. Vis. Sci.* 55(5):3060–66

You Y, Gupta VK, Li JC, Klistorner A, Graham SL. 2013. Optic neuropathies: characteristic features and mechanisms of retinal ganglion cell loss. *Rev. Neurosci.* 24(3):301–21

You Y, Thie J, Klistorner A, Gupta VK, Graham SL, et al. 2012. Normalization of Visual Evoked Potentials Using Underlying Electroencephalogram Levels Improves Amplitude Reproducibility in Rats. *Investig. Opthalmology Vis. Sci.* 53(3):1473

Young H. Kwon, John H. Fingert MHK and WLMA. 2009. Primary open-angle glaucoma. *N. Engl. J. Med.* 360:1113–24

Yu CL, Jin YJ, Burakoff SJ. 2000. Cytosolic tyrosine dephosphorylation of STAT5. Potential role of SHP-2 in STAT5 regulation. *J. Biol. Chem.* 275(1):599–604

Zhang J, Zhao J, Jiang W, Shan X, Yang X, Gao J. 2012. Conditional gene manipulation: Cre-ating a new biological era. *J. Zhejiang Univ. Sci. B.* 13(7):511–24

Zhang SQ, Tsiaras WG, Araki T, Wen G, Minichiello L, et al. 2002. Receptor-Specific Regulation of Phosphatidylinositol 3’-Kinase Activation by the Protein Tyrosine Phosphatase Shp2. *Mol. Cell. Biol.* 22(12):4062–72

Zhang X, Cai ZG, Simons DL, Fu XY, Feng GS, Wu SM. 2011. Loss of Shp2-Mediated Mitogen-Activated Protein Kinase Signaling in Muller Glial Cells Results in Retinal Degeneration. *Mol. Cell. Biol.* 31(14):2973–83

Zhou Y, Pernet V, Hauswirth WW, Di Polo A. 2005. Activation of the extracellular signal-regulated kinase 1/2 pathway by AAV gene transfer protects retinal ganglion cells in glaucoma. *Mol. Ther.* 12(3):402–12